MARCUS ANDRÉ BRAIDO PINHEIRO

USING BIG DATA FROM REMOTE SENSING FOR EVAPOTRANSPIRATION PREDICTION AND WATER MANAGEMENT IN IRRIGATED COFFEE

LAVRAS – MG
2021

MARCUS ANDRÉ BRAIDO PINHEIRO

USING BIG DATA FROM REMOTE SENSING FOR EVAPOTRANSPIRATION PREDICTION AND WATER MANAGEMENT IN IRRIGATED COFFEE

Tese apresentada à Universidade Federal de Lavras, como parte das exigências do Programa de Pós-Graduação em Engenharia Agrícola, área de concentração em Sensoriamento Remoto e Geoprocessamento, para a obtenção do título de Doutor.

Prof. Dr. Marcelo de Carvalho Alves
Orientador
Prof. Dr. João Marcos Louzada
Coorientador

LAVRAS -MG
2021

Ficha catalográfica elaborada pelo Sistema de Geração de Ficha Catalográfica da Biblioteca Universitária da UFLA, com dados informados pelo(a) próprio(a) autor(a).

Pinheiro, Marcus André Braido.
Using bigdata from remote sensing for evapotranspiration prediction and water management in irrigated coffee / Marcus André Braido Pinheiro. - 2021.
88 p. : il.

Orientador(a): Marcelo de Carvalho Alves.
Coorientador(a): João Marcos Louzada.
Tese (doutorado) - Universidade Federal de Lavras, 2021.
Bibliografia.

1. Irrigation management. 2. Evapotranspiration. 3. Latent heat flux. I. Alves, Marcelo de Carvalho. II. Louzada, João Marcos. III. Título.

MARCUS ANDRÉ BRAIDO PINHEIRO

USO DE BIG DATA DE SENSORIAMENTO REMOTO PARA PREDIÇÃO DE EVAPOTRANSPIRAÇÃO E GESTÃO DA ÁGUA NO CAFÉ IRRIGADO

USING BIG DATA FROM REMOTE SENSING FOR EVAPOTRANSPIRATION PREDICTION AND WATER MANAGEMENT IN IRRIGATED COFFEE

Tese apresentada à Universidade Federal de Lavras, como parte das exigências do Programa de Pós-Graduação em Engenharia Agrícola, área de concentração em Sensoriamento Remoto e Geoprocessamento, para a obtenção do título de Doutor.

APROVADA em 23 de Setembro de 2021.

Dr. Marcelo de Carvalho Alves UFLA
Dr. Luiz Gonsaga de Carvalho UFLA
Dr. João Marcos Louzada IFES – Campus Itapina
Dr Jonathan da Rocha Miranda – CNPq/UFPI
Dr. Michel Eustáquio Dantas Chaves - INPE

Prof. Dr. Marcelo de Carvalho Alves
Orientador
Prof. Dr. João Marcos Louzada
Coorientador

LAVRAS – MG
2021

À minha Mãe Maria Geralda pelo apoio, carinho e cobranças em todos os momentos da minha vida e em toda essa caminhada.
Ao meu Pai, Nivaldo que além de pai sempre foi um amigo e companheiro para todos os momentos.
À minha irmã, Ana Paula pelo apoio e pelos momentos de discussão científica para engrandecer o trabalho.
À minha noiva, Omaira que além de companheira, sempre esteve ao meu lado em todos os dias durante essa jornada, cobrando e incentivando todos os dias.
Aos meus amigos que sempre torceram pelo meu sucesso.
Dedico

AGRADECIMENTOS

À Universidade Federal de Lavras, especialmente ao Departamento de Engenharia Agrícola, pela oportunidade.

À CAPES, pela concessão da bolsa de doutorado, que me permitiu desenvolver esse trabalho.

Ao Prof. Dr. Marcelo de Carvalho Alves, pela orientação, paciência, conhecimentos compartilhados e disposição para ajudar e acompanhar durante todo o processo.

[...] A todos funcionários do DEA/UFLA.

A todos os colegas de laboratório, que contribuíram de alguma forma para conclusão deste trabalho.

Aos meus pais, Nivaldo e Geralda pelo amor e apoio incondicional, em todas as minhas decisões nas diferentes etapas da minha vida e a minha irmã Ana Paula.

À Omaira, pelo companheirismo, amor, cobrança e apoio em todos os momentos com uma singular torcida.

O presente trabalho foi realizado com apoio da Coordenação de Aperfeiçoamento de Pessoal de Nível Superior – Brasil (CAPES) – Código de Financiamento 001

MUITO OBRIGADO!!

“O ser humano é o mesmo em qualquer lugar, em qualquer tempo, em qualquer que seja a sua condição. Você pode ser rico ou pobre, mas os problemas que afetam verdadeiramente o ser humano são os mesmos.” (Ariano Suassuna)

RESUMO

A agricultura é a atividade de uso da terra mais importante do mundo. A agricultura não apenas afeta a mudança de cobertura da terra, mas também tem um profundo impacto no desenvolvimento sustentável da economia social, segurança alimentar, água e meio ambiente, serviços ambientais, mudança climática e ciclo do carbono. Desta forma, o Brasil é o maior produtor mundial de café, com uma participação de 32% da produção mundial, sendo o café Arábica responsável pela maior parte da produção. Para se manter no topo da produção, o monitoramento de diversas variáveis assume importância para um ganho contínuo de produção, temos o destaque da evapotranspiração (ET), importante para a gestão de diferentes culturas. Neste trabalho, objetivamos avaliar diferentes métodos de estimativa da evapotranspiração por sensoriamento remoto em diferentes locais nos cafés Arábicas e Robustas. Em primeiro lugar, fazemos uma visão geral dos modelos de evapotranspiração (ET) comumente aplicados, usando dados de sensoriamento remoto para fornecer uma visão geral da estimativa da evapotranspiração em escala regional a partir de dados de satélite. Geralmente, estes modelos variam muito em entradas, principais suposições e precisão dos resultados. Esta revisão resume as teorias básicas dos métodos de estimativa da radiação solar (onda curta), térmica (onda longa) e evapotranspiração (fluxo de calor latente), tanto da terra como de satélite, que são intrinsecamente complexas para medir em larga escala. Nos artigos 2 e 3 aplicamos dois métodos diferentes de estimativa da evapotranspiração por sensoriamento remoto (METRIC e SAFER). As aplicações conjuntas dos algoritmos METRIC e SAFER permitiram compreender a variação do ET no campo irrigado de café com alta resolução espacial (30 e 10 m) e temporal (16 e 5 dias), e a partir desta variação no ET, entender como melhor gerenciar a irrigação nesta cultura. Mesmo assim, a boa precisão do modelo METRIC foi encontrada na estimativa da evapotranspiração, fornecendo assim informações importantes para a entrada de dados no balanço hídrico para a determinação dos projetos de irrigação.

Palavras-chave: Manejo de irrigação, Fluxo de calor Latente, Evapotranspiração, Landsat 8, Sentinel 2.

ABSTRACT

Agriculture is the world's most important land-use activity. Agriculture not only affects land cover change, but also has a profound impact on the sustainable development of the social economy, food security, water and the environment, environmental services, climate change and the carbon cycle. Thus, Brazil is the world's largest coffee producer, with a 32% share of world production, with Arabica coffee accounting for most of the production. To stay on top of production, the monitoring of several variables assumes importance for a continuous production gain, we highlight the evapotranspiration (ET), important for the management of different crops. In this work, we aim to evaluate different methods of estimating evapotranspiration by remote sensing in different locations in Arabica and Robusta coffees. First, we give an overview of commonly applied evapotranspiration (ET) models using remote sensing data to provide an overview of regional-scale evapotranspiration estimation from satellite data. Generally, these models vary widely in inputs, key assumptions, and accuracy of results. This review summarizes the basic theories of methods for estimating solar (shortwave), thermal (longwave), and evapotranspiration (latent heat flux) radiation from both earth and satellite, which are inherently complex to measure on a large scale. In papers 2 and 3 we apply two different methods of estimating evapotranspiration by remote sensing (METRIC and SAFER). The joint applications of the METRIC and SAFER algorithms allowed to understand the variation of ET in the irrigated coffee field with high spatial (30 and 10 m) and temporal (16 and 5 days) resolution, and from this variation in ET, to understand how to better manage irrigation in this crop. Even so, the good accuracy of the METRIC model was found in the estimation of evapotranspiration, thus providing important information for data input in the water balance for the determination of irrigation projects.

Keywords: Irrigation management, Latent heat flux, Evapotranspiration, Landsat 8, Sentinel 2.

SUMÁRIO

1. INTRODUÇÃO

The main and first challenge faced by agriculture is producing enough food for a continued increasing population in a complex context of population growth and urbanization, poverty, increased demands for food, ever-growing competition for water and land, climate change, climate uncertainty and droughts, variable supply reliability, decline in critical ecosystems services, changing regulatory environments and less-participatory water resources governance (FAO, 2012).

Brazil is the largest world's coffee producer, followed by Vietnam and Colombia. Coffee is the major export product of some countries such as Uganda, Burundi, Rwanda and Ethiopia. About 70% of the world crop is grown on smallholdings smaller than 10 ha, and hence it is often a family business that provides maintenance for over 25 million people worldwide.

Among some 100 species of the Coffea genus (DAVIS et al., 2006), only *C. arabica* L. (arabica coffee) and *C. canephora* Pierre ex A. Froehner (robusta coffee) are economically important worldwide, with these species being responsible for about 99% of world bean production. Presently, arabica coffee accounts for about 64% of coffee produced, and Robusta coffee for the rest (FASSIO; SILVA, 2007).

Water scarcity affects first and foremost the 52% of world's population who live in arid and semi-arid regions (WWAP, 2006). Consequently, there is a mounting pressure to reduce irrigation water use, while sustaining agricultural production in these regions (DEHGHANISANIJ et al., 2009). To optimize crop yield and quality, a robust and effective irrigation management strategy, that is adaptable to these regions, must also be developed and adopted by local farmers.

irrigated agriculture composes a global food productive system very important in all the word. Irrigated land comprises less than one-fifth of the total cropped area of the world but produces about two-fifths of the world's food (WWAP, 2006). This sector however competes heavily for the already limited water resources in irrigation regions. Thus, appropriate planning in water resources, and more specifically in irrigation, is becoming increasingly important given the challenges of already-stressed water resources, climate change, growing population, increased prosperity, and potential food short- ages.

For the better irrigation management, evapotranspiration is essential to schedule the irrigation. Thus, Allen et al. (1998), define, the combination of two separate

processes whereby water is lost on the one hand from the soil surface by evaporation and on the other hand from the crop by transpiration is referred to as evapotranspiration (ET).

Evapotranspiration (ET) is an important part of both the water and energy cycle. The spatio-temporal variation of ET has been widely used to inform regional water resources management and allocation, including irrigation scheduling, drought monitoring and forecasting. Remote sensing techniques, characterized by high temporal, spatial, and spectral resolution, have been a viable and economical way to map ET in heterogeneous regions. Many models with different degrees of complexity have been developed in recent decades to obtain trends in spatial and temporal variability of ET (BASTIAANSSEN et al., 1998; JIANG; ISLAM, 1999; SU, 2002), which differ with respect to landscape type and spatial extent of model application, type of remote sensing data, and required ancillary meteorological and land-cover data (KALMA; MCVICAR; MCCABE, 2008).

Remote sensing technology has been developed today for earth observation from different sensors and platforms. All the factors with geospatial distribution and data acquisition frequency result in remote sensing big data with huge volume and high complexity. Remote sensing technology has been developing with new, high-performance sensors with higher spatial, spectral and temporal resolutions. Agricultural remote sensing is a highly specialized field to generate images and spectral data in huge volume and extreme complexity to drive decisions for agricultural development.

In light of that, Big Data has significant potential to address the issues of modern societies, including the needs of consumers, financial analysts, marketing agents, producers, and decision makers. While some of these information technologies have been available for some time, adoption surveys such as (GRIFFIN et al., 2017; HENNESSY; LÄPPLE; MORAN, 2016; SCHIMMELPFENNIG; EBEL, 2016) suggest continued increased rates of adoption of the various forms of these technologies.

A variety of technological advances have created the opportunities of Big Data (SONKA, 2021). In many cases, computational capacity both in terms of speed and volume allows for modern analyses previously not possible.

The objective of this work was to analyze and estimate evapotranspiration through remote sensing using different coffee varieties (Arabica and Robusta), with different estimation models (METRIC and SAFER) for the states of Minas Gerais and Espírito Santo, respectively.

REFERÊNCIAS

ALLEN, R. G. et al. **FAO Irrigation and Drainage Paper Nº 56. Crop Evapotranspiration (guidelines for computation crop water requirements)**. Roma: FAO, 1998.

BASTIAANSSEN, W. G. M. et al. A remote sensing surface energy balance algorithm for land (SEBAL). 1. Formulation. **Journal of Hydrology**, v. 212–213, n. JANUARY, p. 198–212, dez. 1998.

DAVIS, AA. P. et al. An annotatated taxonomic conspectus of the genus coffea (Rubiaceae). **Botanical Journal of the Linnean Society**, v. 152, p. 465–512, 2006.

DEHGHANISANIJ, H. et al. Assessment of wheat and maize water productivities and production function for cropping system decisions in arid and semiarid regions. **Irrigation and Drainage**, v. 58, n. 1, p. 105–115, 2009.

FAO. World agriculture towards 2030/2050: the 2012 revision. **Journal of Surgical Oncology**, v. 12, n. 3, p. 1–154, 2012.

FASSIO, L. H.; SILVA, A. E. S. DA. Importância econômica e social o café Conilon. In: FERRÃO, R. G. et al. (Eds.). . **Café Conilon**. 1. ed. Vitoria, ES: Incaper, 2007. p. 38–40.

GRIFFIN, T. W. et al. Farm's sequence of adoption of information-intensive precision agricultural technology. **Applied Engineering in Agriculture**, v. 33, n. 4, p. 521–527, 2017.

HENNESSY, T.; LÄPPLE, D.; MORAN, B. The digital divide in farming: A problem of access or engagement? **Applied Economic Perspectives and Policy**, v. 38, n. 3, p. 474–491, 2016.

JIANG, L.; ISLAM, S. A methodology for estimation of surface evapotranspiration over large areas using remote sensing observations. **Geophysical Research Letters**, v. 26, n. 17, p. 2773–2776, 1999.

KALMA, J. D.; MCVICAR, T. R.; MCCABE, M. F. Estimating land surface evaporation: A review of methods using remotely sensed surface temperature data. **Surveys in Geophysics**, v. 29, n. 4–5, p. 421–469, 2008.

SCHIMMELPFENNIG, D.; EBEL, R. Sequential adoption and cost savings from precision agriculture. **Journal of Agricultural and Resource Economics**, v. 41, n. 1, p. 97–115, 2016.

SONKA, S. T. Digital Technologies, Big Data, and Agricultural Innovation. In: CAMPOS, H. (Ed.). . **The Innovation Revolution in Agriculture**. 1. ed. [s.l.] Springer, 2021.

SU, Z. The Surface Energy Balance System (SEBS) for estimation of turbulent heat fluxes. **Hydrology and Earth System Sciences**, v. 6, n. 1, p. 85–99, 2002.

WWAP, U. **Water: A shared responsibility**. [s.l: s.n.].

SPACE-TIME CHARACTERIZATION OF REMOTELY SENSED EVAPOTRANSPIRATION UNDER DIFFERENT IRRIGATION COFFEE MANAGEMENT

Marcus André Braido Pinheiro, Marcelo de Carvalho Alves

ABSTRACT

An overview of the commonly applied evapotranspiration (ET) models using remotely sensed data is given to provide insight into the estimation of ET on a regional scale from satellite data. Generally, these models vary greatly in inputs, main assumptions, and accuracy of results. This narrative review summarizes the basic theories of estimation methods of solar (shortwave) radiation, thermal (longwave) radiation and evapotranspiration (latent heat flux) from both the ground and satellite measurements, which are inherently complex to measure a large scale. We discuss the main inputs, assumptions, theories, advantages, and drawbacks of each model. Moreover, approaches to the extrapolation of instantaneous ET to the daily values are also briefly presented. This study infers that the further advances in the satellite remote sensing and worldwide ground-based measurement networks will enhance the capabilities for the potential estimation of the ET parameters as well as monitoring the global water and energy cycles to develop significant environmental studies for the betterment of living on the Earth.

KEYWORDS: energy balance; solar radiation; remote sensing; satellite.

1. INTRODUCTION

Evapotranspiration (ET) is a major unknown variable involved in the understanding of ecohydrological systems and can amount up to 95% of the water balance in dry areas (WILCOX; BRESHEARS; SEYFRIED, 2003). The individual components of ET include evaporation from soil (E) and transpiration through plant stomata (T), and in some instances, evaporation of water intercepted by plant canopy and litter layer. The function of E and T within ecosystems is distinctly different: T is

usually associated with plant productivity, whereas E does not directly contribute to production.

On a global basis, the mean ET from the land surface accounts for approximately 60% of the average precipitation. It is therefore indispensable to have reliable information on the land surface ET when natural hazards such as floods and droughts are predicted and weather forecasting and climate change modeling are performed (BRUTSAERT, 1986).

In agriculture, accurate ET estimation is fundamental to determine water management practices, design irrigation systems and irrigation regimes, and calculate crop yield (ALLEN et al., 1998).

Irrigated agriculture is a consumptive use of water, that is, it changes its conditions as it is removed from the environment and most of it is consumed by the evapotranspiration of plants and soil, not returning directly to water bodies. In numbers, irrigated agriculture removes 46 percent of the country's available water.

On a global scale, concerns about climate change have raised interest in the connection between ET and carbon sequestration (SCOTT et al., 2006), and the influence of ET partitioning on land-atmosphere patterns which affect climate simulations (LAWRENCE et al., 2007).

While several reviews have previously described ET research (BURT et al., 2005; FARAHANI et al., 2007; LI et al., 2009; RANA; KATERJI, 2000; SHUTTLEWORTH, 2007; TANNY, 2013), None of them focused specifically on remote sensing applied to coffee irrigation management as performed in this work.

Estimation of water consumption based on ET models using remotely sensed data has become one of the hot topics in water resources planning and management over watersheds due to the competition for water between trans-boundary water users (BASTIAANSSEN et al., 2005).

For vegetated land surfaces, ET rates are closely related to the assimilation rates of plants and can be used as an indicator of plant water stress (JACKSON et al., 1981). Therefore, accurate estimates of regional ET in the land surface water and energy budget modeling at different temporal and spatial scales are essential in hydrology, climatology, and agriculture.

In various practical applications, there are still no specific ways to directly measure the actual ET over a watershed (BRUTSAERT, 1986). Conventional ET estimation techniques (i.e., pan-measurement, Bowen ratio, eddy correlation system,

and weighing lysimeter, scintillometer, sap flow) are mainly based on site (field)-measurements and many of those techniques are dependent on a variety of model complexities.

Remote sensing technology is recognized as the only viable means to map regional- and meso-scale patterns of ET on the Earth's surface in a globally consistent and economically feasible manner and surface temperature helps to establish the direct link between surface radiances and the components of surface energy balance (CASELLES; SOBRINO; COLL, 1992; IDSO et al., 1975; JACKSON, 1985; KUSTAS; NORMAN, 1996; MCCABE; WOOD, 2006; MORAN et al., 1989). Remote sensing technology has several marked advantages over conventional "point" measurements: 1) it can provide large and continuous spatial coverage within a few minutes; 2) it costs less when the same spatial information is required; 3) it is particularly practical for ungauged areas where man-made measurements are difficult to conduct or unavailable (ENGMAN; GURNEY, 1991; RANGO, 1994).

Combining surface parameters derived from remote sensing data with surface meteorological variables and vegetation characteristics allows the evaluation of ET on local, regional, and global scales (LI et al., 2009; MAUSER; SCHÄDLICH, 1998).

Therefore, with the consideration of the characteristics of the various ET methods developed over the past decades and of the significance of land surface ET to hydrologists, water resources and irrigation engineers, and climatologists, know how to calculate the ET over a regional scale or how to estimate ET precisely based on the remote sensing technology has become a critical question in various ET-related applications and studies. Thus, among the great potential of high-resolution satellite images, remote sensing combined with surface energy balance models is the ability to return the spatial distribution of actual evapotranspiration (ETa) over individual fields and/or irrigation districts.

This paper provides an overview of a variety of methods and models that have been developed to estimate land surface ET on a field, regional and large scales, based mainly on remotely sensed data. For each method or model, we shall detail the main theory and assumptions involved in the model development, and highlight its advantages, drawbacks, and potential.

2. EVAPOTRANSPIRATION

ETa is the process of water transferring from land to the atmosphere and is comprised of evaporation from the Earth's surface and transpiration from plants. These processes are typically estimated together due to the difficulty in partitioning them (PETKOVIĆ et al., 2015; SAWANO et al., 2015).

ET is a fundamental parameter of the hydrological cycle used in studies and agricultural areas (BERTI et al., 2014; BORGES JÚNIOR et al., 2017; MARTÍ et al., 2015) and has an extremely important role in the development and operation of irrigation projects (ABDULLAH et al., 2015). This importance is summarized by the parameter to be responsible for 90% water loss in irrigated vegetated systems (HOOGEVEEN et al., 2015; RANA; KATERJI, 2000).

The determination of ET for further use in irrigation depends on the previous calculation of reference evapotranspiration (ET0). Allen et al. (1998, 2005), introduced some parameters for the calculation of ET0, such as the proposal of a “hypothetical crop” with a height of 0.12 m, surface aerodynamic resistance of 70 s m^{-1}, and albedo de 0.23.

Evapotranspiration of a crop under standard conditions (ETc) is defined as evapotranspiration of a crop free from pests and diseases, without nutritional and water restriction, grown in large fields reaching their productivity under specific climatic conditions (ALLEN et al., 1998; LEWIS; ALLEN, 2017).

From the definition, the ETc is obtained from the ET0 product by the crop coefficient (Kc), considering the water requirements of the crop in each phenological stage, being influenced by the type of plant, distribution in the cultivated area, and vegetative conditions (ALLEN et al., 1998).

Finally, there is the definition of actual evapotranspiration (ETr or ETa), (ALLEN et al., 1998), conceptualizing this parameter as crop evapotranspiration under non-standard conditions that is, crop development occurs under conditions adverse to better growth. ETr is generally lower than ETc (LEWIS; ALLEN, 2017). Limited soil water content, low fertility, high salinity, disease occurrence, and agricultural pests affect its determination (ALLEN et al., 1998; LEWIS; ALLEN, 2017).

3. FACTORS AFFECTING EVAPOTRANSPIRATION

Meteorological variables, crop characteristics, management, and environmental factors are some of the factors that affect evapotranspiration (ALLEN et al., 1998). Solar radiation, wind speed, air temperature, and relative humidity are meteorological variables that affect evapotranspiration (ALLEN et al., 1998; DARSHANA; PANDEY; PANDEY, 2013; DINPASHOH et al., 2011; ISHAK et al., 2010; TABARI; GRISMER; TRAJKOVIC, 2013).

When the study is performed using meteorological variables, it is observed that if there is greater availability of air temperature, wind speed, and solar radiation combined with low relative humidity, the evaporative demand of the atmosphere will be high, increasing the evapotranspiration rate (TAGLIAFERRE et al., 2015).

Among all the meteorological variables addressed, the available energy or radiation balance is the main factor that influences evapotranspiration, being the main source of energy for biological metabolism, causing water loss by vegetative surfaces and temperature variations in the soil-plant-atmosphere (PEREIRA et al., 2015).

However, not only are meteorological variables influencing ET, crop type, variety, phenological stage, and planting density also affect crop evapotranspiration due to differences in perspiration resistance, crop height, canopy roughness, leaf reflective power, soil cover type, and rooting characteristics. The combination of these factors results in different ET levels for different crops, even under similar edaphoclimatic conditions.

As well as the factors mentioned above, salinity, low soil fertility, presence of impenetrable horizons, and lack of disease and pest control can also limit crop development and reduce ET (ALLEN et al., 1998).

Remote sensing-based ETa estimates first appeared in the 1970s (LI et al., 2009). Since then, several approaches have been developed including surface energy balance approaches are listed in this work.

4. IMPORTANCE OF EVAPOTRANSPIRATION IN IRRIGATION MANAGEMENT

Water is among the most valuable natural resources, and it is becoming progressively insufficient to meet the current and future demands. With the increasing complexity and magnitude of environmental concerns due to agricultural intensification,

exacerbated by climate change scenario, the allocation of existing water resources must be optimized (MINACAPILLI et al., 2016; PROVENZANO; SINOBAS, 2014; RALLO et al., 2014a).

By far, agriculture is the most significant consumer of freshwater. Definitely, agriculture accounts for 70% of total global freshwater withdrawals from watercourses and groundwater. The total global freshwater withdrawals for irrigation purposes are estimated to increase of about 10% by 2050.

Energy fluxes and water vapor exchange are always of importance for the interaction between land surface ecosystems and the atmosphere (BALDOCCHI; XU; KIANG, 2004; RODRIGUES et al., 2014; TIMOUK et al., 2009). In agricultural areas, available solar radiation, evapotranspiration (ET), and carbon fluxes ultimately determine yield and water productivity (SHEN et al., 2013). The processes are always influenced by several interacting biophysical and environmental factors, such as climate conditions, crop development, and water supplies (LEI; YANG, 2010; SUYKER; VERMA, 2008).

However, for crop irrigation scheduling applications, ET is often required at locations where such measurements may not be readily available. Also, highly technical, expensive facilities like large lysimeters and EC instrumentation are nonviable to have at every location where crops are cultivated, as is maintaining them for long-term data collection. In this context, state-of-the-science agricultural system models are cheap, viable, and widely accepted tools for developing location-specific ET data for irrigation scheduling and developing crop-ET response functions for predicting crop response to irrigation water (MCNIDER et al., 2015; SASEENDRAN et al., 2015).

The accurate evaluation of actual evapotranspiration fluxes, ETa is essential for irrigation water management and the sustainable use of water resources, especially in areas prone to water scarcity (AUTOVINO; MINACAPILLI; PROVENZANO, 2016; NEGM; JABRO; PROVENZANO, 2017; RALLO et al., 2014b). Optimizing irrigation management requires that water managers and policymakers give accurate estimations of the water volumes for irrigation applications (DROOGERS; IMMERZEEL; LORITE, 2010). Improvement of water use efficiency in irrigated agriculture would undoubtedly lead to saving both water and energy. The reduction of the energy cost in the farms can in fact be indirectly achieved by reducing the volumes of water applied with irrigation.

Rahimzadegan and Janani (2019), used the SEBAL model to estimate ET rates for pistachio crops in Iran, achieving a higher coefficient of determination (R^2=0.8) than direct measurements. Bhattarai and Liu (2019), tested the validity of the SEBAL model using flux sites in Nebraska, USA, and found that the model could predict ET with a high degree of accuracy, with a determination coefficient between estimated and measured ET between 0.78 and 0.89, respectively. Ochege et al. (2019), successfully estimated ET in the Aral Sea Basin using Landsat 7 Enhanced Thematic Mapper (ETM) data based on the SEBAL model. Estimated and directly measured ET values were well correlated with R^2 values ranging from 0.94 to 0.98, respectively.

All above considered there is an urgent need to seek out technological advancements and scalable solutions in the context of Precision Farming (PF) (LIAGHAT; BALASUNDRAM, 2010; MULLA, 2013; VUOLO et al., 2015) to address management strategies on water inputs in response to seasonal drought.

5. SURFACE ENERGY BALANCE MODELS

Over the past decades, several methods and algorithms to estimate actual ET through satellite measurements have been developed. Energy balance models may have advantages over conventional ET estimation methods, especially at regional scales, promoting the spatialization of this parameter.

In addition, the energy balance can detect reduced ET values caused by lack of water, salinity, or even frost, as well as increased ET caused by evaporation of uncovered soil or water present in plant canopies after moisture-increasing events, such as irrigation or precipitation. Most of these estimates are based on the surface energy balance equation. The surface energy balance describes the partitioning of natural radiation absorbed at Earth's surface into physical land surface processes. Evapotranspiration is one of these key processes of the energy balance, because latent heat (energy) is required for evaporation to take place. The energy balance at Earth's surface reads (ALLEN et al., 2011b; BASTIAANSSEN et al., 1998b; SENAY et al., 2016):

$$LE=Rn - G - H,$$

where Rn is the net radiation, G is the soil heat flux, H is the sensible heat flux, and LE is the latent heat flux. Each of the three components of the energy balance equation, including Rn, G and H, can be estimated by combining remote sensing-based

parameters of surface radiometric temperature and shortwave albedo from visible, near-infrared, and thermal infrared wavebands with a set of ground-based meteorological variables of air temperature, wind speed, and humidity and other auxiliary surface measurements.

5.1. Net Radiation Equation (Rn)

Surface net radiation (Rn) represents the total heat energy that is partitioned into G, H, and LE. It can be estimated from the sum of the difference between the incoming (Rs) and the reflected outgoing shortwave solar radiation (0.15 to 5 μm), and the difference between the downwelling atmospheric and the surface emitted and reflected longwave radiation (3 to 100 μm), which can be expressed as (JACKSON, 1985; KUSTAS; NORMAN, 1996):

$$R_n = (1-\alpha_s)R_s + \varepsilon_s\varepsilon_a\sigma T_a^4 - \varepsilon_s\sigma T_s^4,$$

where α_s is surface shortwave albedo, usually calculated as a combination of narrow-band spectral reflectance values in the bands used in the remote sensing, Rs is determined by combined factors of solar constant, solar inclination angle, geographical location and time of year, atmospheric transmissivity and ground elevation (ALLEN; TASUMI; TREZZA, 2007), ε_s is surface emissivity evaluated either as a weighted average between bare soil and vegetation (LI; LYONS, 1999) or as a function of NDVI (BASTIAANSSEN et al., 1998b), ε_a is atmospheric emissivity estimated as a function of vapor pressure (WILFRIED, 1975).

Kustas and Norman (1996), reviewed the uncertainties of various methods of estimating the net shortwave and longwave radiation fluxes and found that a variety of remote sensing methods of surface net radiation estimation had an uncertainty of 5-10% compared with ground-based observations on meteorologically temporal scales. Bisht et al. (2005), proposed a simple scheme to calculate the instantaneous net radiation over large heterogeneous surfaces for clear sky days using only land and atmospheric products obtained using remote sensing data from MODIS-Terra satellite over Southern Great Plain (SGP). Allen; Tasumi and Trezza (2007), detailed an internalized calibration model for calculating ET as a residual of the surface energy balance from remotely sensed data when surface slope and aspect information derived from a digital elevation model were considered.

5.2. Soil Heat Flux (G)

Soil heat flux (G) is the heat energy used for warming or cooling substrate soil volume. It is traditionally measured with sensors buried beneath the surface soil and is directly proportional to the thermal conductivity and the temperature gradient with the depth of the topsoil. To estimate the regional-scale G is expressed as follows:

$$\frac{G}{R_n} = \left(T_s - 273{,}15\right)\left(0{,}0038 + 0{,}0074\alpha\right)\left(1 - 0{,}98NDVI^4\right),$$

where Ts is the surface temperature (°C) and NDVI is the Normalized Differential Vegetation Index.

Many papers have found that the ratio of G to Rn ranges from 0.05 for full vegetation cover or wet bare soil to 0.5 for dry bare soil (DAUGHTRY et al., 1990; JACKSON, 1985; JHAJHARIA et al., 2014; KUSTAS; NORMAN, 1996; LI; LYONS, 1999; REGINATO; JACKSON; PINTER, 1985) and this ratio is simply related in an exponential form to LAI (CHOUDHURY, 1994), NDVI (ALLEN; TASUMI; TREZZA, 2007; BASTIAANSSEN et al., 1998a; MORAN et al., 1989), Ts (ALLEN; TASUMI; TREZZA, 2007) and solar zenith angle (GAO et al., 1998) based on field observations. The value of G has been shown to be variable in both diurnal and yearly cycles over diverse surface conditions (KUSTAS; DAUGHTRY, 1990). However, the assumption that the daily value of G is equal to 0 and can be negligible in the daily energy balance is generally regarded as a good approximation (PRICE, 1982). Comparisons of G between results from these simplified techniques and observations at micrometeorological scales showed an uncertainty of 20-30% (KUSTAS; NORMAN, 1996).

5.3. Sensible Heat Flux (H)

The sensible heat flux (H) is the heat transfer between ground and atmosphere and is the driving force to warm/cool the air above the surface. It is computed using the following equation for heat transport:

$$H = \rho c_p \frac{\left(T_c - T_a\right)}{r_{ah}},$$

where, ρ is the air density (kg/m^3), cp is the air specific heat (1004 J/kg/K), Tc and TA are the surface and the air temperatures (°C), respectively, and rah is the aerodynamic resistance to heat transport (s/m).

Aerodynamic resistance ra is affected by the combined factors of surface roughness (vegetation height, vegetation structure), wind speed, and atmospheric stability. Therefore, aerodynamic resistance to heat transfer must be adjusted according to different surface characteristics except when the water is freely available (BRISSON; SEGUIN; BERTUZZI, 1992). (HATFIELD; PERRIER; JACKSON, 1983) have shown that ra decreased as the wind speed increased, regardless of whether the surface was warmer or cooler than air, and ra decreased if the surface become rougher (HATFIELD; PERRIER; JACKSON, 1983). The commonly applied one being (BRUTSAERT, 1982):

$$r_{ah} = \frac{\ln\left[\left(z_a - d\right)/z_{om} - \Psi_1\right]\ln\left[\left(z_a - d\right)/z_{oh} - \Psi_2\right]}{k^2 u}$$

with neutral stability, $\Psi_1 = \Psi_2 = 0$.

Jackson et al. (1983), found that Ts-Ta varied from -10 to +5^{o}C under medium to low atmospheric humidity, which shows that neutral stability cannot prevail under a wide range of vegetation cover and soil moisture conditions. Under stable and unstable atmospheric stability conditions, the Monin-Obukhov length (BUSINGER JA et al., 1971) was introduced to measure the stability and it needs to be solved with H iteratively (CHOUDHURY et al., 1994):

$$\Lambda = \frac{u^3 \rho c_p T_a}{kgH}$$

where if $\Lambda < 0$, unstable stability; $\Lambda > 0$, stable stability.

For unstable conditions (usually prevailing at daytime) with no predominant free convection, Ψ_1 and Ψ_2 can be expressed as (PAULSON, 1970):

$$\Psi_1 = 2\ln\left(\frac{1+x}{2}\right) + \ln\left(\frac{1+x^2}{2}\right) - 2\arctan\left(x\right) + \frac{\pi}{2}$$

$$\Psi_2 = 2\ln\left(\frac{1+x}{2}\right)$$

with $x = \left(1 - 16\frac{z_a - d}{\Lambda}\right)^{0.25}$

For stable conditions (usually prevailing at night-time), the formula proposed by (BUSINGER JA et al., 1971; WEBB, 1970) was adopted to account for the effects of atmospheric stability on rah:

$$\Psi_1 = \Psi_2 = -5\frac{z_a - d}{\Lambda}$$

Some papers have specified z_{om} is equal to z_{oh} and can be either a function of vegetation height (GURNEY; CAMILLO, 1984; SOER, 1980), in which z_{om} is typically 5 to 15 percent of vegetation height depending on vegetation characteristics.

In view of this, some models have been developed to estimate ET at different temporal and spatial scales using remote sensing data based on ground energy balance, also called Land Surface Energy Balance (LSEB). More complex methods such as SEBAL (BASTIAANSSEN et al., 1998a, 1998b), METRIC (ALLEN et al., 2007; ALLEN; TASUMI; TREZZA, 2007), TSEB (NORMAN; KUSTAS; HUMES, 1995), ALEXI-/-Disalexi (ANDERSON et al., 1997), Surface Energy Balance Index (SEBI) (MENENTI; CHOUDHURY, 1993), Simplified Surface Energy Balance Index (S-SEBI) (ROERINK; SU; MENENTI, 2000), Enhancing the Simplified Surface Energy Balance (SSEB) (SENAY et al., 2007), Operational Simplified Surface Energy Balance (SSEBop) (SENAY et al., 2013), or simpler, using only a few parameters related to the energy balance together with the Penman-Monteith equation, for example, the SAFER (TEIXEIRA, 2010). Although there is no consensus on the best algorithm or approach.

5.4. Surface Energy Balance Algorithms for Land - SEBAL

Developed by Bastiaanssen et al. (1998b), to evaluate ET with minimum ground-based measurements, SEBAL is a one-layer energy balance model that estimates latent heat flux and other energy balance components without information on soil, crop, and management practices.

Since the satellite image provides information for the overpass time only, SEBAL computes an instantaneous ET flux for the image time. The ET flux is calculated for each pixel of the image as a “residual” of the surface energy budget equation.

One of the main considerations in SEBAL, when evaluating pixel by pixel sensible and latent heat fluxes, is to establish the linear relationships between Ts and the surface-air temperature difference dT on each pixel with the coefficients of the linear expressions determined from the extremely dry (hot) and wet (cold) points. The dT can be approximated as a relatively simple linear relation of Ts expressed as:

$$dT = a + bT_s$$

where a and b are empirical coefficients derived from two anchor points (dry and wet points). At the dry (hot) pixel, latent heat flux is assumed to be zero and the surface-air temperature difference at this pixel is obtained by inverting the single-source bulk aerodynamic transfer equation:

$$dT_{dry} = \frac{H_{dry} \times r_{ah}}{\rho C_p}$$

where Hdry is equal to Rn-G. At the wet (cold) pixel, latent heat flux is assigned a value of Rn-G (or a reference ET), which means sensible heat flux under this condition is equal to zero (when reference ET is applied, both H and dT at this pixel will not equal zero anymore). Obviously, the surface-air temperature difference at this point is also zero (wet dT = 0).

SEBAL has been applied for ET estimation, calculation of crop coefficients, and evaluation of basin-wide irrigation performance under various agroclimatic conditions in several countries including Spain, Sri Lanka, China, and the United States (BASTIAANSSEN et al., 2005; SINGH et al., 2008). Timmermans et al. (2007), compared the spatially distributed surface energy fluxes derived from SEBAL with a dual-source energy balance model using data from two large scale field experiments covering sub-humid grassland (Southern Great Plains '97) and semi-arid rangeland (Monsoon '90). Norman, Anderson and Kustas (2006), showed that the assumption of linearity between surface temperature and the air temperature gradient used in defining the sensible heat fluxes did not generally hold true for strongly heterogeneous landscapes.

Teixeira et al. (2009), reviewed the inputs to the SEBAL model and assessed ET and water productivity with SEBAL using ground measurements observed over the semi-arid region of the Low-Middle São Francisco River basin, Brazil. Opoku-duah, Donoghue and Burt (2008), employed the SEBAL model with remote sensing data derived respectively from MODIS and AATSR sensors to estimate ET over large heterogeneous landscapes and found that both sensors underestimated daily ET when compared with eddy correlation observations. The selection of dry pixel and wet pixel can have a significant impact on the heat flux distribution from SEBAL.

5.5. Mapping Evapotranspiration with Internalized Calibration - METRIC

The METRIC model was initially developed to maximize the accuracy of ET at the field scale using Landsat satellite imagery. It is a variant of the SEBAL model, and it has been extended by incorporating reference ET to minimize the computational biases of aerodynamics resistance and to allow the regional advection of heat (ALLEN et al., 2011a; ALLEN; TASUMI; TREZZA, 2007; GOWDA et al., 2011). Following the SEBAL foundation, a linear relationship between the near-surface temperature gradient (dT) and the surface temperature (Ts) is developed in METRIC by employing the Calibration using Inverse Modeling at Extreme Conditions (CIMEC) process with theoretically defined hydrological extremes (cold and hot). The advantage of using the dT vs. Ts relationship is that it eliminates the need for air temperature (Ta) to map H within the modeling domain. Moreover, the use of the CIMEC process excludes the effect of potential biases related to energy balance components, radiometric correction, and model assumptions on the final estimated ET (ALLEN et al., 2011a; IRMAK et al., 2012).

After the establishment of Rn, G, and H from the Landsat 8 image processing, the LE was calculated as a residue of the Energy Balance equation. The LE obtained is equivalent to ET_{inst} at the time of passage of the Landsat 8 satellite, according to Eq. (23).

$$ET_{inst} = 3600\frac{LE}{\lambda\rho_{\omega}} \tag{23}$$

Where ET_{inst} is the instantaneous evapotranspiration ($mm.h^{-1}$), 3600 converts from seconds to hours, $\rho\omega$ is the density of water ($\sim$1000 $kg.m^{-3}$) and λ is the latent heat of vaporization ($J.kg^{-1}$) representing the heat absorbed when a kilogram of water evaporates.

The λ component was calculated according to Eq. (24)

$$\lambda = \left[2{,}501 - 0{,}00236\left(T_s - 273{,}15\right)\right]\times 10^6 \tag{24}$$

Finally, as shown in Eq. (25), the reference ET fraction (ETrF) was calculated as the ratio between the computed ET_{inst} of each pixel and the reference ET (ET_0) calculated from the meteorological station data.

$$ET_rF = \frac{ET_{inst}}{ET_r} \tag{25}$$

The ETrF obtained was later extrapolated to daily values. In the processes, ET_{24} was calculated assuming that the instantaneous ETrF computed at the time of satellite passage is the same as the mean ETrF over the 24 h mean (ALLEN; TASUMI; TREZZA, 2007), according to Eq. (26).

$$ET_{24} = C_{rad}\left(EF\right)\left(ET_{r24}\right) \tag{26}$$

Where C_{rad} is a correction term used to correct the variation over 24 hours versus the instantaneous availability of energy (ALLEN et al., 2007).

This algorithm has been successfully implemented in many homogeneous ecosystems around the world with different levels of accuracy (ALLEN et al., 2013; BHATTARAI et al., 2017; CHOI et al., 2011; FRENCH; HUNSAKER; THORP, 2015; LOSGEDARAGH; RAHIMZADEGAN, 2018; MADUGUNDU et al., 2017; PÔÇAS et al., 2014; TREZZA; ALLEN; TASUMI, 2013).

5.6. Surface energy balance index (SEBI) and Simplified Surface Energy Balance Index (S-SEBI)

The SEBI model is based on the crop water stress index (CWSI), by scaling up the observed temperature in the maximum (max) temperature (dry condition) and the minimum (min) temperature (wet condition). Jackson et al. (1981), which is the fundamental concept for all the SEB models. The observed max and min surface temperatures are interpolated to calculate the relative evaporative fraction (EF) then for a particular surface albedo and roughness, the pixelwise SEBI computes the regional ET from pixelwise max and min surface temperature redefined CWSI and relative EF. Due to the complexity in the determination of the max and min surface temperatures and poor accuracy of SEBI, it was further developed with a simplified form named simplified-SEBI (S-SEBI) (ROERINK; SU; MENENTI, 2000). Here, a reflectance (albedo)-dependent max and min surface temperatures are pointed out to determine the dry and wet conditions for partitioning the available energy into sensible and latent heat fluxes. The ET is calculated in terms of EF, which can be defined as the ratio of ET/latent heat flux (LE) to the available it can be formulated by interpolating the albedo- energy (Rn−G). Under the dry and wet conditions, dependent surface temperatures as

$$EF = \frac{T_H - T_s}{T_H - T_{LE}} \tag{27}$$

where TH is the max surface temperature at dry conditions and represents the max sensible heat flux and min latent heat flux, TLE is the min surface temperature at wet conditions and represents the max latent heat flux and min sensible heat flux and Ts is the surface temperature.

5.7. Simple Algorithm for Evapotranspiration Retrieving - SAFER

Simple Algorithm for Evapotranspiration Retrieving (SAFER) is an algorithm for estimating large-scale ET formulated by Teixeira (2010) which has the advantage of not being mandatory the use of “anchor pixels” nor the use of thermal bands (which can also be used in the absence of measured temperature data), different from SEBAL and METRIC, and for this reason, is a more operationally application than other methods.

SAFER model requires agrometeorological data of reference evapotranspiration (ETo), global radiation (RG), and mean air temperature (TA) to be integrated with radiometric data from digital images. This algorithm has the additional advantage of the possibility of using daily weather data from either conventional or automatic agrometeorological stations. This is an important characteristic because it allows a historical evaluation of the energy balance components on a large scale, as data from automatic sensors are results from relatively recent advances in instrumental technology. SAFER was recently developed in the semiarid conditions of Brazil, which has already been validated with field data from four flux stations involving irrigated crops and natural vegetation (TEIXEIRA et al., 2013).

Initially, it was named as PM2 model (TEIXEIRA et al., 2009) because it was an adaptation of the Penman-Monteith equation, and from (TEIXEIRA et al., 2013) received the current name. It is an algorithm because it requires as main inputs, surface albedo data, NDVI, and surface temperature, which are obtained sequentially from equations that relate radiometric data (from multispectral images) and agrometeorological data. A flowchart with these relationships is presented in Fig. 1.

All the regression coefficients of the parameters in Fig. 1 and equations below were determined in different areas of Brazil, with digital images from different satellites, like Landsat (COAGUILA et al., 2017; DE OLIVEIRA FERREIRA SILVA; HERIBERTO DE CASTRO TEIXEIRA; LILLA MANZIONE, 2019; TEIXEIRA et al., 2017) and MODIS (TEIXEIRA et al., 2015) and field measurements, involving strong

contrasting agroecosystems and under different thermohydrological conditions throughout several years.

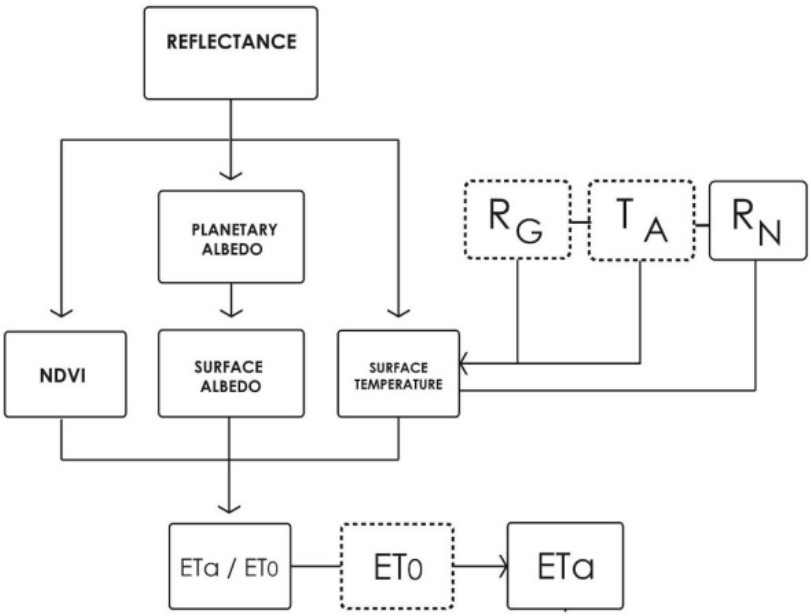

Figure 1 - Flowchart for the large-scale modelling of radiation balances (net radiation, RN), evapotranspiration fraction (ETa ET0−1) and actual evapotranspiration (ETA) by applying the SAFER algorithm with reflectances from satellite images and agrometeorological data (solar radiation, RG, average air temperature, TA, and reference evapotranspiration, ET0).

After reviewing the detailed literature related to the estimation techniques of ET fluxes, we make a summarization as listed in table 1.

Table 1. Summary of the satellite-based evapotranspiration (latent heat flux) estimation models (surface energy balance based)

Name of the models and references	Main concepts	Advantages	Disadvantages
Surface energy balance index (SEBI) (MENENTI; CHOUDHURY, 1993)	Based on the crop water stress index (CWSI) by scaling up the max (dry condition) and min (wet condition) temperature	Direct effects of surface temperature and resistance on latent heat flux	Poor accuracy Ground based measurement is required
Simplified SEBI (S-SEBI) (ROERINK; SU; MENENTI, 2000; VERSTRAETEN; VEROUSTRAETE; FEYEN, 2005)	The observation of temperature is albedo dependent to determine the max (dry condition) and min (wet condition)	Ground based measurement is not required	Extreme temperatures are location dependent
Surface energy balance system (SEBS) (AMATYA et al., 2016; CHEN et al., 2013; MA et al., 2013; SU, 2002)	Estimate the actual ET and other surface fluxes in terms of evaporative fraction and atmospheric turbulent fluxes	Good accuracy The roughness height for heat transfer can be calculated instead of constant value User friendly with RS and GIS software The uncertainties can be partially solved	Requires more parameters The solution of turbulent flux is relatively complex
Surface energy balance algorithm for land (SEBAL) (BASTIAANSSEN et al., 2005; BASTIAANSSEN; MOLDEN; MAKIN, 2000)	A moderate approach based on both the empirical relationship and parameterization scheme	Requires minimum ground-based weather data Automatic internal correction of atmospheric effects on surface temperature	The user dependent specification of anchor pixels
Mapping evapotranspiration at high resolution with internalized calibration (METRIC) (ALLEN et al., 2013; ALLEN; TASUMI; TREZZA, 2007; CARRILLO-ROJAS et al., 2016)	Extended from SEBAL with considering slope aspect	Slope aspect is considered	Uncertainties found in the determination of anchor pixels

5.8. Errors and uncertainties associated with satellite estimations

Several types of errors and uncertainties are found in satellite estimation of SEB components due to various problems and limitations in estimation methods and models, as well as the uneven characteristics of the atmosphere and Earth's surface. Some important sources of uncertainties and possible ways to reduce them are outlined here.

a) *Uncertainties due to coverage problem of satellite data:* Different spatial and temporal scale SEB components are needed for several relevant departments at global and local scales. The simultaneous acquiring of high spatial and temporal resolution imagery is very hard because the satellites with high spatial coverage possess lower temporal frequency and vice versa. Also, the cloud covers obscure entire or parts of the scene in an image, making it nearly impossible to obtain continuous coverage of an area. Hence, the spatio-temporal coverage problem may render the satellite estimation method impractical in relevant applications. There are some gap-filling procedures (ANDERSON et al., 2007) and coupling models (RENZULLO et al., 2008) to resolve this issue.

b) *Uncertainties in net radiation estimation:* Net radiation is the key parameter of SEB, which-ever, the net radiation estimation may lead to quantifies the available energy (Rn −G). How- errors due to the ignorance of diurnal variation and phase difference between the diurnal cycles of each individual component (short and long waves). In most of the SEB methods, total Rn flux is considered without the relative functions of direct and diffuse radiation. It is necessary to consider the effects of diffuse radiation than only direct radiation (ROERINK; SU; MENENTI, 2000).

c) *Errors associated with surface temperature retrieved from satellite measurement:* In the case of satellite estimation, most of the methods are using TIR radiation data to derive sur- face temperature. The atmospheric correction and surface emissivity affect the derivation of surface temperature; hence, the uncertainty is associated with the satellite measurement. The surface temperature problem can be corrected using two methods, namely, direct and indirect methods, where the direct method uses the combination of atmospheric sounding and radiative transfer model, but the indirect methods only use the satellite observations. The along-track scanning radiometer (ATSR) observation can improve the estimation by performing the two nearly simultaneous measurements

of brightness temperature from two different view angles. The consideration of both the directional radiometric surface temperature and emissivity on high spectral resolution (NORMAN; KUSTAS; HUMES, 1995) can reduce the uncertainty to some limit.

d) *Inconsistency in satellite estimation models:* Different models are useful for different land surface types and meteorological conditions. To date, there is no universal model, which could be used throughout the world. So, we need the modifications/improvements of the model to estimate SEB components at a global scale, which leads to uncertainties.

e) *Insufficient near-surface meteorological and flux data:* Most of the satellite-based estimation models need near-surface meteorological data. Basically, the data from meteorological stations are obtained at a satellite pixel by spatial interpolation techniques. Different study regions have different climatic and terrain conditions with sparse/irregular meteorological and surface flux measurement stations. Therefore, the accuracy of the interpolation methods should be improved, as well as the ground-based meteorological and flux measurement networks also need further development.

6. CONCLUSIONS

In the last three decades, satellite remote sensing technologies have developed significantly, and the wide availability of satellite data products has enabled researchers to develop a wide spectrum of satellite-based estimation methods and models. From this review work, we have observed that each method and model have its own advantages and disadvantages relative to other approaches, and there is no consensus on which one is the best. These are the important tools for estimating the SEB components at regional and global scales.

Among other methods and parameterization schemes, the use of the hybrid method may achieve a better generalization, which is highly expected for universal applications. Most of the SEB-based models are estimating latent heat or sensible heat fluxes as the residual of SEB by using satellite data and some additional ground-based meteorological data.

However, the accuracy of surface flux estimation using these methods varies from one model to another, one study area to another, and one study period to another. (SU et al., 2005) reported the accuracy of ET value estimated from SEBS was 10–15%

with respect to ground-based measurement, where the EF ranged from 0.5 to 0.9 mm. A maximum relative difference of 8% between measured and estimated EF was observed in the S-SEBI model (ROERINK; SU; MENENTI, 2000). The typical accuracy of SEBAL was tested under several climatic conditions at field scale and it was found to be 85% and 95% at daily and seasonal scales, respectively (BASTIAANSSEN, 2000; BASTIAANSSEN et al., 2005). The SEBAL and SEBS have some limitations over mountainous areas (ALLEN et al., 2011a; CHEN et al., 2013). These limitations can be solved using METRIC and TESEBS models as they consider the slope aspect (ALLEN et al., 2007; AMATYA et al., 2016).

The reviewed methods and models had enough capability for surface flux estimations, there still were some limitations that lead to errors and uncertainties. Therefore, future research can be focused on several directions. Newly developed methods in the acquisition of satellite and ground data are needed to solve the addressed uncertainties and limitations.

Hybrid methods or integration of some methods can be used to take the advantage of their respective merits and limitation compensating. The use of data fusion and data assimilation techniques can be highly useful for integrated estimations. The satellite estimation methods also have a large area to be improved for using the recent high-resolution satellite data as relevant satellite data are rapidly growing.

REFERENCES

ABDULLAH, S. S. et al. Extreme Learning Machines: A new approach for prediction of reference evapotranspiration. **Journal of Hydrology**, v. 527, p. 184–195, 2015.

ALLEN, R. et al. Satellite-based ET estimation in agriculture using SEBAL and METRIC. **Hydrological Processes**, v. 25, n. 26, p. 4011–4027, 2011a.

ALLEN, R. G. et al. **FAO Irrigation and Drainage Paper Nº 56. Crop Evapotranspiration (guidelines for computation crop water requirements)**. Roma: FAO, 1998.

ALLEN, R. G. et al. **The ASCE Standardized Reference Evapotran- spiration Equation**. Reston, VA, USA: ASCE, 2005.

ALLEN, R. G. et al. Satellite-Based Energy Balance for Mapping Evapotranspiration with Internalized Calibration (METRIC)—Applications. **Journal of Irrigation and Drainage Engineering**, v. 133, n. 4, p. 395–406, 2007.

ALLEN, R. G. et al. Evapotranspiration information reporting: I. Factors governing measurement accuracy. **Agricultural Water Management**, v. 98, n. 6, p. 899–920, 2011b.

ALLEN, R. G. et al. Automated calibration of the METRIC-Landsat evapotranspiration process. **Journal of the American Water Resources Association**, v. 49, n. 3, p. 563–576, 2013.

ALLEN, R. G.; TASUMI, M.; TREZZA, R. Satellite-Based Energy Balance for Mapping Evapotranspiration with Internalized Calibration (METRIC)—Model. **Journal of Irrigation and Drainage Engineering**, v. 133, n. 4, p. 380–394, 2007.

AMATYA, P. M. et al. Mapping regional distribution of land surface heat fluxes on the southern side of the central Himalayas using TESEBS. **Theoretical and Applied Climatology**, v. 124, n. 3–4, p. 835–846, 2016.

ANDERSON, M. C. et al. A two-source time-integrated model for estimating surface fluxes using thermal infrared remote sensing. **Remote Sensing of Environment**, v. 60, n. 2, p. 195–216, 1997.

ANDERSON, M. C. et al. A climatological study of evapotranspiration and moisture stress across the continental United States based on thermal remote sensing: 1. Model formulation. **Journal of Geophysical Research Atmospheres**, v. 112, n. 10, p. 1–17, 2007.

AUTOVINO, D.; MINACAPILLI, M.; PROVENZANO, G. Modelling bulk surface resistance by MODIS data and assessment of MOD16A2 evapotranspiration product in an irrigation district of Southern Italy. **Agricultural Water Management**, v. 167, p. 86–94, 2016.

BALDOCCHI, D. D.; XU, L.; KIANG, N. How plant functional-type, weather, seasonal drought, and soil physical properties alter water and energy fluxes of an oak-grass savanna and an annual grassland. **Agricultural and Forest Meteorology**, v. 123, n. 1–2, p. 13–39, 2004.

BASTIAANSSEN, W. G. . SEBAL-based sensible and latent heat fluxes in the irrigated Gediz Basin, Turkey. **Journal of Hydrology**, v. 229, n. 1–2, p. 87–100, mar. 2000.

BASTIAANSSEN, W. G. M. et al. A remote sensing surface energy balance algorithm for land (SEBAL): 2. Validation. **Journal of Hydrology**, v. 212–213, n. 1–4, p. 213–229, 1998a.

BASTIAANSSEN, W. G. M. et al. A remote sensing surface energy balance algorithm for land (SEBAL). 1. Formulation. **Journal of Hydrology**, v. 212–213, n. JANUARY, p. 198–212, dez. 1998b.

BASTIAANSSEN, W. G. M. et al. SEBAL model with remotely sensed data to improve water-resources management under actual field conditions. **Journal of Irrigation and Drainage Engineering**, v. 131, n. 1, p. 85–93, 2005.

BASTIAANSSEN, W. G. M.; MOLDEN, D. J.; MAKIN, I. W. Remote sensing for irrigated agriculture: examples from research and possible applications. **Agricultural Water Management**, v. 46, n. 2, p. 137–155, dez. 2000.

BERTI, A. et al. Assessing reference evapotranspiration by the Hargreaves method in north-eastern Italy. **Agricultural Water Management**, v. 140, p. 20–25, 2014.

BHATTARAI, N. et al. A new optimized algorithm for automating endmember pixel selection in the SEBAL and METRIC models. **Remote Sensing of Environment**, v. 196, p. 178–192, 2017.

BHATTARAI, N.; LIU, T. LandMOD ET mapper: A new matlab-based graphical user

interface (GUI)for automated implementation of SEBAL and METRIC models in thermal imagery. **Environmental Modelling and Software**, v. 118, n. April, p. 76–82, 2019.

BISHT, G. et al. Estimation of the net radiation using MODIS (Moderate Resolution Imaging Spectroradiometer) data for clear sky days. **Remote Sensing of Environment**, v. 97, n. 1, p. 52–67, 2005.

BORGES JÚNIOR, J. C. F. et al. Equação de Hargreaves-Samani calibrada em diferentes bases temporais para Sete Lagoas, MG. **Revista Engenharia na Agricultura**, v. 25, n. 1, p. 38–49, 2017.

BRISSON, N.; SEGUIN, B.; BERTUZZI, P. Agrometeorological soil water balance for crop simulation models. **Agricultural and Forest Meteorology**, v. 59, n. 3–4, p. 267–287, 1992.

BRUTSAERT, W. **Evaporation into the Atmosphere - Theory, History, and Applications**. 1. ed. Dordrecht: Springer, 1982.

BRUTSAERT, W. Catchment-scale evaporation and the atmospheric boundary layer. **Water Resources Research**, v. 22, n. 9 S, p. 39S-45S, 1986.

BURT, C. M. et al. Evaporation research: Review and interpretation. **Journal of Irrigation and Drainage Engineering**, v. 131, n. 1, p. 37–58, 2005.

BUSINGER JA et al. **Flux- profile relationships in the atmospheric surface layerJournal of the Atmospheric Sciences**, 1971.

CARRILLO-ROJAS, G. et al. Dynamic mapping of evapotranspiration using an energy balance-based model over an andean páramo catchment of southern ecuador. **Remote Sensing**, v. 8, n. 2, 2016.

CASELLES, V.; SOBRINO, J. A.; COLL, C. On the use of satellite thermal data for determining evapotranspiration in partially vegetated areas. **International Journal of Remote Sensing**, v. 13, n. 14, p. 2669–2682, 1992.

CHEN, X. et al. Estimation of surface energy fluxes under complex terrain of Mt. Qomolangma over the Tibetan Plateau. **Hydrology and Earth System Sciences**, v. 17, n. 4, p. 1607–1618, 2013.

CHOI, M. et al. Evapotranspiration estimation using the Landsat-5 Thematic Mapper image over the Gyungan watershed in Korea. **International Journal of Remote Sensing**, v. 32, n. 15, p. 4327–4341, 10 ago. 2011.

CHOUDHURY, B. J. Synergism of multispectral satellite observations for estimating regional land surface evaporation. **Remote Sensing of Environment**, v. 49, n. 3, p. 264–274, 1994.

CHOUDHURY, B. J. et al. Relations between evaporation coefficients and vegetation indices studied by model simulations. **Remote Sensing of Environment**, v. 50, n. 1, p. 1–17, 1994.

COAGUILA, D. N. et al. Water productivity using SAFER - Simple Algorithm for Evapotranspiration Retrieving in watershed. **Revista Brasileira de Engenharia Agrícola e Ambiental**, v. 21, n. 8, p. 524–529, 2017.

DARSHANA; PANDEY, A.; PANDEY, R. P. Analysing trends in reference evapotranspiration and weather variables in the Tons River Basin in Central India. **Stochastic Environmental Research and Risk Assessment**, v. 27, n. 6, p. 1407–1421,

2013.

DAUGHTRY, C. S. T. et al. Spectral estimates of net radiation and soil heat flux. **Remote Sensing of Environment**, v. 32, n. 2–3, p. 111–124, 1990.

DE OLIVEIRA FERREIRA SILVA, C.; HERIBERTO DE CASTRO TEIXEIRA, A.; LILLA MANZIONE, R. agriwater: An R package for spatial modelling of energy balance and actual evapotranspiration using satellite images and agrometeorological data. **Environmental Modelling & Software**, v. 120, n. February, p. 104497, out. 2019.

DINPASHOH, Y. et al. Trends in reference crop evapotranspiration over Iran. **Journal of Hydrology**, v. 399, n. 3–4, p. 422–433, 2011.

DROOGERS, P.; IMMERZEEL, W. W.; LORITE, I. J. Estimating actual irrigation application by remotely sensed evapotranspiration observations. **Agricultural Water Management**, v. 97, n. 9, p. 1351–1359, 2010.

ENGMAN, E. T.; GURNEY, R. J. **Remote Sensing in Hydrology**. London, UK: Chapman and Hall, 1991.

FARAHANI, H. J. et al. EVAPOTRANSPIRATION: PROGRESS IN MEASUREMENT AND MODELING IN AGRICULTURE. **Transactions Of The Asabe**, v. 50, n. 5, p. 1627–1638, 2007.

FRENCH, A. N.; HUNSAKER, D. J.; THORP, K. R. Remote sensing of evapotranspiration over cotton using the TSEB and METRIC energy balance models. **Remote Sensing of Environment**, v. 158, p. 281–294, mar. 2015.

GAO, W. et al. Estimating clear-sky regional surface fluxes in the southern great plains atmospheric radiation measurement site with ground measurements and satellite observations. **Journal of Applied Meteorology**, v. 37, n. 1, p. 5–22, 1998.

GOWDA, P. H. et al. **SEBAL for Estimating Hourly ET Fluxes over Irrigated and Dryland Cotton during BEAREX08**. World Environmental and Water Resources Congress 2011. **Anais**...Reston, VA: American Society of Civil Engineers, 19 maio 2011Disponível em: <http://ascelibrary.org/doi/10.1061/41173%28414%29290>

GURNEY, R. J.; CAMILLO, P. J. MODELLING DAILY EVAPOTRANSPIRATION USING REMOTELY SENSED DATA. **Journal of Hydrology**, v. 69, p. 305–324, 1984.

HATFIELD, J. L.; PERRIER, A.; JACKSON, R. D. Estimation of evapotranspiration at one time-of-day using remotely sensed surface temperatures. **Agricultural Water Management**, v. 7, n. 1–3, p. 341–350, 1983.

HOOGEVEEN, J. et al. GlobWat - A global water balance model to assess water use in irrigated agriculture. **Hydrology and Earth System Sciences**, v. 19, n. 9, p. 3829–3844, 2015.

IDSO, S. B. et al. The utility of surface temperature measurements for the remote sensing of surface soil water status. **Journal of Geophysical Research**, v. 80, n. 21, p. 3044–3049, 1975.

IRMAK, S. et al. Trend and magnitude of changes in climate variables and reference evapotranspiration over 116-yr period in the Platte River Basin, central Nebraska-USA. **Journal of Hydrology**, v. 420–421, p. 228–244, 2012.

ISHAK, A. M. et al. Estimating reference evapotranspiration using numerical weather

modelling. **Hydrological Processes**, v. 24, n. 24, p. 3490–3509, 2010.

JACKSON, R. D. et al. Canopy temperature as a crop water stress indicator. **Water Resources Research**, v. 17, n. 4, p. 1133–1138, 1981.

JACKSON, R. D. et al. Estimation of daily evapotranspiration from one time-of-day measurements. **Agricultural Water Management**, v. 7, n. 1–3, p. 351–362, 1983.

JACKSON, R. D. Evaluating Evapotranspiration at Local and Regional Scales. **Proceedings of the IEEE**, v. 73, n. 6, p. 1086–1096, 1985.

JHAJHARIA, D. et al. Trends in temperature over Godavari River basin in Southern Peninsular India. **International Journal of Climatology**, v. 34, n. 5, p. 1369–1384, 2014.

KUSTAS, W. P.; DAUGHTRY, C. S. T. Estimation of the soil heat flux/net radiation ratio from spectral data. **Agricultural and Forest Meteorology**, v. 49, n. 3, p. 205–223, 1990.

KUSTAS, W. P.; NORMAN, J. M. Use of remote sensing for evapotranspiration monitoring over land surfaces. **Hydrological Sciences Journal**, v. 41, n. 4, p. 495–516, 1996.

LAWRENCE, D. M. et al. The partitioning of evapotranspiration into transpiration, soil evaporation, and canopy evaporation in a GCM: Impacts on land-atmosphere interaction. **Journal of Hydrometeorology**, v. 8, n. 4, p. 862–880, 2007.

LEI, H.; YANG, D. Interannual and seasonal variability in evapotranspiration and energy partitioning over an irrigated cropland in the North China Plain. **Agricultural and Forest Meteorology**, v. 150, n. 4, p. 581–589, 2010.

LEWIS, C. S.; ALLEN, L. N. Potential crop evapotranspiration and surface evaporation estimates via a gridded weather forcing dataset. **Journal of Hydrology**, v. 546, p. 450–463, 2017.

LI, F.; LYONS, T. J. Estimation of regional evapotranspiration through remote sensing. **Journal of Applied Meteorology**, v. 38, n. 11, p. 1644–1654, 1999.

LI, Z. L. et al. A review of current methodologies for regional Evapotranspiration estimation from remotely sensed data. **Sensors**, v. 9, n. 5, p. 3801–3853, 2009.

LIAGHAT, S.; BALASUNDRAM, S. K. A Review: The Role of Remote Sensing in Precision Agriculture S. Liaghat and S.K. Balasundram Department of Agriculture Technology, Faculty of Agriculture, University Putra Malaysia, 43400 Serdang, Selangor, Malaysia. **Agriculture**, v. 5, n. 1, p. 50–55, 2010.

LOSGEDARAGH, S. Z.; RAHIMZADEGAN, M. Evaluation of SEBS, SEBAL, and METRIC models in estimation of the evaporation from the freshwater lakes (Case study: Amirkabir dam, Iran). **Journal of Hydrology**, v. 561, p. 523–531, jun. 2018.

MA, W. et al. Evaluation of SEBS for estimation of actual evapotranspiration using ASTER satellite data for irrigation areas of Australia. **Theoretical and Applied Climatology**, v. 112, n. 3–4, p. 609–616, 2013.

MADUGUNDU, R. et al. Performance of the METRIC model in estimating evapotranspiration fluxes over an irrigated field in Saudi Arabia using Landsat-8 images. **Hydrology and Earth System Sciences**, v. 21, n. 12, p. 6135–6151, 5 dez. 2017.

MARTÍ, P. et al. Parametric expressions for the adjusted Hargreaves coefficient in Eastern Spain. **Journal of Hydrology**, v. 529, p. 1713–1724, 2015.

MAUSER, W.; SCHÄDLICH, S. Modelling the spatial distribution of evapotranspiration on different scales using remote sensing data. **Journal of Hydrology**, v. 212–213, n. 1–4, p. 250–267, 1998.

MCCABE, M. F.; WOOD, E. F. Scale influences on the remote estimation of evapotranspiration using multiple satellite sensors. **Remote Sensing of Environment**, v. 105, n. 4, p. 271–285, 2006.

MCNIDER, R. T. et al. An integrated crop and hydrologic modeling system to estimate hydrologic impacts of crop irrigation demands. **Environmental Modelling and Software**, v. 72, p. 341–355, 2015.

MENENTI, M.; CHOUDHURY, B. J. **Parameterization of land surface evaporation by means of location dependent potential evaporation and surface temperature range**. Exchange processes at the land surface for a range of space and time scales. Proc. international symposium, Yokohama, 1993. **Anais**...1993

MINACAPILLI, M. et al. Using scintillometry to assess reference evapotranspiration methods and their impact on the water balance of olive groves. **Agricultural Water Management**, v. 170, p. 49–60, 2016.

MORAN, M. S. et al. Mapping surface energy balance components by combining landsat thematic mapper and ground-based meteorological data. **Remote Sensing of Environment**, v. 30, n. 1, p. 77–87, 1989.

MULLA, D. J. Twenty five years of remote sensing in precision agriculture: Key advances and remaining knowledge gaps. **Biosystems Engineering**, v. 114, n. 4, p. 358–371, 2013.

NEGM, A.; JABRO, J.; PROVENZANO, G. Assessing the suitability of American National Aeronautics and Space Administration (NASA) agro-climatology archive to predict daily meteorological variables and reference evapotranspiration in Sicily, Italy. **Agricultural and Forest Meteorology**, v. 244–245, n. October 2016, p. 111–121, 2017.

NORMAN, J. M.; ANDERSON, M. C.; KUSTAS, W. P. Are single-source, remote-sensing surface-flux models too simple? **AIP Conference Proceedings**, v. 852, n. 1, p. 170–177, 2006.

NORMAN, J. M.; KUSTAS, W. P.; HUMES, K. S. Source approach for estimating soil and vegetation energy fluxes in observations of directional radiometric surface temperature. **Agricultural and Forest Meteorology**, v. 77, n. 3–4, p. 263–293, 1995.

OCHEGE, F. U. et al. Mapping evapotranspiration variability over a complex oasis-desert ecosystem based on automated calibration of Landsat 7 ETM+ data in SEBAL. **GIScience and Remote Sensing**, v. 56, n. 8, p. 1305–1332, 2019.

OPOKU-DUAH, S.; DONOGHUE, D.; BURT, T. Intercomparison of Evapotranspiration Over the Savannah Volta Basin in West Africa Using Remote Sensing Data. **Sensors**, v. 8, n. 4, p. 2736–2761, 17 abr. 2008.

PAULSON, C. A. **The Mathematical Representation of Wind Speed and Temperature Profiles in the Unstable Atmospheric Surface LayerJournal of Applied Meteorology**, 1970.

PEREIRA, L. S. et al. Crop evapotranspiration estimation with FAO56: Past and future. **Agricultural Water Management**, v. 147, p. 4–20, 2015.

PETKOVIĆ, D. et al. Determination of the most influential weather parameters on reference evapotranspiration by adaptive neuro-fuzzy methodology. **Computers and Electronics in Agriculture**, v. 114, p. 277–284, jun. 2015.

PÔÇAS, I. et al. Satellite-based evapotranspiration of a super-intensive olive orchard: Application of METRIC algorithms. **Biosystems Engineering**, v. 128, p. 69–81, dez. 2014.

PRICE, J. C. On the Use of Satellite Data to Infer Surface Fluxes at Meteorological Scales. **Journal of Applied Meteorology**, v. 21, p. 1111–1121, 1982.

PROVENZANO, G.; SINOBAS, L. R. Special issue on trends and challenges of sustainable irrigated agriculture. **Journal of Irrigation and Drainage Engineering**, v. 140, n. 9, p. 1–3, 2014.

RAHIMZADEGAN, M.; JANANI, A. Estimating evapotranspiration of pistachio crop based on SEBAL algorithm using Landsat 8 satellite imagery. **Agricultural Water Management**, v. 217, n. August 2018, p. 383–390, maio 2019.

RALLO, G. et al. Improvement of FAO-56 model to estimate transpiration fluxes of drought tolerant crops under soil water deficit: Application for olive groves. **Journal of Irrigation and Drainage Engineering**, v. 140, n. 9, 2014a.

RALLO, G. et al. Detecting crop water status in mature olive groves using vegetation spectral measurements. **Biosystems Engineering**, v. 128, n. 0, p. 52–68, 2014b.

RANA, G.; KATERJI, N. Measurement and estimation of actual evapotranspiration in the field under Mediterranean climate: A review. **European Journal of Agronomy**, v. 13, n. 2–3, p. 125–153, 2000.

RANGO, A. Application of remote sensing methods to hydrology and water resources. **Hydrological Sciences Journal**, v. 39, n. 4, p. 309–320, 1994.

REGINATO, R. J.; JACKSON, R. D.; PINTER, P. J. Evapotranspiration calculated from remote multispectral and ground station meteorological data. **Remote Sensing of Environment**, v. 18, n. 1, p. 75–89, 1985.

RENZULLO, L. J. et al. Multi-sensor model-data fusion for estimation of hydrologic and energy flux parameters. **Remote Sensing of Environment**, v. 112, n. 4, p. 1306–1319, 2008.

RODRIGUES, T. R. et al. Seasonal variation in energy balance and canopy conductance for a tropical savanna ecosystem of south central Mato Grosso, Brazil. **Journal of Geophysical Research: Biogeosciences**, v. 119, n. 1, p. 1–13, 2014.

ROERINK, G. J.; SU, Z.; MENENTI, M. S-SEBI: A simple remote sensing algorithm to estimate the surface energy balance. **Physics and Chemistry of the Earth, Part B: Hydrology, Oceans and Atmosphere**, v. 25, n. 2, p. 147–157, 2000.

SASEENDRAN, S. A. et al. Developing and normalizing average corn crop water production functions across years and locations using a system model. **Agricultural Water Management**, v. 157, p. 65–77, 2015.

SAWANO, S. et al. Development of a simple forest evapotranspiration model using a process-oriented model as a reference to parameterize data from a wide range of environmental conditions. **Ecological Modelling**, v. 309–310, p. 93–109, ago. 2015.

SCOTT, R. L. et al. Partitioning of evapotranspiration and its relation to carbon dioxide exchange in a Chihuahuan Desert shrubland. **Hydrological Processes**, v. 20, n. 15, p. 3227–3243, 15 out. 2006.

SENAY, G. B. et al. A coupled remote sensing and simplified surface energy balance approach to estimate actual evapotranspiration from irrigated fields. **Sensors**, v. 7, n. 6, p. 979–1000, 2007.

SENAY, G. B. et al. Operational Evapotranspiration Mapping Using Remote Sensing and Weather Datasets: A New Parameterization for the SSEB Approach. **Journal of the American Water Resources Association**, v. 49, n. 3, p. 577–591, 2013.

SENAY, G. B. et al. Evaluating Landsat 8 evapotranspiration for water use mapping in the Colorado River Basin. **Remote Sensing of Environment**, v. 185, p. 171–185, 2016.

SHEN, Y. et al. Energy/water budgets and productivity of the typical croplands irrigated with groundwater and surface water in the North China Plain. **Agricultural and Forest Meteorology**, v. 181, p. 133–142, 2013.

SHUTTLEWORTH, W. J. Putting the "vap" into evaporation. **Hydrology and Earth System Sciences**, v. 11, n. 1, p. 210–244, 2007.

SINGH, R. K. et al. Application of SEBAL Model for Mapping Evapotranspiration and Estimating Surface Energy Fluxes in South-Central Nebraska. **Journal of Irrigation and Drainage Engineering**, v. 134, n. 3, p. 273–285, jun. 2008.

SOER, G. J. R. Estimation of regional evapotranspiration and soil moisture conditions using remotely sensed crop surface temperatures. **Remote Sensing of Environment**, v. 9, n. 1, p. 27–45, 1980.

SU, H. et al. Modeling evapotranspiration during SMACEX: Comparing two approaches for local- and regional-scale prediction. **Journal of Hydrometeorology**, v. 6, n. 6, p. 910–922, 2005.

SU, Z. The Surface Energy Balance System (SEBS) for estimation of turbulent heat fluxes. **Hydrology and Earth System Sciences**, v. 6, n. 1, p. 85–99, 2002.

SUYKER, A. E.; VERMA, S. B. Interannual water vapor and energy exchange in an irrigated maize-based agroecosystem. **Agricultural and Forest Meteorology**, v. 148, n. 3, p. 417–427, 2008.

TABARI, H.; GRISMER, M. E.; TRAJKOVIC, S. Comparative analysis of 31 reference evapotranspiration methods under humid conditions. **Irrigation Science**, v. 31, n. 2, p. 107–117, 2013.

TAGLIAFERRE, C. et al. Influência dos Elementos Meteorológicos na Evapotranspiração de Referência Estimada Utilizando-se o Irrigâmetro no Município de Guanambi-BA. **Revista Engenharia na Agricultura - REVENG**, v. 23, n. 3, p. 251–260, 30 jun. 2015.

TANNY, J. Microclimate and evapotranspiration of crops covered by agricultural screens: A review. **Biosystems Engineering**, v. 114, n. 1, p. 26–43, 2013.

TEIXEIRA, A. H. D. C. et al. Use of MODIS images to quantify the radiation and energy balances in the Brazilian Pantanal. **Remote Sensing**, v. 7, n. 11, p. 14597–14619, 2015.

TEIXEIRA, A. H. DE C. et al. Reviewing SEBAL input parameters for assessing evapotranspiration and water productivity for the Low-Middle São Francisco River

basin, Brazil. **Agricultural and Forest Meteorology**, v. 149, n. 3–4, p. 477–490, mar. 2009.

TEIXEIRA, A. H. DE C. Determining Regional Actual Evapotranspiration of Irrigated Crops and Natural Vegetation in the São Francisco River Basin (Brazil) Using Remote Sensing and Penman-Monteith Equation. **Remote Sensing**, v. 2, n. 5, p. 1287–1319, 6 maio 2010.

TEIXEIRA, A. H. DE C. et al. Large-Scale Water Productivity Assessments with MODIS Images in a Changing Semi-Arid Environment: A Brazilian Case Study. **Remote Sensing**, v. 5, n. 11, p. 5783–5804, 6 nov. 2013.

TEIXEIRA, A. H. DE C. et al. Large-scale radiation and energy balances with Landsat 8 images and agrometeorological data in the Brazilian semiarid region. **Journal of Applied Remote Sensing**, v. 11, n. 1, p. 016030, 2017.

TIMMERMANS, W. J. et al. An intercomparison of the Surface Energy Balance Algorithm for Land (SEBAL) and the Two-Source Energy Balance (TSEB) modeling schemes. **Remote Sensing of Environment**, v. 108, n. 4, p. 369–384, 2007.

TIMOUK, F. et al. Response of surface energy balance to water regime and vegetation development in a Sahelian landscape. **Journal of Hydrology**, v. 375, n. 1–2, p. 178–189, 2009.

TREZZA, R.; ALLEN, R.; TASUMI, M. Estimation of Actual Evapotranspiration along the Middle Rio Grande of New Mexico Using MODIS and Landsat Imagery with the METRIC Model. **Remote Sensing**, v. 5, n. 10, p. 5397–5423, 23 out. 2013.

VERSTRAETEN, W. W.; VEROUSTRAETE, F.; FEYEN, J. Estimating evapotranspiration of European forests from NOAA-imagery at satellite overpass time: Towards an operational processing chain for integrated optical and thermal sensor data products. **Remote Sensing of Environment**, v. 96, n. 2, p. 256–276, 2005.

VUOLO, F. et al. Satellite-based irrigation advisory services: A common tool for different experiences from Europe to Australia. **Agricultural Water Management**, v. 147, p. 82–95, 2015.

WEBB, E. K. Profile relationships: The log-linear range, and extension to strong stability. **Quarterly Journal of the Royal Meteorological Society**, v. 96, n. 407, p. 67–90, 1970.

WILCOX, B. P.; BRESHEARS, D. D.; SEYFRIED, M. S. Water balance on rangelands. In: STEWART, B. A.; HOWELL, T. A. (Eds.). . **Encyclopedia of Water Science**. [s.l.] Marcel Dekker, 2003. p. 791–794.

WILFRIED, B. On a Derivable Formula for Long-Wave Radiation From Clear Skies FLD). **Water Resources Research**, v. 11, n. 5, p. 742–744, 1975.

REMOTE EVAPOTRANSPIRATION ESTIMATION IN COFFEE CROP UNDER DIFFERENT IRRIGATION MANAGEMENT USING THE METRIC ALGORITHM

Marcus Andre Braido Pinheiro, Marcelo de Carvalho Alves, João Marcos Louzada

ABSTRACT

Brazil is the world's largest producer of coffee, with a share of 32% of world production, with Arabica coffee responsible for the majority of production. In order to keep on top of production, the monitoring of several variables assumes importance for a continuous production gain, we have the highlight of evapotranspiration (ET), important for managing different crops. This work aimed to apply the METRIC algorithm to quantify the actual evapotranspiration (ETa) in three different irrigation management and to validate the accuracy of the algorithm in coffee plantations in the municipality of Carmo do Rio Claro, MG, Brazil. METRIC methodology was applied for the calculation of ETa in different coffee irrigation systems, Dryland, Central Pivot, Self-propelled and Dripping. NDVI and NDWI maps were generated. After the calculation, the results were evaluated by performance measurement criteria, Nash-Sutcliffe Efficiency (EF), Root Mean Square Error (RMSE), Mean Absolute Error (MAE), and Coefficient of Determination (R^2), there was also spatialization of the values of ETa, Latent Heat Flux (LE), Land Surface Temperature (LST), albedo, NDVI and NDWI for the management. Based on the results, a good accuracy of the METRIC algorithm was observed in the estimation of evapotranspiration when compared to the meteorological station ET method, thus providing important information for data entry in the water balance for the determination of irrigation projects. It was also observed a good correspondence between the studied variables, showing a relationship between ETa, NDVI, and NDWI.

KEYWORDS: Energy Balance, Landsat 8, Irrigation Management, *Coffea Arabica* L.

1. INTRODUCTION

Brazil in 2018, according to estimates by the Companhia Nacional de Abastecimento (CONAB, 2019), obtained 61.66 million bags of coffee, distributed over an area of 1.86 million hectares. Irrigated agriculture can be a crucial factor in maintaining high levels of productivity under water stress situations and due to climatic anomalies.

Thus, with the increased application of irrigation in agriculture, there is a need to improve irrigation management and to develop the adoption of sustainable irrigation management practices. So, when it comes to coffee cultivation, irrigation is an important tool that helps increase productivity.

In irrigation management, evapotranspiration (ET) is of great importance in the management of water resources. The calculation of ET is performed empirically through the standard FAO Penman-Monteith equation (ALLEN et al., 1998) and experimentally with high accuracy using the Eddy correlation method (KIZER; ELLIOTT, 1991), Bowen 's ratio, and weighing lysimeters (GEBLER et al., 2015; WRIGHTL, 1991) and by a variety of methods.

ET is a vital component for describing the hydrological cycle in ecological systems, estimating water balance, agricultural zoning, and design of irrigation and drainage systems (BERTI et al., 2014; BORGES JÚNIOR et al., 2017). The term evapotranspiration is understood as a process comprising the loss of water to the atmosphere by evaporation of water present in the soil and transpiration of plants (ALENCAR et al., 2011; MELO; FERNANDES, 2012).

However, the methods can only determine the ET rate at a single point or a small area and may not extend to large areas. Therefore, there are ET estimation models that can be used to overcome such limitations. Among these estimation models, satellite images can be used to determine ET in large areas, promoting the spatialization of the parameter. More broadly, models for estimating ET from satellite imagery provide an accurate estimate of ET in large areas using minimal weather data and applying various algorithms (ALLEN; TASUMI; TREZZA, 2007; ANDERSON et al., 2012; BASTIAANSSEN; CHANDRAPALA, 2003).

Among the several algorithms that perform the estimation of evapotranspiration using remote sensing, stands out the *Mapping Evapotranspiration at high Resolution and with Internalized Calibration* (METRIC) (ALLEN; TASUMI; TREZZA, 2007). The model has been successfully implemented in several homogeneous ecosystems

around the world, with different levels of accuracy (ALLEN et al., 2013; BHATTARAI et al., 2017; CHOI et al., 2011; FRENCH; HUNSAKER; THORP, 2015; LOSGEDARAGH; RAHIMZADEGAN, 2018; MADUGUNDU et al., 2017; PÔÇAS et al., 2014; TREZZA; ALLEN; TASUMI, 2013). However, the best and most appropriate choice of a method for monitoring and quantifying ET is still a challenge, as there is a shortage of spatially validated data, especially for irrigation schemes in developing countries.

Considering that there are rapid changes in atmospheric environmental conditions and based on the hypothesis that evapotranspiration (ET) can be spatialized in coffee plantations for better crop management, this work aimed to apply the METRIC algorithm to quantify ET in four different irrigation management and validate the accuracy of the algorithm in the municipality of Carmo do Rio Claro, Minas Gerais, Brazil.

2. MATERIAL AND METHODS

2.1. Study area

The study area is located in the municipality of Carmo do Rio Claro, in the state of Minas Gerais, Brazil, with an altitude of 798 m, latitude 20°58'17" S and longitude 46°7'57" W (Figure 1). The climate of the municipality is classified as subtropical mesothermic (Cwa), according to the Köppen-Geiger classification, and characterized by dry winters and humid summers (PEEL; FINLAYSON; MCMAHON, 2007).

The coffee cultivated in the study areas is *Coffea arabica* L., cultivar Acaiá 474/19, and cultivated under different irrigation systems.

In 2012, the area under a dryland system had 30 hectares, 6 years, 3.6 m per 0.7 m spacing, and density of 3,968 plants.ha^{-1}, was cut into the ground in September 2013. The area under the self-propelled irrigation system had 2.6 ha, 7 years, spacing of 3.5 m per 0.7 m, and density of 4,081 plants.ha^{-1}. The area under the drip irrigation system had 11 ha, 2.5 years, the spacing of 3.6 m per 0.7 m and density of 3,968 plants.ha^{-1}. The area under the central pivot irrigation had 17 ha, 10 years, 4.0 m per 0.5 m spacing, and density of 5,000 plants.ha^{-1}.

Irrigation was performed throughout the year according to the water requirement of the plants, calculated based on the measurement of tensiometers.

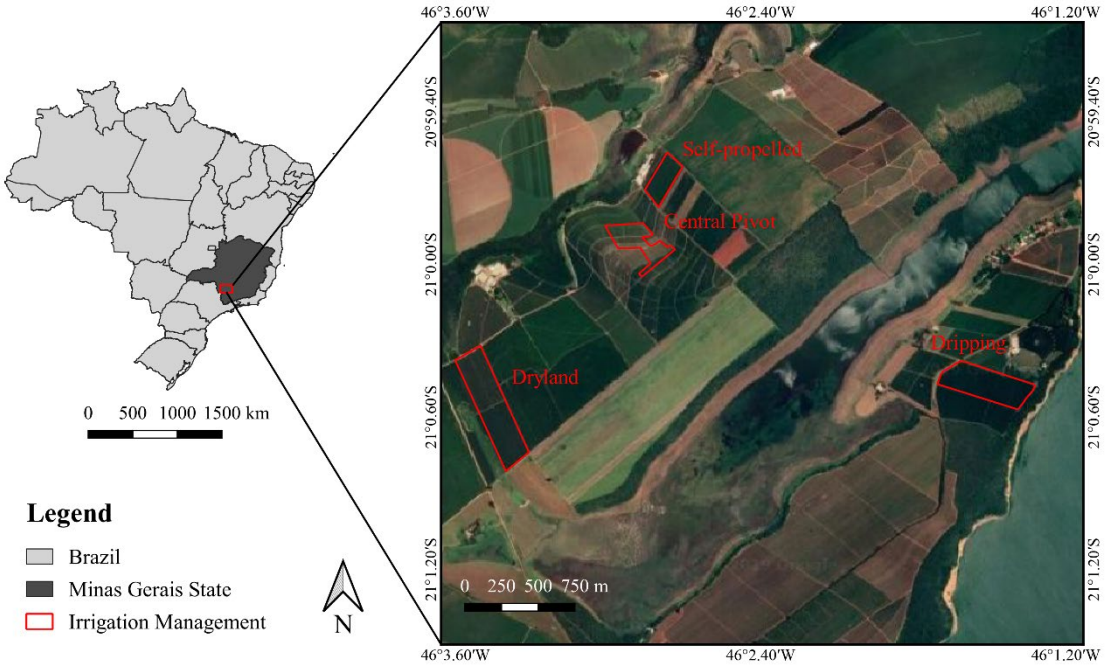

Figure 1 - Region of Carmo do Rio Claro, Minas Gerais State, with different irrigation management.

2.2. Data Used

2.2.1. Orbital Data

For the development of the study, 10 images acquired from the Landsat 8 satellite (OLI-/-TIRS) were used during the grain filling period of coffee beans from 2013 to 2019 (Table 1), according (CAMARGO; CAMARGO, 2001; PEREIRA; CAMARGO; CAMARGO, 2008). The images were acquired from the United States Geological Survey (USGS, 2013) through the Earth Explorer platform. The criteria for image selection was no cloud presence in the study areas. All the images were in path 219 and rows 74 and 75. Level 1 and Level 2 images were acquired, without atmospheric correction with the digital numbers of pixels and already with the LaSRC atmospheric correction (VERMOTE et al., 2018), respectively.

Images of the Shuttle Radar Topography Mission (SRTM), Arc-Second Global 1, were acquired from the grids: S21W046V3, S21W047V3, S22W046V3, and S22W047V3, also acquired from USGS, through the Earth Explorer platform.

Table 1 - Satellite images used to calculate METRIC.

Image number	Date	Day of the Year (DOY)
1	20/11/2013	324
2	15/05/2014	135
3	07/11/2014	311
4	10/01/2015	10
5	04/05/2016	125
6	30/12/2016	365
7	08/06/2017	159
8	10/05/2018	130
9	10/03/2019	69
10	14/06/2019	165

2.2.2. *In situ* measurements

The meteorological data used in the study were obtained from an automatic weather station present in the municipal district of Passos, Minas Gerais, Brazil. The data were provided by the Instituto Nacional de Meteorologia - INMET. The station is located at latitude coordinates 20º44'42.853" S and longitude 46º 38' 2.098" W, with an altitude of 782 meters and 67 kilometers away from the study area (Figure 2).

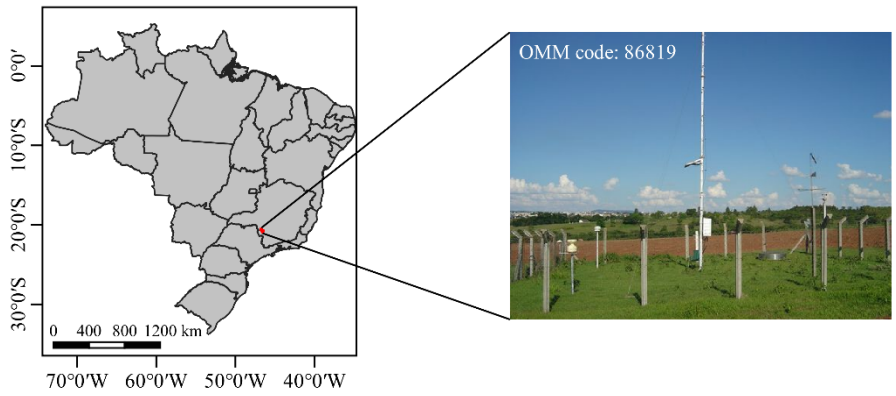

Figure 2 - Description of Meteorological Station in municipality of Passos – MG.

2.3. METRIC Methodology

After the acquisition of Landsat 8 images, SRTM, and meteorological station data. We used the Water package (OLMEDO et al., 2016) present in the software R for

the application of the METRIC algorithm. When the data were read by the software, the methodology proposed by (ALLEN; TASUMI; TREZZA, 2007) was started.

METRIC is a model that has been gaining scientific recognition in recent years. The model is based on principles and techniques used by the SEBAL model (BASTIAANSSEN et al., 1998). In particular, METRIC is automatically calibrated for each image using a soil-based calculation and reference evapotranspiration (ET_0), which is obtained based on hourly weather data. The METRIC algorithm was developed exclusively to estimate ET from Landsat data (ALLEN; TASUMI; TREZZA, 2007).

During the calculation of ET by the METRIC algorithm, surface characteristics such as albedo, vegetation indices, emissivity, and surface temperature were estimated as intermediate products. Anchor pixels (hot and cold) were selected and energy components such as net radiation (Rn), soil heat flux (G), and sensible heat flux (H) were also estimated.

Finally, the latent heat flux (LE) (Equation 1) was predicted as a residue of the surface radiation balance (ALLEN et al., 2007; ALLEN; TASUMI; TREZZA, 2007). Consequently, the instant ET (ETinst) for each pixel was calculated. In addition, the leaf area index (LAI) was obtained and the reference evapotranspiration (ET_0) was used as a factor for METRIC-based ET (ET_{METRIC}) estimation.

$$LE = R_n - G - H \quad (1)$$

The first step in the METRIC model was to calculate the net radiation (Rn) using the surface radiation balance (Equation 2). The Rn estimation was performed in a series of steps, adding short-wave liquid radiation and long-wave liquid radiation (ALLEN; TASUMI; TREZZA, 2007; BRUNSELL; GILLIES, 2002; HIPPS, 1989).

$$R_n = R_{s\downarrow} - \alpha R_{s\downarrow} - R_{L\downarrow} - R_{L\uparrow} - \left(1 - \varepsilon_o\right) R_{L\downarrow} \quad (2)$$

Where $R_{S\downarrow}$ is the short-wave input radiation ($W.m^{-2}$), α is the broadband surface albedo (dimensionless), and $R_{L\downarrow}$ and $R_{L\uparrow}$ are the long-wave radiation entering and exiting the atmosphere ($W.m^{-2}$), respectively. εo is the thermal emissivity of the wide-band surface (dimensionless). The term (1-εo) $R_{L\downarrow}$ represents the fraction of the received long-wave radiation reflected from the surface.

The received bandwidth and the short-wave radiation ($R_{S\downarrow}$), which represents the main energy source for ET, are calculated for the Landsat-8 image over time as a constant for the whole image, assuming clear sky conditions as Equation 3.

$$R_{S\downarrow} = \frac{G_{SC} \cos\theta_{ref} \tau_{SW}}{d^2} \quad (3)$$

Where G_{SC} is the solar constant (1367 W.m^{-2}), θ_{ref} is the angle of solar incidence, τ_{sw} is the broadband atmospheric transmissivity, and d^2 is the square of the relative of the Earth-Sun distance.

The τ_{sw} is calculated using Equation 4, which was elaborated on (ALLEN et al., 2005).

$$\tau_{SW} = 0,35 + 0,627 \exp\left[\frac{-0,00146P}{K_t \cos Z} - 0,075\left(\frac{W}{\cos Z}\right)^{0,4}\right] \quad (4)$$

Where P is the atmospheric pressure (kPa), W is the amount of water present in the atmosphere (mm), Z is the zenith solar angle (extracted from the image metadata) and K_t is the air turbidity coefficient (K_t = 1.0 for clean air and 0.5 for extremely polluted air, in this study K_t = 1.0).

P and W are calculated using the vapor pressure measured or estimated near the surface, according to Equations 5 and 6, according to (ALLEN et al., 2005; GARRISON; ADLER, 1990), respectively.

$$P = 101,3\left(\frac{293 - 0,0065_z}{293}\right)^{5,26} \quad (5)$$

$$W = 0,14 e_a P_{air} + 2,1 \quad (6)$$

Where the constant 293 is the standard air temperature (K), z is the elevation above sea level (m), and ea is the vapor pressure near the surface (kPa).

The parameter d^2 was calculated from Equation 7, as a function of the DOY, as described in (DUFFIE; BECKMAN, 2013).

$$d^2 = \frac{1}{1 + 0,033\cos\left(\frac{DOY\,2\pi}{365}\right)} \quad (7)$$

The broadband surface albedo (α), however, is calculated using Equation 8 as described in (BASTIAANSSEN et al., 1998; ZHONG; YINHAI, 1988).

$$\alpha = \frac{\left(\alpha_{toa} - \alpha_{atm}\right)}{\tau_{SW}^2} \quad (8)$$

Where α_{toa} is the planetary albedo of each pixel; The atmospheric albedo of α_{atm} and τ_{sw} are obtained from equation 4, following (SILVA et al., 2016).

The Long-wave Radiation Output (RL↑) radiation emitted from the surface is driven by surface temperature and surface emissivity. The RL↑ is calculated using the Stefan-Boltzmann equation (Equation 9).

$$R_{L\uparrow} = \varepsilon_o \sigma T_s^4 \tag{9}$$

Where ε_o is the broadband emissivity (dimensionless), σ is the Stefan-Boltzmann constant ($5{,}67 \times 10^{-8}$ W.m^{-2} K^{-4}) and Ts is the surface temperature (K).

In this study, Ts was counted as LST and obtained from Equation 10.

$$LST = TB_{10} + C_1\left(TB_{10} - TB_{11}\right) + C_2\left(TB_{10} - TB_{11}\right)^2 + C_0 + \left(C_3 + C_4 W\right) \left(1-\varepsilon\right) + \left(C_5 + C_6 W\right)\Delta\varepsilon \tag{10}$$

Where LST is the surface temperature of the earth (K), C_0=-0,268; C_1=1,378; C_2=0,183; C_3=54,3; C_4=-2,238; C_5=-129,2; C_6=16,4, TB10, and TB11 are the brightness temperatures of bands 10 and 11 of Landsat 8 (K), ε is the average LSE of TIRS bands, W is the atmospheric water vapor content, and Δε is the difference in LSE.

The brightness temperature (TB) was calculated using Equation 11.

$$TB = \frac{K_2}{Ln\left(\frac{K_1}{L_\lambda} + 1\right)} \tag{11}$$

Where K_1 = 1321,08 e 1201,14 for bands 10 and 11 respectively, and K_2= 777,89 e 480,89 for bands 10 and 11 respectively, and L_λ is the spectral radiance of the top of the atmosphere.

This spectral radiance at the top of the atmosphere was determined by multiplying the multiplicative scaling factors of Equation 12.

$$L_\lambda = M_L \times Q_{cal} + A_L \tag{12}$$

Where M_L= 0,000342, Q_{cal} is the image of band 10 or 11, and A_L = 0,1

Subsequently, the Land Surface Emissivity (LSE) was calculated using Equation 13. The ε_s = 0,971; 0,977 and ε_v = 0,987; 0,989 are values of soil and vegetation emissivity of bands 10 and 11, respectively.

$$LSE = \varepsilon_s\left(1 - FVC\right) + \varepsilon_v FVC \tag{13}$$

Where Fractional plant cover (FVC) was estimated based on the Normalized Difference Vegetation Index (NDVI) obtained in the experimental area by Equation 14.

$$FVC = \frac{NDVI - NDVI_s}{NDVI_v - NDVI_s} \tag{14}$$

Where the NDVIs and NDVIv are the NDVI reclassified to the areas of soil and vegetation, respectively.

After generating LSE for both TIRS bands, the mean and difference of LSE were obtained according to Equations 15 and 16.

$$\varepsilon = \frac{\varepsilon_{10} - \varepsilon_{11}}{2} \quad (15)$$

$$\Delta\varepsilon = \varepsilon_{10} - \varepsilon_{11} \quad (16)$$

Surface emissivity was calculated using Equation 17 after (TASUMI; ALLEN; TREZZA, 2008) based on vegetative and ground thermal emissivity. The LAI was calculated according to Equation 18 proposed by (BASTIAANSSEN et al., 1998).

$$\varepsilon_0 = 0,95 + 0,01LAI \quad \text{para LAI} \leq 3 \quad (17)$$

$$LAI = \frac{-\ln\left[\frac{(0,69 - SAVI)}{0,59}\right]}{0,91} \quad (18)$$

Soil adjusted vegetation index (SAVI) was calculated based on the TOA reflectance of bands 4 and 5 according to (HUETE, 1988).

The arriving long-wave radiation (RL↓), through the descending thermal radiation of the atmosphere (W.m^{-2}), was estimated using the equation of Stefan-Boltzmann, Equation 19, described in (ALLEN; TASUMI; TREZZA, 2007).

$$R_{L\downarrow} = \varepsilon_a \sigma T_a^4 \quad (19)$$

Where ε_a is the broadband surface emissivity (dimensionless), σ is the constant of Stefan-Boltzmann (5,67 × 10^{-8} W.m^{-2} K^{-4}) and Ta is the temperature of the air near the surface replaced by a cold pixel temperature (Tcold).

The ε_a was calculated using Equation 20, as described in (BASTIAANSSEN, 1995).

$$\varepsilon_a = 0,85\left(-\ln \tau_{SW}\right)^{0,09} \quad (20)$$

Where τ_{sw} is the broadband atmospheric transmissivity calculated from Equation 4.

For the estimation of soil heat flux (G), this study adopted the empirical model described by (BASTIAANSSEN; MOLDEN; MAKIN, 2000) which represent values near midday for the estimation with Landsat 8, as a G / Rn ratio based on the NDVI, according to Equation 21.

$$\frac{G}{R_n} = \left(T_s - 273{,}15\right)\left(0{,}0038 + 0{,}0074\alpha\right)\left(1 - 0{,}98NDVI^4\right) \quad (21)$$

Where Ts is the surface temperature (K) and α is the surface albedo.

Subsequently, the G_{METRIC} was obtained by multiplying G/Rn by Rn.

The sensible heat flux (H_{METRIC}) was estimated from an aerodynamic function expressed in Equation 22. In calculating the r_{ah}, the wind speed measurements were used.

$$H = \rho_{air} C_p \frac{\Delta T}{r_{ah}} \quad (22)$$

Where ρ is the density of the air ($kg.m^{-3}$), Cp is the specific heat capacity of the air ($J.kg^{-1}$ .K); ΔT is the temperature gradient of the air near the surface and r_{ah} is the aerodynamic resistance to heat transfer ($S.m^{-1}$) between two heights near the surface as (ALLEN; TASUMI; TREZZA, 2007).

After the establishment of Rn, G, and H from the Landsat 8 image processing, the LE was calculated as a residue of the Energy Balance equation. The LE obtained is equivalent to ET_{inst} at the time of passage of the Landsat 8 satellite, according to Equation 23.

$$ET_{inst} = 3600 \frac{LE}{\lambda \rho_\omega} \quad (23)$$

Where ET_{inst} is the instantaneous evapotranspiration ($mm.h^{-1}$), 3600 converts from seconds to hours, ρω is the density of water (~1000 $kg.m^{-3}$) and λ is the latent heat of vaporization ($J.kg^{-1}$) representing the heat absorbed when a kilogram of water evaporates.

The λ component was calculated according to Equation 24.

$$\lambda = \left[2{,}501 - 0{,}00236\left(T_s - 273{,}15\right)\right] \times 10^6 \quad (24)$$

Finally, as shown in Equation 25, the reference ET fraction (ETrF) was calculated as the ratio between the computed ET_{inst} of each pixel and the reference ET (ET_0) calculated from the meteorological station data.

$$ET_rF = \frac{ET_{inst}}{ET_0} \quad (25)$$

The ETrF obtained was later extrapolated to daily values. In the processes, ET_{24} was calculated assuming that the instantaneous ETrF computed at the time of satellite

passage is the same as the mean ETrF over the 24 h mean (ALLEN et al., 2007), according to Equation 26.

$$ET_{24} = C_{rad}\left(EF\right)\left(ET_{r24}\right) \quad (26)$$

Where C_{rad} is a correction term used to correct the variation over 24 hours versus the instantaneous availability of energy (ALLEN; TASUMI; TREZZA, 2007).

2.4. Calculation of NDVI and NDWI

After the estimation of Evapotranspiration by Landsat 8 images, the calculation of the NDVI (ROUSE et al., 1974) and NDWI (GAO, 1996) was performed for the different irrigation managements evaluated, according to Equations 27 and 28. The calculation was performed using the RStoolbox R package (LEUTNER; HORNING; SCHWALB-WILLMANN, 2019).

$$NDVI = \frac{NIR - RED}{NIR + RED} \quad (27)$$

$$NDWI = \frac{NIR - SWIR2}{NIR + SWIR2} \quad (28)$$

Where RED = Band 4 of Landsat 8, referring to the wavelength of red (0.636 a 0.673 μm); NIR = Band 5 of Landsat 8, referring to the near-infrared wavelength (0.851 a 0.879 μm) and SWIR2 = Band 7 of Landsat 8, referring to the short-wave infrared wavelength (2.11 a 2.29 μm).

2.5. METRIC model evaluation

The validation of the evapotranspiration estimation by the METRIC model was performed by applying different performance meters, among them are the Root Mean Square Errors (RMSE), Mean Absolute Error (MAE), Nash-Sutcliffe efficiency (EF), and Determination coefficient (R^2).

O RMSE (WILLMOTT; MATSUURA, 2005) is the root square of the residue variance. Indicates the absolute fit of the model to the data. Indicates the proximity of the ET_{METRIC} values to the ETr values. The RMSE was calculated according to Equation 29.

$$RMSE = \sqrt{\frac{\sum_{i=1}^{n}\left(ET_r - ET_{METRIC}\right)^2}{n}} \quad (29)$$

The MAE (WILLMOTT et al., 2015) indicates how much the predicted values are distanced from the calculated value of the standard equation, and was calculated according to Equation 30.

$$MAE = \frac{\sum_{i=1}^{n} \left| ET_r - ET_{METRIC} \right|}{n} \tag{30}$$

where ET_r é a ET calculada pela equação padrão FAO Penman Montheith e ET_{METRIC} é a evapotranspiração estimada por imagem de satélite.

EF efficiency, proposed by Nash and Sutcliffe (MORIASI et al., 2007; NASH; SUTCLIFFE, 1970; WILLMOTT et al., 2015), is defined as one minus the sum of the absolute quadratic differences between the ET_{METRIC} and ETr values normalized by the variance of the ETr values during the period under investigation. EF values range from -∞ to 1, with 1 being a perfect fit. High EF values are indicative of a more efficient model, however, EF values in the range of (-∞ to 0) indicate the unacceptable performance of the tested model. EF was calculated using Equation 31.

$$EF = 1 - \left[\frac{\sum_{i=1}^{n} \left(ET_r - ET_{METRIC} \right)^2}{\sum_{i=1}^{n} \left(ET_r - \overline{ET_r} \right)^2} \right] \tag{31}$$

where $\overline{ET_r}$ is the mean Evapotranspiration calculated by the standard method.

The coefficient of determination, R^2 was calculated using Equation 32. It indicates the relative adjustment between the ET_{METRIC} and ETr values (HEIJ et al., 2004).

$$R^2 = 1 - \frac{\sum_{i=1}^{n} \left(ET_r - ET_{METRIC} \right)^2}{\sum_{i=1}^{n} \left(ET_r \right)^2} \tag{32}$$

3. RESULTS AND DISCUSSION

In order to better evaluate the results, the mean values and standard deviation of LST, albedo, Rn, G, and H for each irrigation management studied (Tables 2 to 6) were calculated for all dates evaluated. NDVI, NDWI, albedo, LST, LE, and ET_{METRIC} maps were also generated. Finally, the performance of the METRIC algorithm against the calculation of the real evapotranspiration by the meteorological station was evaluated.

In addition, Figure 3 shows the precipitation and mean temperature in the studied period. The variable with the greatest variation was precipitation. Between

October and March of all year evaluated, there were high-intensity precipitations followed by long dry periods. DOY 10/2015 and 365/2016 occurred in a period of intense precipitation rate and high mean temperature. However DOY 159/2017 and 165/2019 occurred in days of low rainfall and low mean temperature, while the DOY 135/2014 followed days of low intensity rain, which occurs in all summer of 2013/2014.

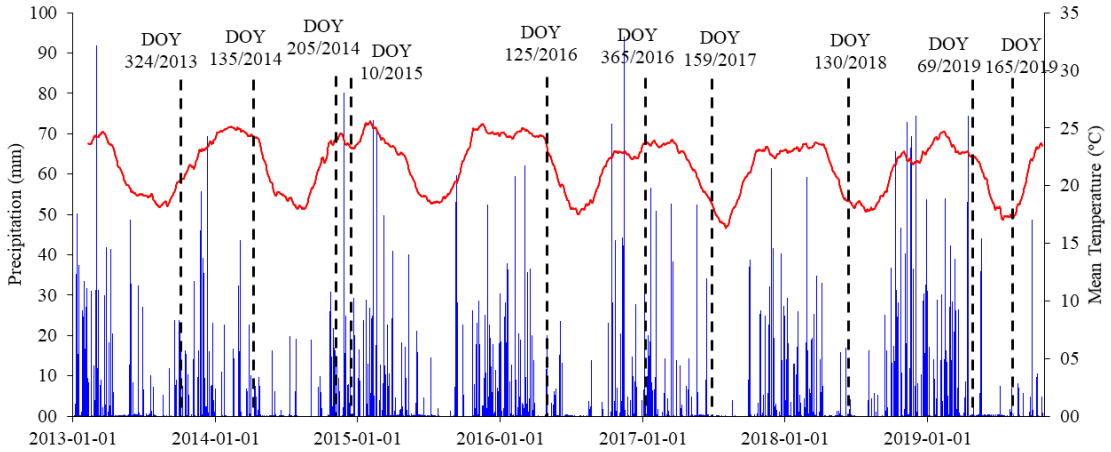

Figure 3 - Precipitation and Mean Temperature at a daily scale between 01 January 2013 and 23 October 2019 in the municipality of Carmo do Rio Claro – MG. The temporal location of the DOYs of the present research is indicated by the dotted line (DOY = day of year).

3.1. Land Surface Temperature (LST) and albedo evaluation

It was observed that, for dryland management, the surface temperature ranged from 21.82 to 41.45 ºC, with the highest values in the dates present in the rainy periods (close to summer), with a reduction in dry seasons (close to winter). The same pattern occurs for different irrigation management, but with lower LST variations (Table 2). This pattern may be related to the irrigation that was applied in the area, maintaining the surface with fewer variations of humidity, which can be seen in Figure 6. It's important to highlight that the surface temperature is largely dependent mainly on the solar radiation that is absorbed, being converted into thermal energy by the transfer of longwave radiation from the surfaces to the lower part of the atmosphere.

Allen et al. (2013), studying agricultural areas in the state of Idaho, USA, concluded that high LST values are associated with low values of latent heat flux, which occurs on less vegetated surfaces. The authors found large peak LST (43.85 to 56.85 ° C) in a large number of pixels present in the desert image area. This phenomenon was

observed in the study area, in which areas with higher values of LE (Figure LE), have a lower temperature.

Table 2 Mean values and standard deviation of Land surface temperature (ºC), estimated by the METRIC algorithm in the different dates of the study.

DOY	LST (ºC)			
	Dryland	Central Pivot	Self-Propelled	Dripping
324/2013	37.47 ± 1.20	36.31 ± 1.30	32.99 ± 0.47	36.31 ± 0.73
135/2014	24.45 ± 0.74	25.69 ± 0.85	26.71 ± 0.44	28.43 ± 0.65
205/2014	41,45 ± 1.85	39.85 ± 1.11	39.06 ± 3.15	41.01 ± 1.21
10/2015	38.12 ± 0.84	35.35 ± 0.60	33.92 ± 0.69	38.85 ± 0.72
145/2016	23.55 ± 0.59	25.94 ± 1.24	26.10 ± 1.11	26.33 ± 0.56
365/2016	34.89 ± 1.02	37.47 ± 2.24	34.67 ± 0.93	35.31 ± 0.97
159/2017	24.69 ± 0.54	26.47 ± 0.70	26.17 ± 1.25	25.95 ± 0.51
130/2018	23.97 ± 0.66	28.26 ± 1.40	26.50 ± 0.76	24.92 ± 0.60
69/2019	31.13 ± 1.09	34.72 ± 1.56	32.74 ± 1.48	31.08 ± 0.71
165/2019	21.82 ± 0.68	23.85 ± 0.72	25.25 ± 0.28	23.47 ± 0.52

Albedo presented small spatial variation and is strongly associated with land use and the presence of heterogeneous vegetation cover. When it is evaluated in the time series, the albedo was affected by environmental characteristics throughout the year, besides the presence of anthropic action by the management of adjacent agricultural areas (Figure 4).

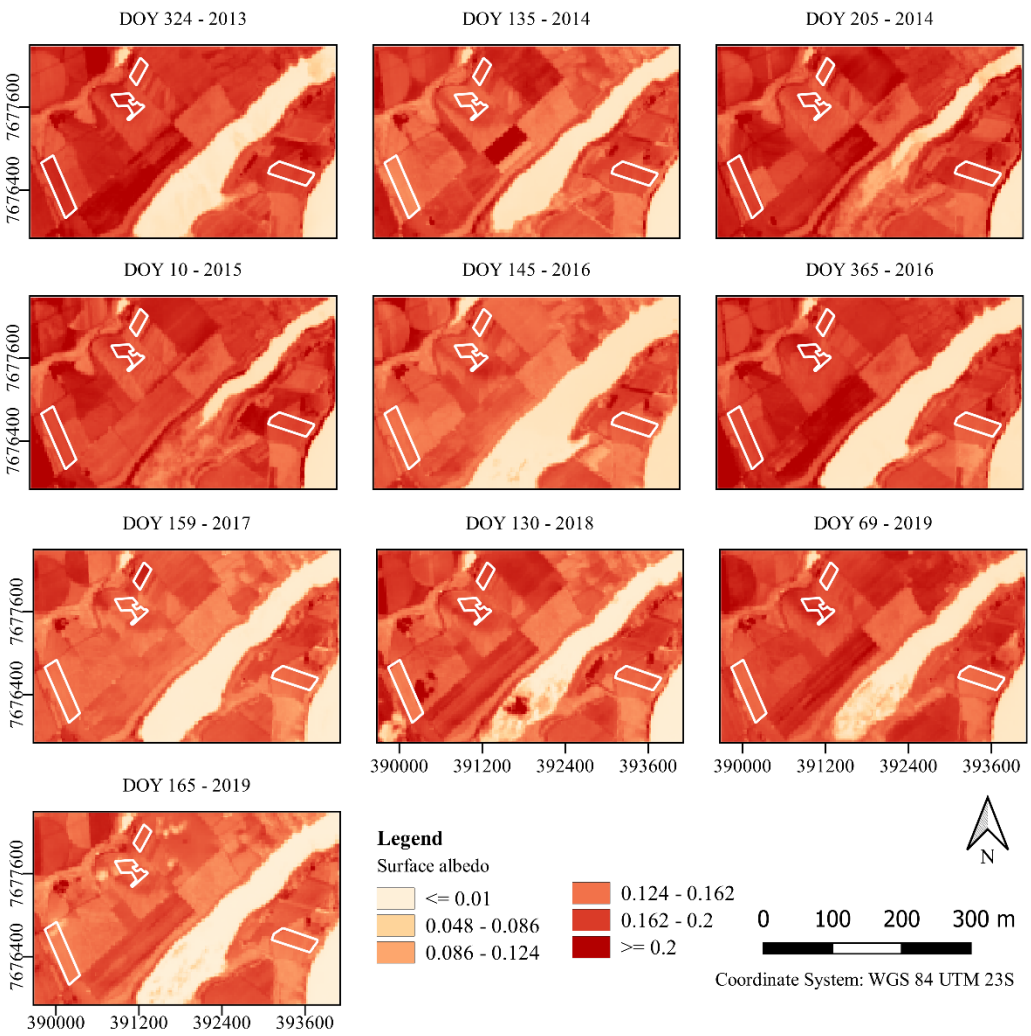

Figure 4 - Albedo at Dryland, Central Pivot, Self-Propelled and Dripping irrigation management in different evaluated dates.

In addition, it was found that the higher the NDVI (Figure 5), the lower the value of albedo estimated by METRIC in dryland management (Table 3). This means that the lower the NDVI, the more exposed soil there is, consequently promoting an increase in the albedo value, which was also observed by (RAHIMZADEGAN; JANANI, 2019). However, again, as in the LST, the greatest discrepancy of the values occurred in the management of the crop in the dryland.

Table 3 Mean values and standard deviation of Albedo, estimated by the METRIC algorithm in the different dates of the study.

DOY	albedo			
	Dryland	Central Pivot	Self-Propelled	Dripping
324/2013	0.17 ± 0.004	0.17 ± 0.008	0.15 ± 0.002	0.16 ± 0.003
135/2014	0.11 ± 0.006	0.14 ± 0.008	0.15 ± 0.004	0.15 ± 0.004
205/2014	0.16 ± 0.004	0.16 ± 0.005	0.15 ± 0.006	0.16 ± 0.005
10/2015	0.15 ± 0.004	0.16 ± 0.011	0.14 ± 0.006	0.16 ± 0.004
145/2016	0.13 ± 0.005	0.14 ± 0.010	0.14 ± 0.005	0.14 ± 0.003
365/2016	0.16 ± 0.004	0.17 ± 0.009	0.15 ± 0.007	0.14 ± 0.005
159/2017	0.12 ± 0.005	0.13 ± 0.008	0.17 ± 0.008	0.13 ± 0.004
130/2018	0.12 ± 0.009	0.15 ± 0.010	0.16 ± 0.005	0.13 ± 0.004
69/2019	0.13 ± 0.004	0.17 ± 0.006	0.15 ± 0.004	0.13 ± 0.005
165/2019	0.11 ± 0.010	0.13 ± 0.010	0.14 ± 0.004	0.12 ± 0.004

A fact to be highlighted is that with the increase of the albedo, the absorption of solar energy decreases and as a result, the LST also reduces. (ALLEN et al., 2007; RAHIMZADEGAN; JANANI, 2019) observed these events in beet crops in Idaho, USA, and pistachio in Iran, respectively. The fact was also observed in the present study.

Another factor that contributes to seasonal albedo variations is the surface humidity during the rainy season or the management of irrigation. Many authors (LI et al., 2006; LOBELL; ASNER, 2002; TEIXEIRA et al., 2014, 2008) have found linear relationships between albedo and surface moisture.

3.2. Evaluation of the net radiation (Rn) and the soil heat flux (G)

The mean values of Rn ranged from 404.92 to 731.48 W among the different irrigation management systems (Table 4), with the highest values observed during the rainy season. The values were within the predicted by (ALLEN et al., 2002), in which it inferred that the values should be between 100 to near 700 $W.m^{-2}$.

Net radiation is directly related to the entry of longwave and shortwave radiation. As these two parameters are directly related to surface temperature, in areas with higher surface temperatures, the net radiation is higher (ALLEN et al., 2011).

He et al. (2017), studied almond orchards in California, USA, found that Rn, ET, and NDVI obtained close spatial patterns in which, the lower the vigor of the almond

crop, the lower the values. However, in this work, it was observed that only Rn and ET have close spatial patterns.

Table 4 Mean values and standard deviation of net radiation (Rn) estimated by the METRIC algorithm in the different dates of the study.

DOY	Rn (W)			
	Dryland	Central Pivot	Self-Propelled	Dripping
324/2013	692.17 ± 8.7	673.55 ± 16.9	731.48 ± 9.4	692.69 ± 14.2
135/2014	469.14 ± 14.4	489.22 ± 8.5	494.25 ± 15.3	456.36 ± 14.3
205/2014	684.90 ± 9.3	676.32 ± 14.0	716.46 ± 12.7	679.08 ± 12.7
10/2015	676.52 ± 11.0	645.51 ± 19.7	704.06 ± 12.2	652.32 ± 16.7
145/2016	479.42 ± 13.9	499.61 ± 9.2	520.58 ± 13.1	483.05 ± 14.9
365/2016	689.40 ± 9.9	642.48 ± 17.9	699.02 ± 12.3	680.76 ± 18.1
159/2017	404.92 ± 13.9	439.34 ± 10.3	426.11 ± 16.4	421.40 ± 15.7
130/2018	474.63 ± 15.2	486.89 ± 9.9	497.71 ± 14.4	481.87 ± 15.6
69/2019	618.37 ± 12.0	581.84 ± 14.1	636.05 ± 12.3	614.21 ± 19.1
165/2019	405.55 ± 18.7	436.71 ± 9.6	442.88 ± 16.6	420.04 ± 14.3

When analyzing the heat flux in the soil (G) (Table 5), it was verified that the mean values were between 32,84 to 74,20 W. With the largest discrepancies between the dates in the Self-propelled system. (MADUGUNDU et al., 2017) found values ranging from 28.6 to 143.73 $W.m^{-2}$ for irrigated alfalfa fields during the year 2013. Close values to G were also found by (HAM; HEILMAN; LASCANO, 1991) in the study of the latent heat flux in the cotton crop in Lubbock, Texas, USA.

Table 5 Mean values and standard deviation of soil heat flux (G) estimated by the METRIC algorithm in the different dates of the study.

DOY	G (W)			
	Dryland	Central Pivot	Self-Propelled	Dripping
324/2013	74.20 ± 10.6	49.48 ± 1.5	45.39 ± 2.6	62.59 ± 5.0
135/2014	52.83 ± 4.4	44.38 ± 2.8	46.52 ± 4.1	57.64 ± 6.2
205/2014	52.06 ± 9.5	42.98 ± 0.7	45.91 ± 13.5	52.95 ± 7.0
10/2015	45.61 ± 7.9	48.41 ± 3.2	42.47 ± 3.1	56.86 ± 4.6
145/2016	41.81 ± 4.8	44.53 ± 5.5	50.52 ± 8.9	56.57 ± 3.5
365/2016	41.98 ± 5.3	49.36 ± 11.9	71.16 ± 4.6	48.91 ± 8.4
159/2017	40.91 ± 5.0	46.01 ± 4.3	32.84 ± 9.4	50.34 ± 3.5
130/2018	52.82 ± 5.2	50.95 ± 9.1	41.37 ± 3.9	51.53 ± 5.4
69/2019	46.07 ± 5.6	44.68 ± 4.5	45.20 ± 9.3	47.08 ± 3.3
165/2019	44.14 ± 6.7	46.59 ± 3.9	50.95 ± 3.7	51.61 ± 3.8

3.3. Analysis of the sensible heat flux (H)

The evaluation of H shows that the values estimated by METRIC ranged from 83.34 to 344.25 W in different irrigation management systems (Table 6). However, the greatest variation between the analyzed dates was observed for the dryland crop, in which the lowest value was obtained and one of the highest values estimated in the studied period. Sensible heat flux (H) is the form of thermal energy that is released or is absorbed by the earth's surface into the atmosphere by convection and conduction, and there have always been difficulties in estimating it on a large scale using orbital data information (LIAQAT; CHOI, 2015).

It was observed that in the rainy season, the values of H were higher than in periods with more scarce rains. This pattern was also observed by (CARRASCO-BENAVIDES et al., 2014), in which the authors evaluated the application of METRIC to irrigated vines in the Talca Valley, Chile. (CHOI et al., 2011), evaluating the METRIC algorithm in a river basin in Korea, verified that high H values occur in areas without vegetation, as in urban areas, and low values of sensible heat flux are found in vegetated areas.

Table 6 Average values of sensible heat flux (H), estimated by the METRIC algorithm in the different dates of the study.

DOY	H (W)			
	Dryland	Central Pivot	Self-Propelled	Dripping
324/2013	340.23 ± 8.8	344.25 ± 11.9	322.07 ± 5.4	333.69 ± 7.4
135/2014	201.65 ± 3.5	211.84 ± 4.7	217.75 ± 2.8	221.73 ± 3.2
205/2014	279.54 ± 4.9	283.09 ± 2.2	285.81 ± 6.9	275.54 ± 5.4
10/2015	217.75 ± 8.5	191.20 ± 5.4	179.07 ± 6.5	225.82 ± 7.2
145/2016	144.28 ± 4.7	159.74 ± 9.2	160.97 ± 9.7	166.98 ± 3.9
365/2016	205.89 ± 10.3	233.09 ± 23.6	201.70 ± 9.4	209.51 ± 9.9
159/2017	95.53 ± 5.4	115.92 ± 8.2	114.82 ± 14.0	109.18 ± 5.5
130/2018	103.09 ± 7.7	162.02 ± 16.6	142.70 ± 9.9	116.14 ± 7.0
69/2019	148.28 ± 13.2	197.99 ± 19.0	173.43 ± 18.2	147.09 ± 8.6
165/2019	83.34 ± 7.5	110.62 ± 10.0	128.42 ± 4.0	103.26 ± 6.0

3.4. Analysis of NDVI and NDWI

After analyzing the NDVI values, it was found that the values were relatively high in the areas of irrigation management studied (Figure 5). From the comparison of the NDVI behavior in the coffee plants, it was verified that higher values occurred in

November and December when the plants showed higher vigor (ALLEN; TASUMI; TREZZA, 2006) (Figure 5).

Al Zayed et al. (2016), infer that NDVI is strongly related to the ET value, demonstrating reasonable compliance between values, a fact confirmed by R^2 values of 0.69; 0.62; 0.81 for SEBAL, METRIC, and SSEB, respectively.

Another important fact to emphasize in relation to NDVI is the annual variation, that is, how the values change with each observed image, can be indicative of vegetation stress, which may be caused by climate change (LIU; MASSAMBANI; NOBRE, 1994).

The NDWI pattern follows what was found for the NDVI values since, in the places where the highest vigor occurred, a higher value of moisture was also observed in the crop (Figure 6). Thus, in general, in the periods between November and January, NDWI values were higher than winter dates.

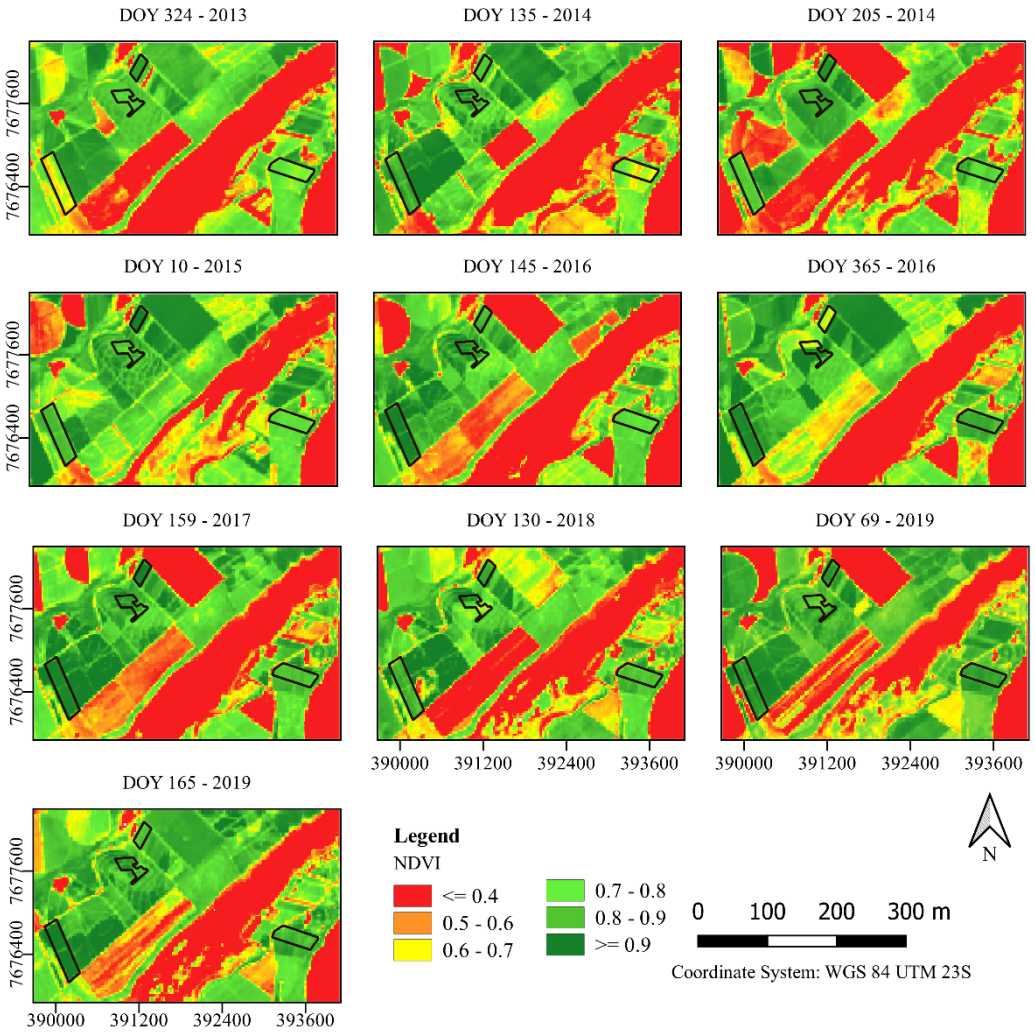

Figure 5 - NDVI at Dryland, Central Pivot, Self-Propelled and Dripping irrigation management, in the different evaluated dates.

Thus, NDWI can be a good alternative to verify through orbital sensors how the coffee crop is when it is desired to evaluate the humidity present in the use of different irrigation methods. Since NDWI has shown good results to estimate the variation in vegetation moisture condition, drought monitoring and water budget management (BAJGAIN et al., 2015).

Emphasizing the importance of the index in culture, (NOGUEIRA; MOREIRA; VOLPATO, 2018; PICINI et al., 1999), show that coffee cultivation was highly dependent on water availability, which was a factor that affected coffee productivity.

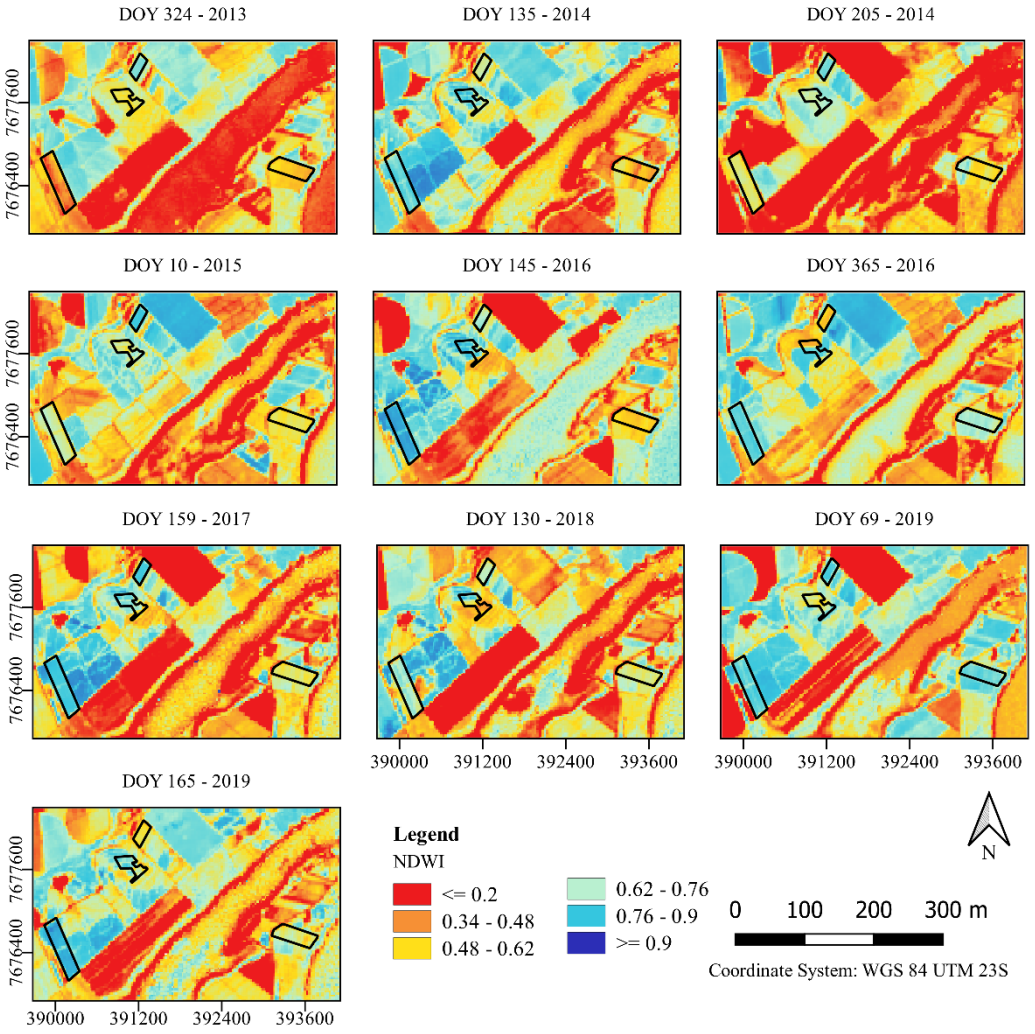

Figure 6 - NDWI at Dryland, Central Pivot, Self-Propelled and Dripping irrigation management, in the different evaluated dates.

3.5. Evaluation of the evapotranspiration estimation performed by METRIC algorithm

It was observed that the ET values were very varied in the different dates. When the variation between the irrigation management was evaluated, it was verified that the management with the self-propelled promoted higher ETr values (Figure 7 and 8).

This fact may be related to the type of irrigation, which is administered in large quantities by means of a powerful cannon on the crop, which may cause an increase in humidity in the studied area, increasing Etr values.

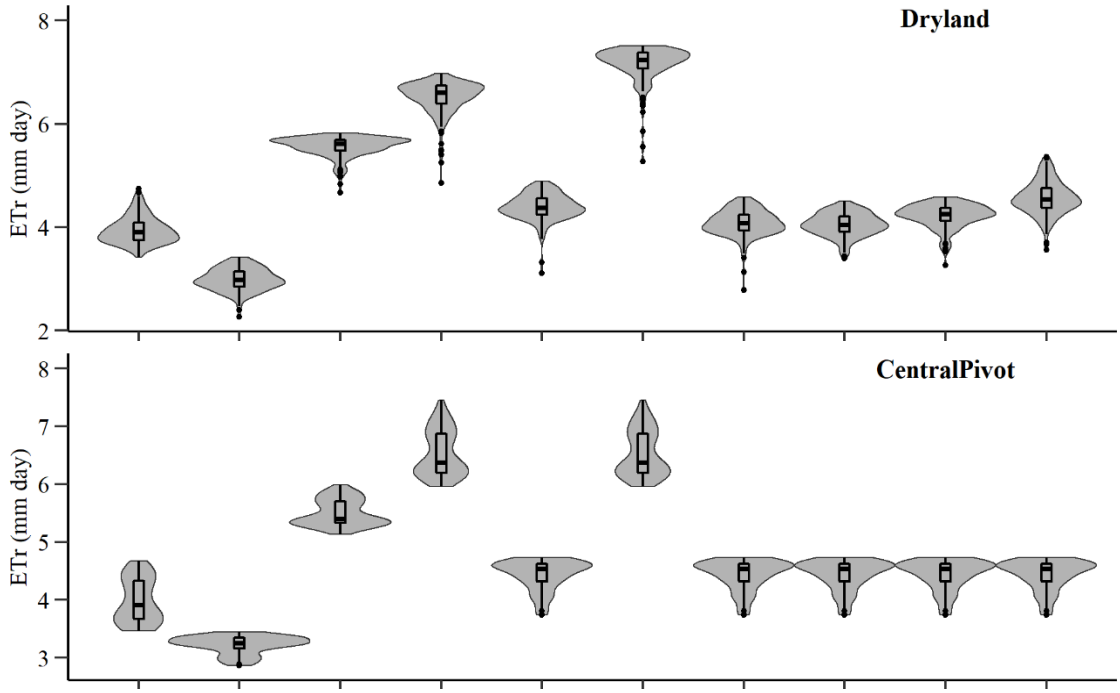

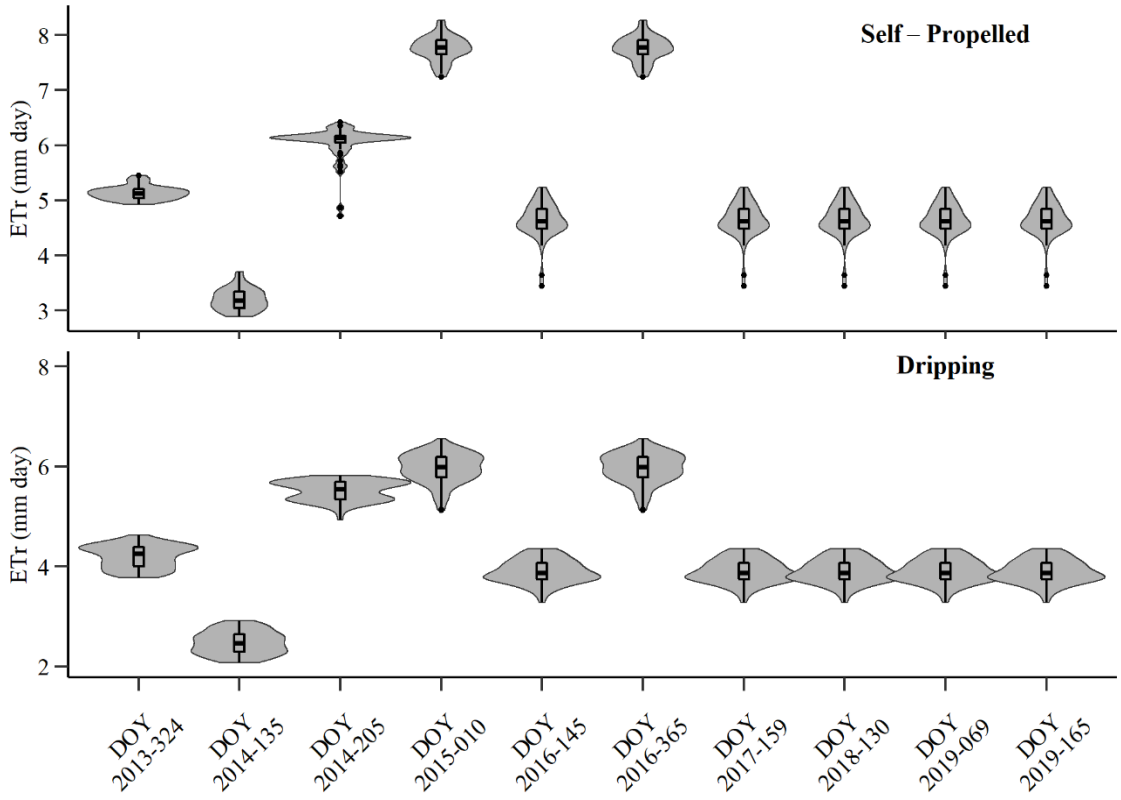

Figure 7 - Violin and boxplot chart for different irrigation management and each DOY.

Figure 7 shows how the density of probability of ETr. In addition, a boxplot was generated, demonstrating the median, dispersion, symmetry, and outliers of ETr in different dates and irrigation management.

It is possible to verify that when the values of ETr is low (DOY 145/2016, 59/2017, 130/2018, 069/2019 and 165/2019) the behavior of data is almost the same. However, in high values of ETr, the distribution varies in different DOY and irrigation management.

Another fact to be observed is that in the November, December, and January periods ET values were higher (close to 6 mm per day) than those found in the periods close to winter, such as March, May, and June (between 2 to 4 mm daily). This fact occurs because the plants were more photosynthetically active in the rainy periods, since the temperature in that period was also higher (CAMARGO; CAMARGO, 2001; RAHIMZADEGAN; JANANI, 2019).

In Figure 8, it is possible to highlight the DOY 135/2014, in which the lowest ET values of all studied series were observed, this fact is due to the drought period that occurred during the year 2014 (Figure 3), and the collection of information made in the month next to the winter (May), where ET values are usually lower, this characteristic

corroborates the lower values of NDVI and NDWI found in Figures 5 and 6, respectively.

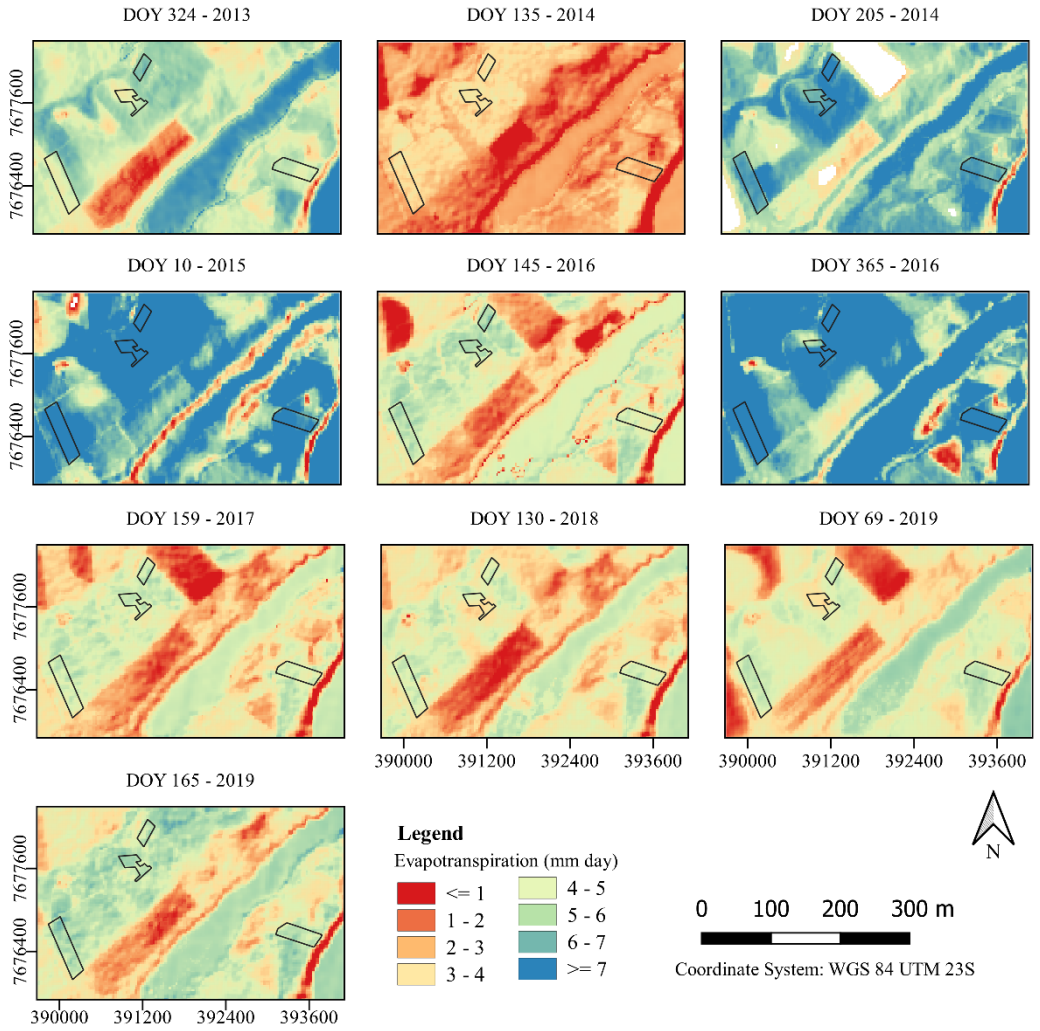

Figure 8 - ET_{METRIC} at Dryland, Central Pivot, Self-propelled and Dripping irrigation management, in the different evaluated dates.

Another fact to be highlighted in the ET_{METRIC} analysis is the fact that the values of NDVI and NDWI are related to the behavior of how the culture loses water to the atmosphere. Although not a direct relation, the variations occurred in the indexes impacted on variations observed in ET_{METRIC} maps, as in the image of November 20, 2013.

Finally, in the evaluation of the accuracy and precision of the METRIC algorithm in the study region (Figure 9), METRIC has a satisfactory performance in the region. The calculated ET value on the pixel at which the weather station was present was compared to the ETr value calculated by the meteorological station.

From the comparison of ETr, the values of R, RMSE, MAE, and EF calculated between ET_{METRIC} and ETr are shown in Figure 9, and the meteorological station method is considered the standard method.

An important fact to note regarding the METRIC model applied in the study region is that, when applied in the months close to winter (May, June, and July), the error associated to these values was lower than when the model was applied in the months close to summer (November, December, and January).

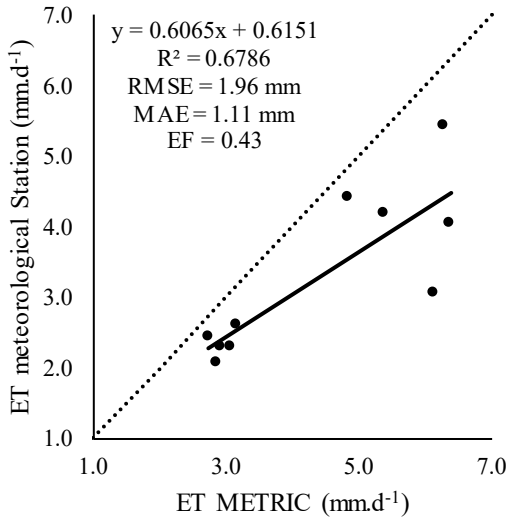

Figure 9 - Regression between evapotranspiration calculated by METRIC (ET METRIC) and ETr calculated by the meteorological station (ET Meteorological Station).

In addition, the median R^2 values (Figure 9) indicate that the fit was not perfect, but acceptable among the methods of obtaining the ETr.

The EF values found in the study were 0.43 for the METRIC model. This result indicates that the ET_{METRIC} model has satisfactorily adjusted to the ETr by the meteorological station method. (ELNMER et al., 2019) evaluating evapotranspiration on the Nile Delta under different remote sensing methodologies, found EF values for the METRIC model close to 0.9, demonstrating a good fit of the model. (DU et al., 2013; SANTOS; SILVA, 2010) also found satisfactory values evaluating methodologies for calculating ETr by Remote Sensing.

The MAE showed that the ET_{METRIC} was 1.11 $mm.d^{-1}$ distant from ETr. However, when RMSE showed that the ET_{METRIC} was a little distant from the values found by the meteorological station ETr calculation method, with a value of 1.96 mm^2 per day of error. (ELNMER et al., 2019), found values of 0.499 $mm.d^{-1}$ in a study in

Egypt. (WELIGEPOLAGE, 2005) verified differences of 0.4 $mm.d^{-1}$ in a study with seven dates in Hupselse Beek - The Netherlands.

4. CONCLUSIONS

In order to have effective use of irrigation water management, it is necessary to have accuracy in the determination of the essential parameters to use in irrigated agriculture. Since the rational use of water is gaining importance in the current scenario, knowing how much water is required to be applied in the crop is a mandatory factor to have coffee plantations with high yields.

NDWI can be a good alternative to verify through orbital sensors how the coffee crop is, when it is desired to evaluate the humidity present in the use of different irrigation methods.

Good accuracy of the METRIC model was found in the estimation of evapotranspiration, thus providing important information for data entry in the water balance for the determination of irrigation projects. The results of this study improve the understanding of the performance and reliability of the model used to estimate ET, especially in relation to its application in coffee crops, as well as in different irrigation management along the space and time, eliminating problems of ET estimation in only one station fixed in the area.

FUNDING

This work was supported by the Coordenação de Aperfeiçoamento de Pessoal de Nível Superior (Capes).

ACKNOWLEDGMENTS

This work was conducted with the support of the Conselho Nacional de Desenvolvimento Científico e Tecnológico (CNPq), the Fundação de Amparo à Pesquisa do Estado de Minas Gerais (FAPEMIG), the Coordenação de Aperfeiçoamento de Pessoal de Nível Superior (Capes) and the Universidade Federal de Lavras (UFLA).

REFERENCES

AL ZAYED, I. S. et al. Satellite-based evapotranspiration over Gezira Irrigation Scheme, Sudan: A comparative study. **Agricultural Water Management**, v. 177, p. 66–76, nov. 2016.

ALENCAR, L. P. DE et al. Tendências crescentes nos elementos do clima e suas implicações na evapotranspiração da cultura do milho em Viçosa - MG. **Engenharia Agrícola**, v. 31, n. 4, p. 631–642, 2011.

ALLEN, R. et al. S E B A L Sebal (Surface Energy Balance Algorithms for Land) – Advanced Training and Users Manual – Idaho Implementation. p. 97, 2002.

ALLEN, R. et al. Satellite-based ET estimation in agriculture using SEBAL and METRIC. **Hydrological Processes**, v. 25, n. 26, p. 4011–4027, 2011.

ALLEN, R. G. et al. **FAO Irrigation and Drainage Paper Nº 56. Crop Evapotranspiration (guidelines for computation crop water requirements)**. Roma: FAO, 1998.

ALLEN, R. G. et al. **The ASCE Standardized Reference Evapotran- spiration Equation**. Reston, VA, USA: ASCE, 2005.

ALLEN, R. G. et al. Satellite-Based Energy Balance for Mapping Evapotranspiration with Internalized Calibration (METRIC)—Applications. **Journal of Irrigation and Drainage Engineering**, v. 133, n. 4, p. 395–406, 2007.

ALLEN, R. G. et al. Automated calibration of the METRIC-Landsat evapotranspiration process. **Journal of the American Water Resources Association**, v. 49, n. 3, p. 563–576, 2013.

ALLEN, R. G.; TASUMI, M.; TREZZA, R. Benefits from tying satellite-based energy balance to reference evapotranspiration. **AIP Conference Proceedings**, v. 852, p. 127–137, 2006.

ALLEN, R. G.; TASUMI, M.; TREZZA, R. Satellite-Based Energy Balance for Mapping Evapotranspiration with Internalized Calibration (METRIC)—Model. **Journal of Irrigation and Drainage Engineering**, v. 133, n. 4, p. 380–394, 2007.

ANDERSON, M. C. et al. Use of Landsat thermal imagery in monitoring evapotranspiration and managing water resources. **Remote Sensing of Environment**, v. 122, p. 50–65, jul. 2012.

BAJGAIN, R. et al. Sensitivity analysis of vegetation indices to drought over two tallgrass prairie sites. **ISPRS Journal of Photogrammetry and Remote Sensing**, v. 108, p. 151–160, out. 2015.

BASTIAANSSEN, W. **Regionalization of Surface Flux Densi- ties and Moisture Indicators in Composite Terrain: A Remote Sensing Approach under Clear Skies in Mediterranean Climates**. [s.l.] Wageningen Agricultural University, 1995.

BASTIAANSSEN, W. G. .; CHANDRAPALA, L. Water balance variability across Sri Lanka for assessing agricultural and environmental water use. **Agricultural Water Management**, v. 58, n. 2, p. 171–192, fev. 2003.

BASTIAANSSEN, W. G. M. et al. A remote sensing surface energy balance algorithm for land (SEBAL). 1. Formulation. **Journal of Hydrology**, v. 212–213, n. JANUARY,

p. 198–212, dez. 1998.

BASTIAANSSEN, W. G. M.; MOLDEN, D. J.; MAKIN, I. W. Remote sensing for irrigated agriculture: examples from research and possible applications. **Agricultural Water Management**, v. 46, n. 2, p. 137–155, dez. 2000.

BERTI, A. et al. Assessing reference evapotranspiration by the Hargreaves method in north-eastern Italy. **Agricultural Water Management**, v. 140, p. 20–25, 2014.

BHATTARAI, N. et al. A new optimized algorithm for automating endmember pixel selection in the SEBAL and METRIC models. **Remote Sensing of Environment**, v. 196, p. 178–192, 2017.

BORGES JÚNIOR, J. C. F. et al. Equação de Hargreaves-Samani calibrada em diferentes bases temporais para Sete Lagoas, MG. **Revista Engenharia na Agricultura**, v. 25, n. 1, p. 38–49, 2017.

BRUNSELL, N.; GILLIES, R. Incorporation of surface emissivity into a thermal atmospheric correction. **Photogrammetric Engineering and Remote Sensing**, v. 68, n. 12, p. 1263–1269, 2002.

CAMARGO, Â. P. DE; CAMARGO, M. B. P. DE. Definição e Esquematização das Fases Fenológicas do Cafeeiro Arábica nas Condições Tropicais do Brasil. **Bragantia**, v. 60, n. 1, p. 65–68, 2001.

CARRASCO-BENAVIDES, M. et al. Parameterization of the Satellite-Based Model (METRIC) for the Estimation of Instantaneous Surface Energy Balance Components over a Drip-Irrigated Vineyard. **Remote Sensing**, v. 6, n. 11, p. 11342–11371, 14 nov. 2014.

CHOI, M. et al. Evapotranspiration estimation using the Landsat-5 Thematic Mapper image over the Gyungan watershed in Korea. **International Journal of Remote Sensing**, v. 32, n. 15, p. 4327–4341, 10 ago. 2011.

CONAB. Acompanhamento da safra Brasileira. 2° Levantamento da Safra de Café de 2019 - Maio. **Companhia Nacionla de Abastecimento**, v. 5, n. 2, p. 1–65, 2019.

DU, J. et al. Evapotranspiration estimation based on MODIS products and surface energy balance algorithms for land (SEBAL) model in Sanjiang Plain, Northeast China. **Chinese Geographical Science**, v. 23, n. 1, p. 73–91, 10 fev. 2013.

DUFFIE, J. A.; BECKMAN, W. A. **Solar Engineering of Thermal Processes**. Quarta ed. Madison, Wisconsin: Wiley, 2013.

ELNMER, A. et al. Mapping daily and seasonally evapotranspiration using remote sensing techniques over the Nile delta. **Agricultural Water Management**, v. 213, n. November 2018, p. 682–692, mar. 2019.

FRENCH, A. N.; HUNSAKER, D. J.; THORP, K. R. Remote sensing of evapotranspiration over cotton using the TSEB and METRIC energy balance models. **Remote Sensing of Environment**, v. 158, p. 281–294, mar. 2015.

GAO, B. NDWI—A normalized difference water index for remote sensing of vegetation liquid water from space. **Remote Sensing of Environment**, v. 58, n. 3, p. 257–266, dez. 1996.

GARRISON, J. D.; ADLER, G. P. Estimation of precipitable water over the United

States for application to the division of solar radiation into its direct and diffuse components. **Solar Energy**, v. 44, n. 4, p. 225–241, 1990.

GEBLER, S. et al. Actual evapotranspiration and precipitation measured by lysimeters: A comparison with eddy covariance and tipping bucket. **Hydrology and Earth System Sciences**, v. 19, n. 5, p. 2145–2161, 2015.

HAM, J. M.; HEILMAN, J. L.; LASCANO, R. J. Soil and Canopy Energy Balamces of a Row Crop at Partial Cover. **Agronomy Journal**, v. 83, n. 4, p. 744–753, 1991.

HE, R. et al. Evapotranspiration estimate over an almond orchard using Landsat satellite observations. **Remote Sensing**, v. 9, n. 5, p. 1–21, 2017.

HEIJ, C. et al. **Econometric methods with applications in business and economics**. Oxford University Press, 2004.

HIPPS, L. E. The infrared emissivities of soil and Artemisia tridentata and subsequent temperature corrections in a shrub-steppe ecosystem. **Remote Sensing of Environment**, v. 27, n. 3, p. 337–342, 1989.

HUETE, A. . A soil-adjusted vegetation index (SAVI). **Remote Sensing of Environment**, v. 25, n. 3, p. 295–309, ago. 1988.

KIZER, M. A.; ELLIOTT, R. L. Eddy correlation systems for measuring evaporatranspiration. **Transactions of the American Society of Agricultural Engineers**, v. 34, n. 2, p. 387–392, 1991.

LEUTNER, B.; HORNING, N.; SCHWALB-WILLMANN, J. **RStoolbox: Tools for Remote Sensing Data Analysis**, 2019. Disponível em: <https://cran.r-project.org/package=RStoolbox>

LI, S. G. et al. Energy partitioning and its biophysical controls above a grazing steppe in central Mongolia. **Agricultural and Forest Meteorology**, v. 137, n. 1–2, p. 89–106, 2006.

LIAQAT, U. W.; CHOI, M. Surface energy fluxes in the Northeast Asia ecosystem: SEBS and METRIC models using Landsat satellite images. **Agricultural and Forest Meteorology**, v. 214–215, p. 60–79, dez. 2015.

LIU, W. T. H.; MASSAMBANI, O.; NOBRE, C. A. Satellite recorded vegetation response to drought in brazil. **International Journal of Climatology**, v. 14, n. 3, p. 343–354, abr. 1994.

LOBELL, D. B.; ASNER, G. P. Moisture effects on soil reflectance. **Soil Science Society of America Journal**, v. 66, n. 3, p. 722–727, 2002.

LOSGEDARAGH, S. Z.; RAHIMZADEGAN, M. Evaluation of SEBS, SEBAL, and METRIC models in estimation of the evaporation from the freshwater lakes (Case study: Amirkabir dam, Iran). **Journal of Hydrology**, v. 561, p. 523–531, jun. 2018.

MADUGUNDU, R. et al. Performance of the METRIC model in estimating evapotranspiration fluxes over an irrigated field in Saudi Arabia using Landsat-8 images. **Hydrology and Earth System Sciences**, v. 21, n. 12, p. 6135–6151, 5 dez. 2017.

MELO, G. L. DE; FERNANDES, A. L. T. Evaluation of empirical methods to estimate reference evapotranspiration in Uberaba, State of Minas Gerais, Brazil. **Engenharia**

Agrícola, v. 32, n. 5, p. 875–888, 2012.

MORIASI, D. N. et al. Model Evaluation Guidelines for Systematic Quantification of Accuracy in Watershed Simulations. **Transactions of the ASABE**, v. 50, n. 3, p. 885–900, 2007.

NASH, J. E.; SUTCLIFFE, J. V. River flow forecasting through conceptual models part I — A discussion of principles. **Journal of Hydrology**, v. 10, n. 3, p. 282–290, abr. 1970.

NOGUEIRA, S. M. C.; MOREIRA, M. A.; VOLPATO, M. M. L. Relationship Between Coffee Crop Productivity and Vegetation Indexes Derived From Oli / Landsat-8 Sensor Data With and Without Topographic Correction. **Engenharia Agrícola**, v. 38, n. 3, p. 387–394, 2018.

OLMEDO, F. G. et al. water: Tools and Functions to Estimate Actual Evapotranspiration Using Land Surface Energy Balance Models in R. **The R Journal**, v. 8, n. 2, p. 1–18, 2016.

PEEL, M. C.; FINLAYSON, B. L.; MCMAHON, T. A. Updated world map of the Köppen-Geiger climate classification. **Hydrology and Earth System Sciences**, v. 11, n. 5, p. 1633–1644, 11 out. 2007.

PEREIRA, A. R.; CAMARGO, Â. P. DE; CAMARGO, M. B. P. DE. **Agrometeorologia de cafezais no Brasil**. Campinas: Instituto Agrônomico, 2008.

PICINI, A. G. et al. Desenvolvimento e teste de modelos agrometeorológicos para a estimativa de produtividade do cafeeiro. **Bragantia**, v. 58, n. 1, p. 157–170, 1999.

PÔÇAS, I. et al. Satellite-based evapotranspiration of a super-intensive olive orchard: Application of METRIC algorithms. **Biosystems Engineering**, v. 128, p. 69–81, dez. 2014.

RAHIMZADEGAN, M.; JANANI, A. Estimating evapotranspiration of pistachio crop based on SEBAL algorithm using Landsat 8 satellite imagery. **Agricultural Water Management**, v. 217, n. August 2018, p. 383–390, maio 2019.

ROUSE, J. W. et al. **Monitoring Vegetation Systems in the Great Plains with ERTS**. Third Earth Resources Technology Satellite-1 Symposium. **Anais**...Washington, D.C: NASA. Goddart Space Flight Center, 1974Disponível em: <https://ntrs.nasa.gov/search.jsp?R=19740022614>

SANTOS, C. A. C. DOS; SILVA, B. B. DA. Obtenção dos fluxos de energia à superfície utilizando o algoritmo S-SEBI. **Revista Brasileira de Meteorologia**, v. 25, n. 3, p. 365–374, 2010.

SILVA, B. B. DA et al. Procedures for calculation of the albedo with OLI-Landsat 8 images: Application to the Brazilian semi-arid. **Revista Brasileira de Engenharia Agrícola e Ambiental**, v. 20, n. 1, p. 3–8, jan. 2016.

TASUMI, M.; ALLEN, R. G.; TREZZA, R. At-Surface Reflectance and Albedo from Satellite for Operational Calculation of Land Surface Energy Balance. **Journal of Hydrologic Engineering**, v. 13, n. 2, p. 51–63, 2008.

TEIXEIRA, A. H. D. C. et al. Energy balance with Landsat images in irrigated central pivots with corn crop in the São Paulo State , Brazil. **Proc SIPE**, v. 9239, p. 1–10,

2014.

TEIXEIRA, A. H. DE C. et al. Analysis of energy fluxes and vegetation-atmosphere parameters in irrigated and natural ecosystems of semi-arid Brazil. **Journal of Hydrology**, v. 362, n. 1–2, p. 110–127, nov. 2008.

TREZZA, R.; ALLEN, R.; TASUMI, M. Estimation of Actual Evapotranspiration along the Middle Rio Grande of New Mexico Using MODIS and Landsat Imagery with the METRIC Model. **Remote Sensing**, v. 5, n. 10, p. 5397–5423, 23 out. 2013.

USGS. EarthExplorer Help Documentation. **How To Download Lansat Data**, n. September, p. 73, 2013.

VERMOTE, E. et al. **LaSRC (Land Surface Reflectance Code): Overview, application and validation using MODIS, VIIRS, LANDSAT and Sentinel 2 data's**. IGARSS 2018 - 2018 IEEE International Geoscience and Remote Sensing Symposium. **Anais**...IEEE, jul. 2018Disponível em: <https://ieeexplore.ieee.org/document/8517622/>

WELIGEPOLAGE, K. **ESTIMATION OF SPATIAL AND TEMPORAL DISTRIBUTION OF EVAPOTRANSPIRATION BY SATELLITE REMOTE SENSING A case study in Hupselse Beek, The Netherlands**. [s.l.] International Institute for Geo-Information Science and Earth Observation, 2005.

WILLMOTT, C. J. et al. Assessment of three dimensionless measures of model performance. **Environmental Modelling and Software**, v. 73, p. 167–174, 2015.

WILLMOTT, C. J.; MATSUURA, K. Advantages of the mean absolute error (MAE) over the root mean square error (RMSE) in assessing average model performance. **Climate Research**, v. 30, n. 1, p. 79–82, 2005.

WRIGHTL, J. L. **Using Weighing Lysimeters to Develop Evapotranspiration Crop Coefficients**. Lysimetenr for Evapotranspiration and Environmental Measurements. **Anais**...Honolulu: ASCE, 1991

ZHONG, Q.; YINHAI, L. Satellite observation of surface albedo over the Qinghai-Xizang Plateau Region. **Advances in Atmospheric Sciences**, v. 5, n. 1, p. 57–65, 12 fev. 1988.

ACTUAL EVAPOTRANSPIRATION ESTIMATION OF ROBUSTA COFFEE FIELD USING SAFER ALGORITHM

Marcus Andre Braido Pinheiro; Marcelo de Carvalho Alves

ABSTRACT

Agriculture is the most important land use activity in the world. Agriculture not only affects the change of land cover but also has a profound impact on the sustainable development of social economy, food security, water and environment, ecosystem services, climate change, and carbon cycles. Against this background, robusta coffee is the most important culture in the State of Espírito Santo, Brazil. The aim of this study was to estimate evapotranspiration using the SAFER algorithm in an irrigated Robusta coffee crop. In addition to map the actual ET (ETSAFER) estimated by the algorithm, in order to observe the behavior of evapotranspiration within the field. In order to apply the SAFER algorithm, we use the Agriwater R package, we use 15 Sentinel 2 satellite images from 2019 to 2021 and meteorological station data to input the information's in the R software. Boxplots were used to compare the different data through the dates. By the application of the package, we could generate kc values, Land Surface Temperature (LST), NDVI, and Evapotranspiration data from the 15 dates. The application of the SAFER algorithm allowed understand the variation of ET in the coffee drip-irrigated field with high spatial (10 m) and temporal (5 days) resolution, and from this variation in ET, understand how to best manage irrigation in this crop. Therefore, water management of agricultural crops can be performed with free satellite imagery and simple weather data.

KEYWORDS: Land Surface Temperature, Sentinel 2, Irrigation Management, *Coffea canephora*

1. INTRODUCTION

Coffee is one of the most important agricultural commodities in international trade, playing a crucial role in the economy of several African, American, and Asian countries (INTERNATIONAL COFFEE ORGANIZATION, 2019; LEWIN;

GIOVANNUCCI; VARANGIS, 2004; MAFUSIRE et al., 2010). The total world production was estimated to be more than 150 million 60-kg bags of coffee beans over the past five years, of which 80 to 85% were exported (INTERNATIONAL COFFEE ORGANIZATION, 2020). Current coffee bean production is dominated by arabica coffee (Coffea arabica L.), which represents roughly 60%; the remaining 40% being for Robusta coffee (*C. canephora* Pierre ex A. Froehner) (INTERNATIONAL COFFEE ORGANIZATION, 2020). Brazil has a planted area of 2.2 million hectares, which corresponds to 48.8 million bags. Of this amount, Robusta coffee contributes 15.4 million bags in an area of 410.3 thousand hectares (CONAB, 2021).

Coffee production is strongly influenced by environmental conditions and is thus threatened by the increasing variability and changes in climate patterns across several major producing regions worldwide (BUNN et al., 2015; DAMATTA et al., 2019).

Extreme weather events associated with the El Niño Southern Oscillation (ENSO) (e.g, droughts, and frosts) can influence substantially both arabica and robusta coffee commodity markets (CASHIN; MOHADDES; RAISSI, 2017; SEPHTON, 2019; UBILAVA, 2012). It is therefore vital to develop decision support tools for increasing the preparedness of the various stakeholders of the coffee industry, from smallholder farmers to agribusinesses to governments.

Thus, evapotranspiration (ET) is an important process in the terrestrial water and energy cycles. As such, quantifying ET improves understanding of the water cycle and hydrological processes in terrestrial ecosystems (STOCKER; RAIBLE, 2005). The implementation of highly efficient agricultural water-saving measures undoubtedly has a significant effect on the water cycle in agricultural regions. Compared to other hydrological processes in the land-surface water cycle, the relationship between ET and agricultural water-saving measures is arguably more sensitive and direct (MCCABE; WOOD, 2006).

Site-specific irrigation management requires knowing crop ET for each management zone. Conventional ET estimation techniques, such as Bowen ratio, eddy covariance, surface renewal, weighing lysimeter, soil water balance, and scintillometer, can provide relatively accurate estimates of ET at field scale but are not spatially explicit and some are expensive and not readily available to growers (WANG; DICKINSON, 2012).

ET algorithms based on remote sensing data is widely used because these one allows estimating ET for larger and more heterogeneous areas (ALLEN et al., 2011;

BASTIAANSSEN et al., 1998; HSSAINE et al., 2018; SUN et al., 2011; TEIXEIRA et al., 2013c) and provide knowledge about the spatial-temporal distribution of ET (CAO et al., 2021; LIAQAT; CHOI; AWAN, 2015). Furthermore, operational costs are relatively lower.

Among the existing models, the Simple Algorithm for Evapotranspiration Retrieving (SAFER) stands out because it was developed for use in irrigated areas of semiarid regions (TEIXEIRA, 2010). SAFER is a biophysically realistic model of simple operation that is efficient in the spatial mapping of surface evapotranspiration estimates (COAGUILA et al., 2017; TEIXEIRA et al., 2013a, 2016).

According to (TEIXEIRA, 2010), SAFER requires information on images obtained from remote sensors, such as the Normalized Difference Vegetation Index (NDVI) (ROUSE et al., 1974), albedo (α) and surface temperature (Ts). Such information can be used to obtain the evapotranspiration fraction of the surface, which, when associated with the reference evapotranspiration (ET_0) proposed by Penman-Monteith (ALLEN et al., 1998), enables the mapping of surface evapotranspiration (ET_{SAFER}).

The aim of this study was to estimate evapotranspiration using the SAFER algorithm in an irrigated Robusta coffee crop and map the actual ET (ET_{SAFER}) estimated by the algorithm, in order to observe the behavior of evapotranspiration within the field.

2. MATERIAL AND METHODS

2.1. Study Area

The study was conducted on a commercial coffee field in the municipality of Marilândia, located in the northwest region of the state of Espírito Santo, Brazil (Figure 1). The site is in the rectangle bounded by geographic coordinate pairs (Datum SIRGAS 2000): -40.541; -19.407; -40.532, -19.402, with an average altitude of 95 m. The climate of the region is Aw, that is, tropical with rainy summers and dry winters, with annual precipitation of 1134.0 mm (DA SILVA et al., 2010). The cultivated field covers an area of 10.36 ha, the entire cultivated area is irrigated by dripping, the harvest happens between May and July, was present in a sloped area, the highlighted area is shown in Figure 1.

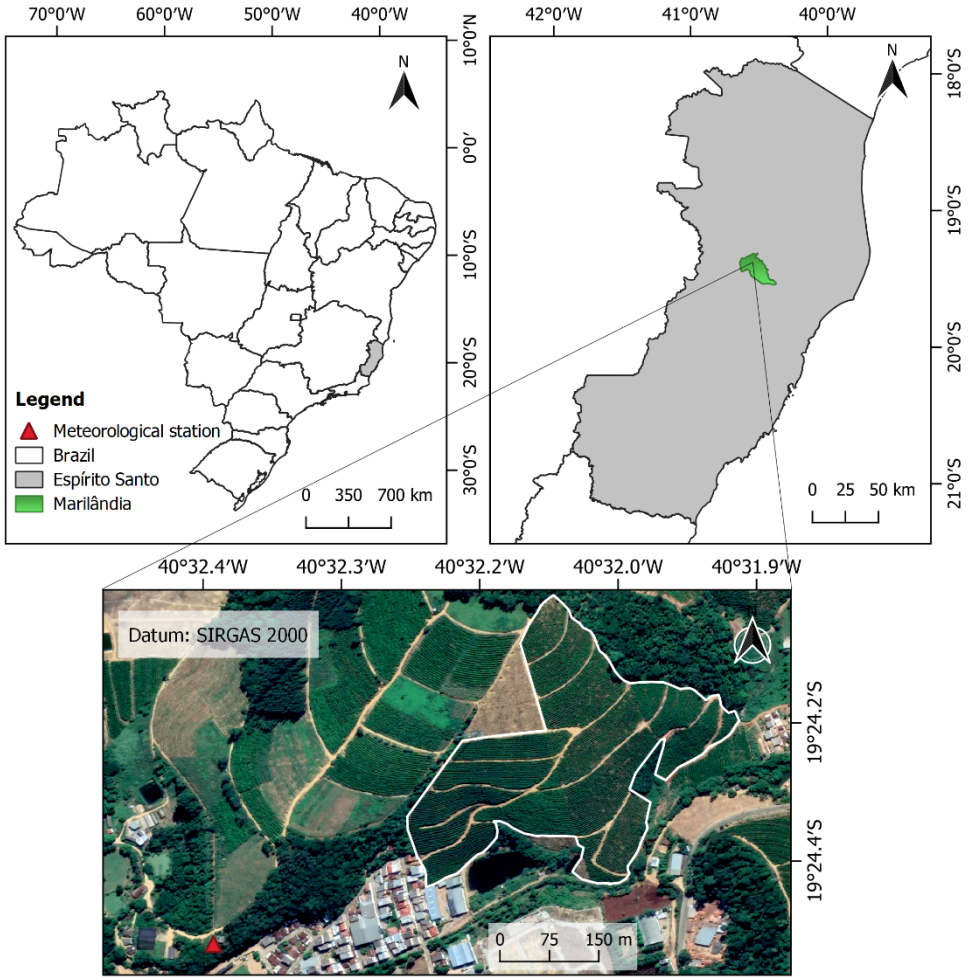

Figure 1 - Location of study site. Meteorological station is in red.

2.2. Meteorological data

Weather freely available 60-minute data from one agrometeorological station from Instituto Nacional de Meteorologia (INMET) installed at 300 m from the experimental area was used in this study.

Data of wind speed at 2m height (U_2, m/s), maximum and minimum temperature (Tmax Tmin, ºC), solar radiation (Ra, MJ m^2 d^{-1}), relative humidity (RH, %), and rainfall (mm) were used, during the years 2019 to 2021. These data were used to determine daily reference evapotranspiration (ET_0) and SAFER coffee evapotranspiration (ET_{SAFER}).

2.3. Orbital data

Satellite images (spectral bands) obtained free of charge from the Google Earth Engine (GEE) (GORELICK et al., 2017) Cloud computing platform was used for

mapping the evapotranspiration. 15 images from 2019 (02/25, 03/17, 06/20, 07/05, 07/15 and 08/19), 2020 (01/11, 02/10, 06/09, 06/24, 07/09, 07/14, 09/27 and 10/02) and 2021 (03/06) were used. These dates were chosen because there were no clouds in the areas of interest.

The images come from the MultiSpectral Instrument (MSI) sensor aboard the Sentinel 2 satellite. The Sentinel 2 mission is a constellation with two twin satellites. The MSI sensor have 13 bands, in this study, we use the bands with a spatial resolution of 10 m, a temporal resolution of 5 days and a radiometric resolution of 12 bits.

The bands used have wavelengths referring to the spectral ranges of blue B2(0.46 – 0.52 μm), green B3(0.53-0.59 μm), red B4(0.63-0.69μm) and near-infrared B8(0.797-0.887 μm).

2.4. Actual crop evapotranspiration (ET) estimation

Meteorological data were obtained by the INMET automatic meteorological station (CITAR). The data collected were temperature, relative air humidity, solar radiation and wind speed. The estimation of reference evapotranspiration (ET_0) by the Penman-Monteith method FAO-56 (Equation 1) is according to Allen et al. (1998):

$$\frac{ET_0 = 0.408s\left(R_n - G\right) + \gamma \frac{900}{t+273}\ U_2\left(e_s - e_a\right)}{s + \gamma\left(1 + 0.34\ U_2\right)}, \quad (1)$$

where ET_0 is the reference evapotranspiration, mm d^{-1}; Rn is the net radiation on the surface, MJ m^{-2} d^{-1}; G is the soil heat flux, MJ m^{-2} d^{-1}; t is the average air temperature, °C; U_2 is the wind speed at a height of 2 m, m s^{-1}; *es* is the saturation vapor pressure, kPa; e_a is the partial vapor pressure, kPa; *s* is the slope of the saturation vapor pressure curve, kPa $ºC^{-1}$; and γ is the psychrometric coefficient, kPa $ºC^{-1}$.

Evapotranspiration mapping was performed using SAFER, as described by (TEIXEIRA, 2010). To obtain SAFER evapotranspiration, it is necessary to have information of monochromatic reflectance for the bands corresponding to the blue (B2), green (B3), red (B4) and near-infrared (B8) wavelengths. These data are necessary to calculate the planetary albedo, surface albedo, brightness temperature, surface temperature, and NDVI. Subsequently, the evapotranspiration fraction (ET/ET_0) is estimated, as described by (TEIXEIRA; TONIETTO; LEIVAS, 2016), and demonstrated in the flowchart of Figure 2.

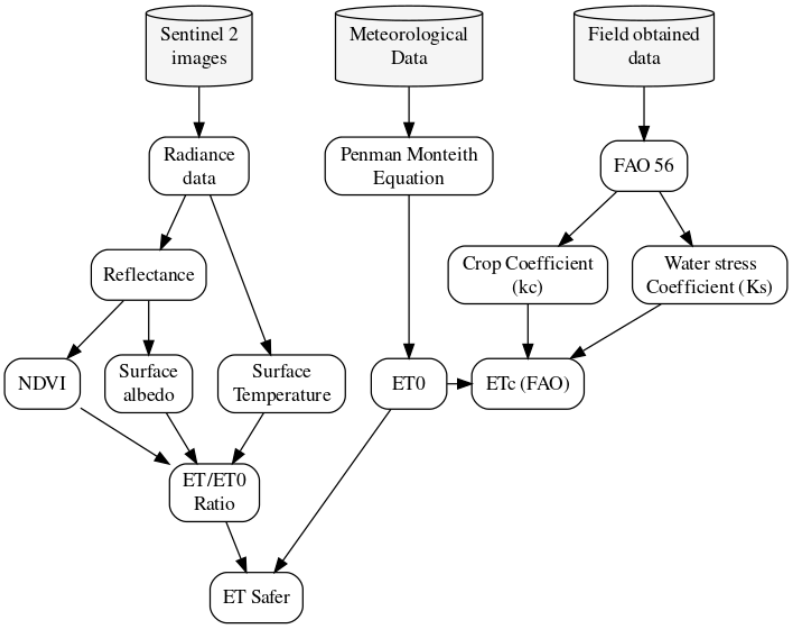

Figure 2 – Flowchart of ET_0 and ET_{SAFER} measurement.

For the Land Surface Temperature (LST) calculation, was used air temperature together with satellite measurements by applying the residual method. According to (SILVA; MANZIONE; ALBUQUERQUE FILHO, 2018), the daily LST values can be estimated by Equation (2).

$$LST = \sqrt[4]{\frac{\varepsilon_A \sigma T_A^4 + \alpha_L \tau_{sw}}{\varepsilon_S \sigma}} \quad (2)$$

where s_w is the shortwave atmosphere transmissivity defined as 44% of RG to the incident solar radiation at the top of atmosphere , values ε_A and ε_S are respectively the atmospheric and surface emissivity's, σ is the Stefan-Boltzmann constant (5.67×10^8 W m^2 K^4) and α_L coefficient can be explained by daily variations (SILVA; MANZIONE; ALBUQUERQUE FILHO, 2018; TEIXEIRA et al., 2014a) by Equation (3).

$$\alpha_L = cT_A - d \quad (3)$$

where T_A is the daily average air temperature from agrometeorological station inside the study area with leaf area index (LAI) of 2.88 and estimated albedo of 0.23, RG is the 24-h values of global solar radiation and c and d are regression coefficients equal to 6.99 and 39.93 (TEIXEIRA et al., 2014a).

Following (TEIXEIRA et al., 2008, 2014b), ε_A and ε_S were calculated as Equation (4 and 5):

$$\varepsilon_A = \alpha_A \left(-\ln \tau_{sw}\right)^{b_A} \quad (4)$$

$$\varepsilon_S = \alpha_S \ln NDVI + b_S \quad (5)$$

where α_A, b_A, α_S and b_S are regression which, from (TEIXEIRA, 2010), were considered, respectively, 0.94, 0.10, 0.06 and 1.00. Teixeira et al. (2009) calibrated ε_A and ε_S with R^2 of 0.75 and 0.90 respectively.

Albedo is defined as the ratio between reflected and incident sunlight and is an important parameter in the study of climate change, desertification, fires, and environmental impacts (SILVA et al., 2005). For estimating surface albedo, first, top-of-atmosphere albedo (α_{TOA}) data were obtained by Equation (6).

$$\alpha_{TOA} = \sum(\omega_P \rho_\lambda) \quad (6)$$

where: ω_P is the weight coefficient for each band and ρ_λ is the surface reflectance of bands 2, 3, 4 and 8 (MSI). The weights for the different bands were computed as the ratio of the amount of the incoming shortwave radiation from the sum in each band and the sum of incoming shortwave radiation for the bands at the top of the atmosphere (TOA).

Then, α_{TOA} was transformed to surface albedo data (TEIXEIRA, 2010) using Equation (7).

$$\alpha_0 = b\alpha_{TOA} + c \quad (7)$$

where b and c are regression coefficients, which for a 24-h period was considered as 1.70 and 0.13, obtained from field and satellite measurements (TEIXEIRA et al., 2009, 2013b, 2014b) and was calibrated with an R^2 = 0.96 (TEIXEIRA, 2010).

The NDVI is an indicator related to the land cover and vegetation stages (ROUSE et al., 1974) obtained from satellite image as Equation (8):

$$NDVI = \frac{\rho_{NIR} - \rho_{RED}}{\rho_{NIR} + \rho_{RED}} \quad (8)$$

where: ρ_{NIR} and ρ_{RED} refer to the reflectance of the near infrared band and the red band, respectively.

Applying the SAFER algorithm, the ratio of the actual (ET) to the reference (ET_0) evapotranspiration, ET_f, was modeled at the satellite overpass time (TEIXEIRA, 2010; TEIXEIRA et al., 2013c, 2017) as follows Equation (9):

$$ET_f = \exp\left[a + b\left(\frac{T_0}{\alpha_0 NDVI}\right)\right] \quad (9)$$

where: *a* and *b* are regression coefficients, 1.8 and –0.008, respectively, applicable for the Brazilian semiarid conditions, according to (TEIXEIRA et al., 2013c).

This equation (ET_f) was established for Brazilian semiarid conditions involving irrigated crops and natural vegetation under different meteorological and hydrological conditions, based on simultaneous field data from four flux towers and Landsat images (TEIXEIRA, 2010). Following the technical formalism, the term ETr also could be called "crop coefficient" when modeling is performed on irrigated areas, respecting the nomenclature from the FAO-56 manual (ALLEN et al., 1998), and "evapotranspiration fraction" in areas without irrigation, as natural vegetation and rainfed crops, because it is a less restricted term.

Amazirh et al. (2017), estimated T_0 using Landsat images and the Planck equation for irrigated wheat crops and compared the results with *in situ* measurements. The authors found RMSE values ranging from 0.91 to 2.36 °C. Oliveira-Guerra et al. (2018) and Rahimzadegan & Janani (2019) used the same procedures to calculate ET_0 to obtain evapotranspiration in their respective research.

In this way, SAFER evapotranspiration (ET_{SAFER}) was calculated using Equation (10):

$$ET_{SAFER} = ET_f \; ET_0 \tag{10}$$

where ET_f is the evapotranspiration fraction, and ET_0 is the reference evapotranspiration calculated by the Penman-Monteith (PM) equation.

ET_{SAFER} is composed of soil evaporation and plant transpiration and depends primarily on energy supply, the vapor pressure gradient between surface and atmosphere, and wind speed (aggregates in reference evapotranspiration). Evaporation in soil, specifically, is directly dependent on soil moisture. Soil water content and its ability to conduct water to the roots should be considered (ALLEN et al., 1998).

2.5. Statistical analysis

In this study, we use the boxplot to better understand the data distribution among the dates studied. For the data analysis, the R software (R CORE TEAM, 2021) was used to work with meteorological and satellite data. We used Agriwater R package to perform ET_{SAFER} estimation.

3. RESULTS AND DISCUSSION

Figure 3 shows the daily temperature (Maximum and Minimum) and precipitation during the entire period studied. As seen, 2019 was an atypical year, with scarce rainfall (656.0 mm). However, 2020 has already started with high rainfall (1381.4 mm), a characteristic that lasted until the end of March, with a dry winter and more concentrated rainfall in November. Corroborating the local climatic classification. The volume of precipitation on 03/02/2020 (151.4 mm) stands out.

Evaluating historical data, da Silva et al. (2010) states that the municipality of Marilândia has two distinct periods, a rainy period in which the monthly average precipitation is 150 mm, ranging between 80 and 205 mm (October to March) and a dry period in which the monthly average precipitation is 39 mm, ranging between 28 and 60 mm. Information consistent with those found in our study.

The temperature (maximum and minimum) had standard characteristics for the local climatic classification, with hot summers and cooler winters.

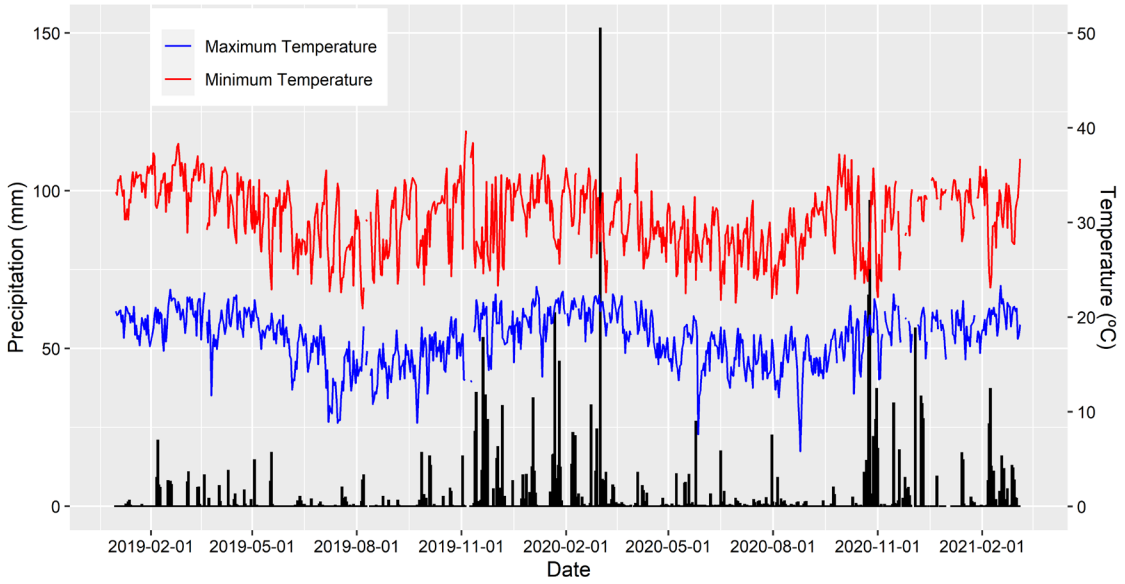

Figure 3 – Meteorological characterization of the area.

Figure 4 shows a boxplot of kc values. Pixel values ranged from 0 to 1.83, with 25 % of the data (third quartiles) normally between 0.76 and 1.83, with an mean value of 0.566. In 2020, between Day of the Year (DOY) 161 to 196 shows the high median values of kc, most likely due to the large volume of rain that occurred on earlier dates, making the coffee crop more vigorous. NDVI data (Figure 6) on the same dates corroborate the kc data analyzed, however the kc did not show any outliers.

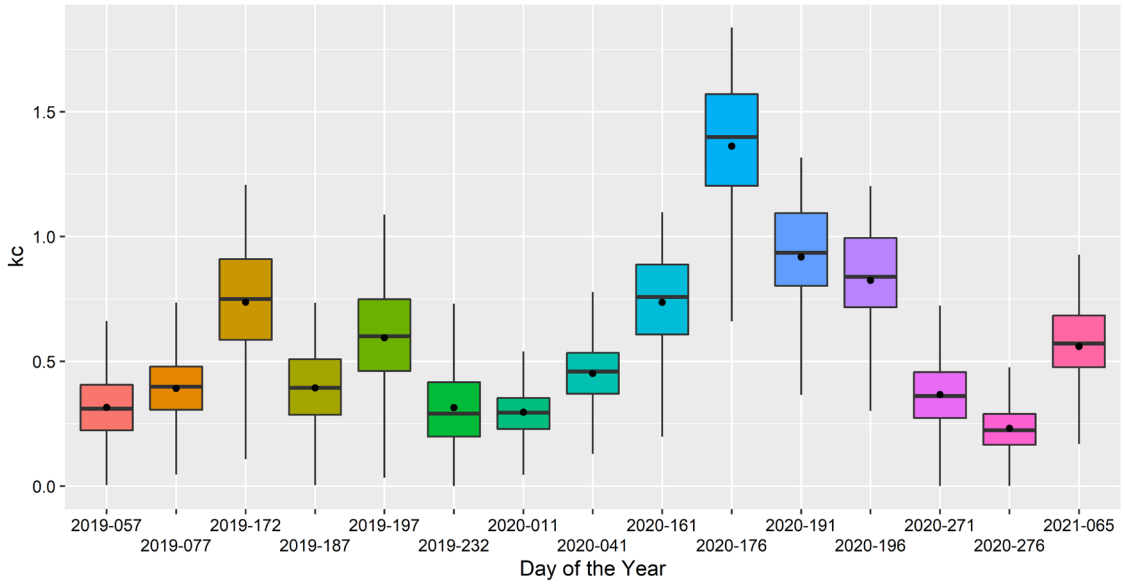

Figure 4 - Boxplot of kc values for different dates of irrigated coffee field.

Costa et al. (2019), evaluating evapotranspiration using the SEBAL algorithm in coffee plantations, found a mean Kc value of 0.6 for young coffee plants, with a standard deviation of 0.43, on mean. Already in adult plants, the mean Kc value was 0.85, with a mean standard deviation of 0.48.

Silva, Manzione, and Albuquerque Filho (2018), applied SAFER in sugarcane crops in the central-western part of São Paulo State, Brazil, and reported that some ET_f (also called kc) values were close to zero, as observed in our study. Teixeira et al. (2015) verified some pixels with ET_f values close to 1.40, with values normally ranging between 0.2 and 1.2.

Figure 5 shows a boxplot of LST values for the coffee field in the different seasons of 2019, 2020, and 2021. LST ranged from 20.77 to 43.87 °C. The different dates had different LST values. However, there is little variation within the same date. The mean LST was approximately 32.2 °C. Maximum LST values were observed during the summer season when there is the highest air temperature (T_0) and radiation.

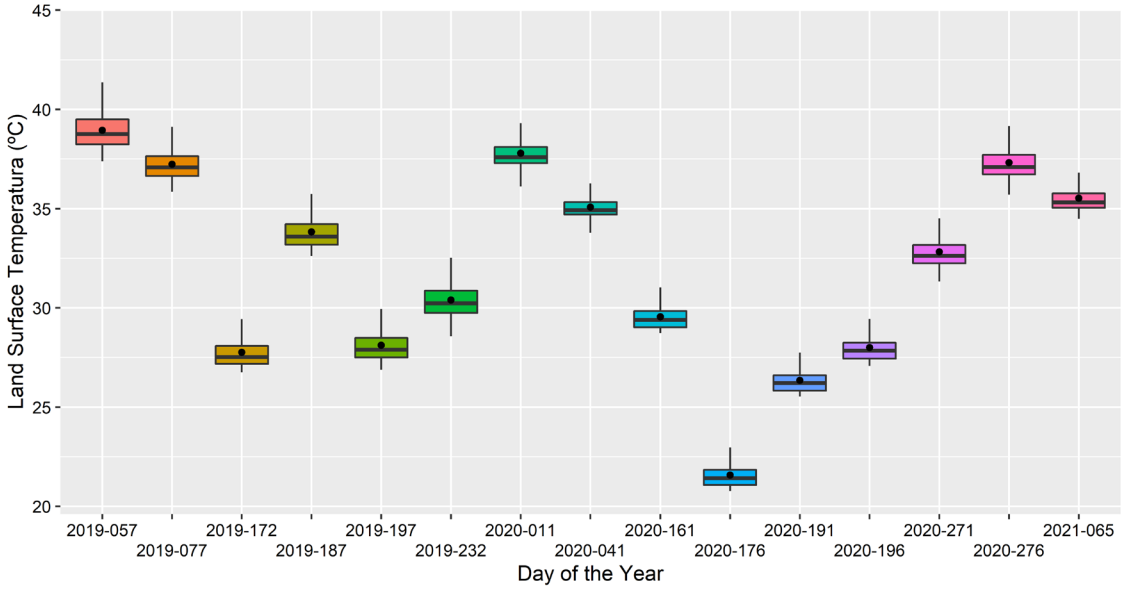

Figure 5 - Boxplot of (LST) values for different dates of irrigated coffee field.

The LST is indirectly related to the latent heat flux (LE) through the energy balance equation (Seguin et al., 1983). It provides important information on surface moisture conditions (LAOUNIA et al., 2017).

Thus, variability of these parameters within the same field is more influenced by the different crop phenological stages, unlike natural vegetation, where the variability of these parameters can primarily be attributed to variations in global solar radiation and surface moisture conditions (TEIXEIRA et al., 2017). According to (TEIXEIRA et al., 2013c), the large dispersion of values also depends on the coincidence between the imaging days and the presence of irrigation in the field.

NDVI values followed the climatic season, with winter with lower values and summer with higher values (Figure 6). Maximum NDVI values were approximately 0.9, while minimum values were close to 0.15, with a mean value of approximately 0.7. The minimum value, approximately 0.15, was commonly observed in bare soil (probably in the crop streets), while the maximum value was observed after the period of massive raining season.

Costa et al. (2019), found the NDVI with a maximum value of 0.87 in a coffee field when analyzing the evapotranspiration on coffee plants in center pivots in the Northwestern region of the state of Minas Gerais.

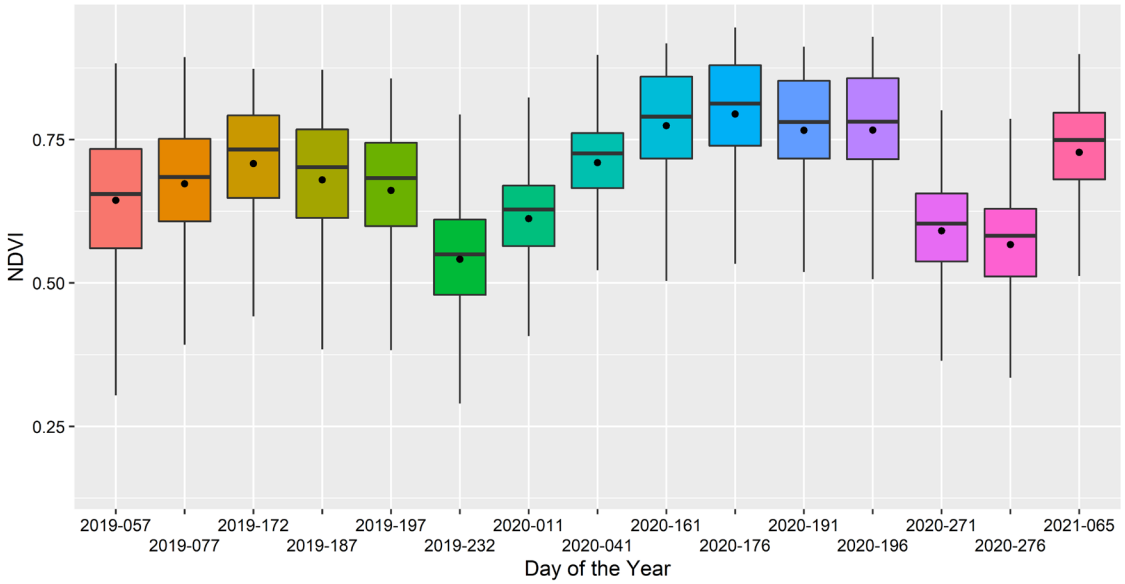

Figure 6 - Boxplot of NDVI values for different dates of irrigated coffee field.

Figure 7 shows a boxplot of evapotranspiration values. Pixel values ranged from 0 to 5.55 mm, with a mean value of 2.0 mm. In 2020, the DOY 176 shows approximately the high values of ET. In 2021, the DOY 065 also shows the high values of evapotranspiration, corresponding to the climatic behavior of the region (rainy summer and dry winter). The values follow the same pattern as the values found in the calculation of NDVI and kc (Figures 4 and 6) and inverse of the LST (Figure 5).

Silva, Teixeira, and Manzione (2019), show this behavior when they developed the modeling of the SAFER algorithm, in which, higher values of ET occur with lower values of LST, higher values of NDVI, and kc.

The evapotranspiration amplitude of 5.55 mm day^{-1} (difference between the highest and lowest ET), despite the predominance of a high canopy, confirms the high heterogeneity of the system regarding land use and dependence on the rainfall regime for the economic development of the cropland, and results close to the values in the dry season were reported in Northwestern São Paulo by (COAGUILA et al., 2017). Filgueiras et al. (2019) and Purevdorj et al. (1998), studied direct relationships between vegetation cover and satellite indexes including NDVI. (RIBEIRO et al., 2017) concluded that NDVI was efficient in differentiating phenological stages of the corn and soybean crop respectively.

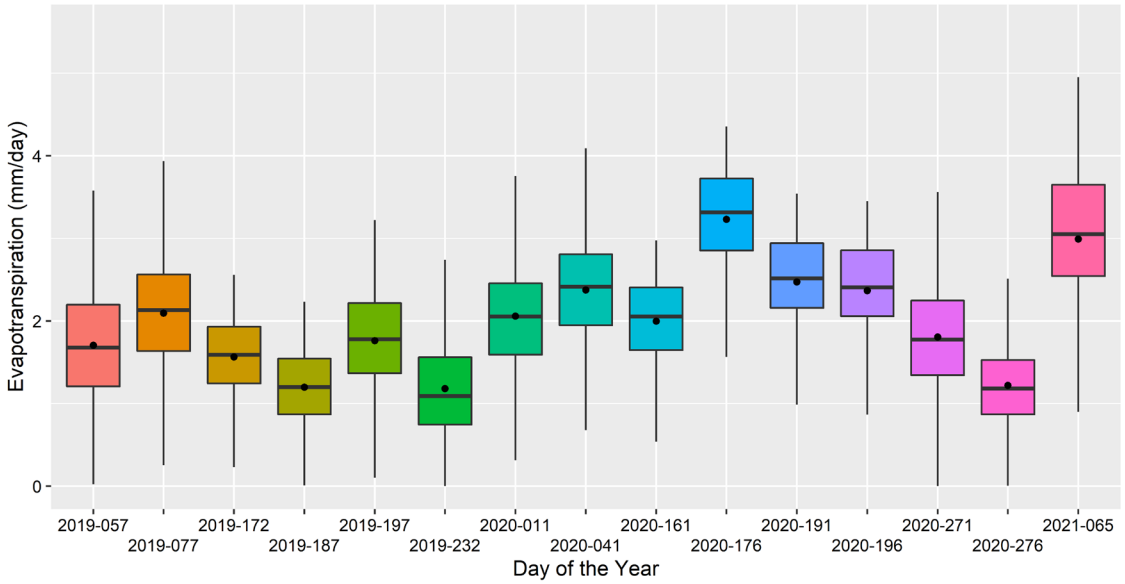

Figure 7 - Boxplot of Evapotranspiration values for different dates of irrigated coffee field.

The different images acquired during the coffee crop cycle can demonstrate the spatial and temporal distribution of the evapotranspiration calculated by the SAFER algorithm (Figure 8), which is a great advantage of the method for irrigation management.

Also in Figure 8, we can conclude that within the same area, there are different evapotranspiration behaviors. This can occur due to poor management of the method. Thus, with the images, one can identify possible failures and correct the management to avoid water and productivity losses.

Seeking the best irrigation management, the interpretation of the irrigated area can happen pixel by pixel, making the analysis very detailed. However different analyzes of the ET can be performed. Producers who do not have detailed control of irrigation, as is the situation in the studied area, an advance is to subdivide the area and larger plots. The subdivision makes decision-making more adapted to the reality of each type of management, whether with high technology or not.

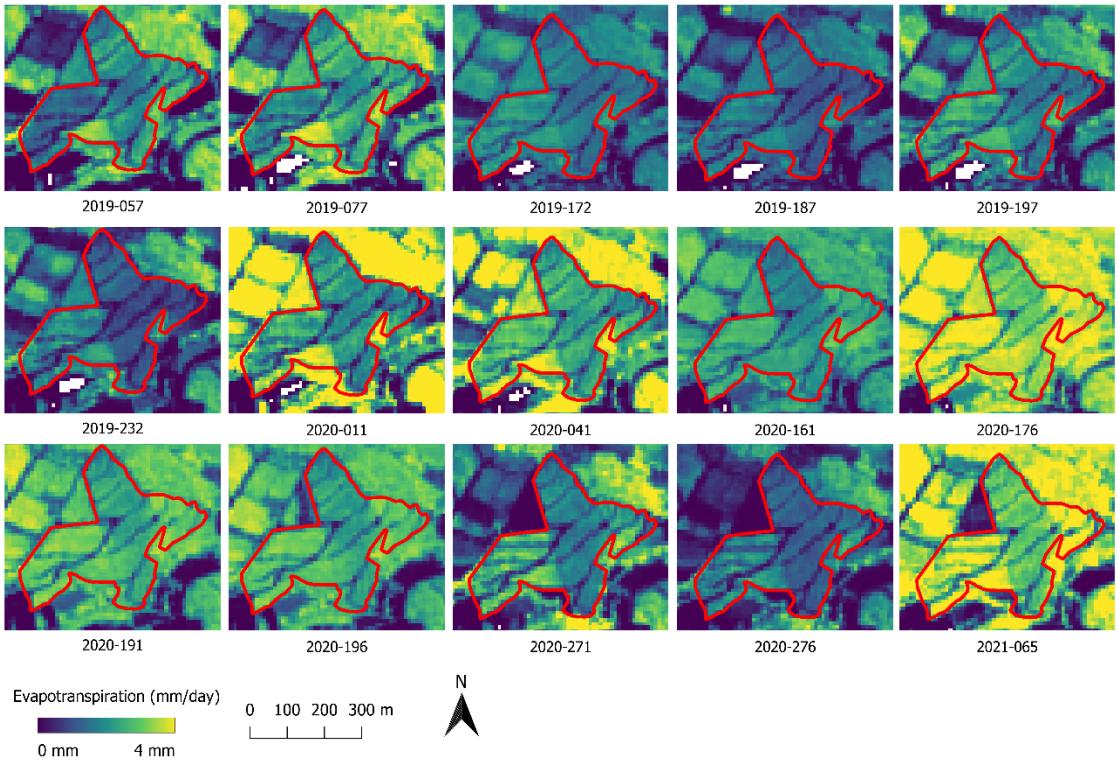

Figure 8 – spatial data of ET_{SAFER} calculated with ET_0 estimated by standard PM

4. CONCLUSIONS

The joint applications of the SAFER algorithm and the FAO Penman-Monteith method allowed understand the variation of ET in the coffee drip-irrigated field with high spatial (10 m) and temporal (5 days) resolution, and from this variation in ET, understand how to best manage irrigation in this crop.

The present study is unprecedented, but future research should be conducted considering other regions and a larger number of irrigated fields, with different irrigation management. Even so, the results found in this research are promising and can serve as a basis for future studies and can assist farmers and technicians in obtaining surface evapotranspiration with a high spatial and temporal resolution.

Therefore, water management of agricultural crops can be performed with free satellite imagery and simple weather data.

REFERENCES

ALLEN, R. et al. Satellite-based ET estimation in agriculture using SEBAL and METRIC. **Hydrological Processes**, v. 25, n. 26, p. 4011–4027, 2011.

ALLEN, R. G. et al. **FAO Irrigation and Drainage Paper Nº 56. Crop Evapotranspiration (guidelines for computation crop water requirements)**. Roma: FAO, 1998.

AMAZIRH, A. et al. Modified Penman–Monteith equation for monitoring evapotranspiration of wheat crop: Relationship between the surface resistance and remotely sensed stress index. **Biosystems Engineering**, v. 164, n. 0, p. 68–84, dez. 2017.

BASTIAANSSEN, W. G. M. et al. A remote sensing surface energy balance algorithm for land (SEBAL). 1. Formulation. **Journal of Hydrology**, v. 212–213, n. JANUARY, p. 198–212, dez. 1998.

BUNN, C. et al. A bitter cup: climate change profile of global production of Arabica and Robusta coffee. **Climatic Change**, v. 129, n. 1–2, p. 89–101, 2015.

CAO, M. et al. Multiple sources of uncertainties in satellite retrieval of terrestrial actual evapotranspiration. **Journal of Hydrology**, v. 601, n. July, p. 126642, 2021.

CASHIN, P.; MOHADDES, K.; RAISSI, M. Fair weather or foul? The macroeconomic effects of El Niño. **Journal of International Economics**, v. 106, p. 37–54, 2017.

COAGUILA, D. N. et al. Water productivity using SAFER - Simple Algorithm for Evapotranspiration Retrieving in watershed. **Revista Brasileira de Engenharia Agrícola e Ambiental**, v. 21, n. 8, p. 524–529, 2017.

CONAB, C. N. DE A. Acompanhamento da Safra Brasileira - CAFÉ. **Observatório Agrícola**, v. 8, n. 2, p. 1–60, 2021.

COSTA, J. DE O. et al. Spatial variability of coffee plant water consumption based on the SEBAL algorithm. **Scientia Agricola**, v. 76, n. 2, p. 93–101, 2019.

DA SILVA, J. G. F. et al. **Estimativa da evapotranspiração de referência para o município de Marilândia – ES.** IX Congreso Latinoamericano y del Caribe de Ingeniería Agrícola - CLIA 2010 XXXIX Congresso Brasileiro de Engenharia Agrícola - CONBEA 2010. **Anais**...Vitória, ES: 2010

DAMATTA, F. M. et al. Why could the coffee crop endure climate change and global warming to a greater extent than previously estimated? **Climatic Change**, v. 152, n. 1, p. 167–178, 2019.

FILGUEIRAS, R. et al. Crop NDVI monitoring based on sentinel 1. **Remote Sensing**, v. 11, n. 12, 2019.

GORELICK, N. et al. Google Earth Engine: Planetary-scale geospatial analysis for everyone. **Remote Sensing of Environment**, v. 202, n. 2016, p. 18–27, dez. 2017.

HSSAINE, B. A. et al. Combining a two source energy balance model driven by MODIS and MSG-SEVIRI products with an aggregation approach to estimate turbulent fluxes over sparse and heterogeneous vegetation in Sahel region (Niger). **Remote**

Sensing, v. 10, n. 6, 2018.

INTERNATIONAL COFFEE ORGANIZATION. Country Coffee Profile: Vietnam. **International Coffee Council**, v. 124th Sess, n. March, p. 25, 2019.

INTERNATIONAL COFFEE ORGANIZATION. **Historical Data on the Global Coffee Trade**. Disponível em: <https://www.ico.org/new_historical.asp>. Acesso em: 3 jul. 2021.

LAOUNIA, N. et al. Evapotranspiration and Surface Energy Fluxes Estimation Using the Landsat-7 Enhanced Thematic Mapper Plus Image over a Semiarid Agrosystem in the North-West of Algeria. **Revista Brasileira de Meteorologia**, v. 32, n. 4, p. 691–702, dez. 2017.

LEWIN, B.; GIOVANNUCCI, D.; VARANGIS, P. **Coffee Markets New Paradigms in Global Supply and Demand**. Washington, D.C: The International Bank for Reconstruction and Development, 2004.

LIAQAT, U. W.; CHOI, M.; AWAN, U. K. Spatio-temporal distribution of actual evapotranspiration in the Indus Basin Irrigation System. **Hydrological Processes**, v. 29, n. 11, p. 2613–2627, 30 maio 2015.

MAFUSIRE, A. et al. Coffee Production in Africa and the Global Market Situation. **Commodity Market Brief**, v. 1, n. 2, p. 1–9, 2010.

MCCABE, M. F.; WOOD, E. F. Scale influences on the remote estimation of evapotranspiration using multiple satellite sensors. **Remote Sensing of Environment**, v. 105, n. 4, p. 271–285, 2006.

OLIVERA-GUERRA, L. et al. Estimating the water budget components of irrigated crops: Combining the FAO-56 dual crop coefficient with surface temperature and vegetation index data. **Agricultural Water Management**, v. 208, n. June, p. 120–131, set. 2018.

PUREVDORJ, T. et al. Relationships between percent vegetation cover and vegetation indices. **International Journal of Remote Sensing**, v. 19, n. 18, p. 3519–3535, 25 dez. 1998.

R CORE TEAM. **R: A language and environment for statistical computing. R Foundation for Statistical Computing**Vienna, Austria, 2021. Disponível em: <https://www.r-project.org/>

RAHIMZADEGAN, M.; JANANI, A. Estimating evapotranspiration of pistachio crop based on SEBAL algorithm using Landsat 8 satellite imagery. **Agricultural Water Management**, v. 217, n. August 2018, p. 383–390, maio 2019.

RIBEIRO, R. B. et al. Variabilidade Espaço-Temporal Da Condição Da Vegetação Na Agricultura Irrigada Por Meio De Imagens Sentinel-2ª. **Revista Brasileira de Agricultura Irrigada**, v. 11, n. 6, p. 1884–1893, 2017.

ROUSE, J. W. et al. **Monitoring Vegetation Systems in the Great Plains with ERTS**. Third Earth Resources Technology Satellite-1 Symposium. **Anais**...Washington, D.C: NASA. Goddart Space Flight Center, 1974Disponível em: <https://ntrs.nasa.gov/search.jsp?R=19740022614>

SEPHTON, P. S. El Niño, La Niña, and a cup of Joe. **Energy Economics**, v. 84, n.

xxxx, p. 104503, 2019.

SILVA, C. DE O. F.; MANZIONE, R. L.; ALBUQUERQUE FILHO, J. Large-Scale Spatial Modeling of Crop Coefficient and Biomass Production in Agroecosystems in Southeast Brazil. **Horticulturae**, v. 4, n. 4, p. 44, 22 nov. 2018.

SILVA, C. DE O. F.; TEIXEIRA, A. H. DE C.; MANZIONE, R. L. agriwater: An R package for spatial modelling of energy balance and actual evapotranspiration using satellite images and agrometeorological data. **Environmental Modelling and Software**, v. 120, n. February, p. 104497, 2019.

SILVA, V. D. P. R. et al. Desenvolvimento de um sistema de estimativa da evapotranspiração de referência. **Revista Brasileira de Engenharia Agrícola e Ambiental**, v. 9, n. 4, p. 547–553, 2005.

STOCKER, T. F.; RAIBLE, C. C. Water cycle shifts gear. **Nature**, v. 434, n. 7035, p. 830–833, 13 abr. 2005.

SUN, Z. et al. Evapotranspiration estimation based on the SEBAL model in the Nansi Lake Wetland of China. **Mathematical and Computer Modelling**, v. 54, n. 3–4, p. 1086–1092, 2011.

TEIXEIRA, A. DE C. et al. Large-Scale Water Productivity Assessments with MODIS Images in a Changing Semi-Arid Environment: A Brazilian Case Study. **Remote Sensing**, v. 5, n. 11, p. 5783–5804, 6 nov. 2013a.

TEIXEIRA, A. H. D. C. et al. Energy balance with Landsat images in irrigated central pivots with corn crop in the São Paulo State , Brazil. **Proc SIPE**, v. 9239, p. 1–10, 2014a.

TEIXEIRA, A. H. D. C. et al. Use of MODIS images to quantify the radiation and energy balances in the Brazilian Pantanal. **Remote Sensing**, v. 7, n. 11, p. 14597–14619, 2015.

TEIXEIRA, A. H. DE C. et al. Analysis of energy fluxes and vegetation-atmosphere parameters in irrigated and natural ecosystems of semi-arid Brazil. **Journal of Hydrology**, v. 362, n. 1–2, p. 110–127, nov. 2008.

TEIXEIRA, A. H. DE C. et al. Reviewing SEBAL input parameters for assessing evapotranspiration and water productivity for the Low-Middle São Francisco River basin, Brazil. **Agricultural and Forest Meteorology**, v. 149, n. 3–4, p. 477–490, mar. 2009.

TEIXEIRA, A. H. DE C. Determining Regional Actual Evapotranspiration of Irrigated Crops and Natural Vegetation in the São Francisco River Basin (Brazil) Using Remote Sensing and Penman-Monteith Equation. **Remote Sensing**, v. 2, n. 5, p. 1287–1319, 6 maio 2010.

TEIXEIRA, A. H. DE C. et al. A Comparative Study of Techniques for Modeling the Spatiotemporal Distribution of Heat and Moisture Fluxes at Different Agroecosystems in Brazil. In: PETROPOULOS, G. P. (Ed.). . **Remote sensing of energy fluxes and soil moisture content**. Boca Raton, FL: CRC Press, 2013b. p. 165–188.

TEIXEIRA, A. H. DE C. et al. Large-Scale Water Productivity Assessments with MODIS Images in a Changing Semi-Arid Environment: A Brazilian Case Study. **Remote Sensing**, v. 5, n. 11, p. 5783–5804, 6 nov. 2013c.

TEIXEIRA, A. H. DE C. et al. **Irrigation Performance Assessments for Corn Crop With Landsat Images in the São Paulo State, Brazil**. Anais do II Inovagri International Meeting - 2014. **Anais**...Fortaleza, Ceará, Brasil: INOVAGRI/INCT-EI/INCTSal, 2014bDisponível em: <http://www.bibliotekevirtual.org/index.php/2013-02-07-03-02-35/simposios/221-ii-inovagri-2014/1414-ii-inovagri-2014-a099.html>

TEIXEIRA, A. H. DE C. et al. Sugarcane Water Productivity Assessments in the São Paulo state, Brazil. **International Journal of Remote Sensing Applications**, v. 6, n. 0, p. 84, 2016.

TEIXEIRA, A. H. DE C. et al. Large-scale radiation and energy balances with Landsat 8 images and agrometeorological data in the Brazilian semiarid region. **Journal of Applied Remote Sensing**, v. 11, n. 1, p. 016030, 2017.

TEIXEIRA, A. H. DE C.; TONIETTO, J.; LEIVAS, J. F. Large-scale water balance indicators for different pruning dates of tropical wine grape. **Pesquisa Agropecuária Brasileira**, v. 51, n. 7, p. 849–857, jul. 2016.

UBILAVA, D. El Niño, La Niña, and world coffee price dynamics. **Agricultural Economics**, v. 43, n. 1, p. 17–26, 2012.

WANG, K.; DICKINSON, R. E. A review of global terrestrial evapotranspiration: Observation, modeling, climatology, and climatic variability. **Reviews of Geophysics**, v. 50, n. 2, p. 1–54, jun. 2012.